

## **Diabetes, Obesity, and Enteric Infections**

**HYPERGLYCEMIA AND COMPONENTS OF AN OBESOGENIC DIET WORSEN THE  
OUTCOMES OF ENTERIC INFECTION**

By

**TREVOR C. LAU, B.Sc.**

A Thesis Submitted to the School of Graduate Studies in Partial Fulfilment  
of the Requirements for the Degree Doctor of Philosophy

**DESCRIPTIVE NOTE**

McMaster University DOCTOR OF PHILOSOPHY (2019) Hamilton,  
Ontario (Biochemistry and Biomedical Sciences)

TITLE: Hyperglycemia and components of an obesogenic diet worsen the  
outcomes of enteric infection

AUTHOR: Trevor C. Lau, B.Sc. (McMaster University)

SUPERVISOR: Dr. Jonathan D. Schertzer

NUMBER OF PAGES: XV, 173

### **Lay Abstract**

Obesity and diabetes are major public health issues that are connected in many ways, including how diet changes glucose metabolism. Diabetics have a higher risk of contracting infections and also have worse outcomes from infections. It was unknown what factors of obesity or diabetes influence how the immune system combats bacterial infections. The gut is an important site as it is where diet, the immune system, and metabolism all directly interact. We discovered that high blood sugar was associated with death related to dehydration in diabetic, but not necessarily obese mice infected with a diarrhea causing bacteria. Diet-induced obesity in mice infected with bacteria associated with Crohn's disease, showed an overgrowth of bacteria and worse intestinal damage. We isolated the key dietary factor responsible, which was low fibre rather than high fat or sugar. Even one day of lower dietary fibre promoted overgrowth of infectious bacteria in the gut.

## Abstract

Obesity is a major predictor for type 2 diabetes. The etiology and comorbidities of these two diseases are associated. Diabetics are twice as likely to contract any type of infection and at greater risk of worse clinical outcomes to infection. However, the individual effects of diet, glycemia and obesity on risk and severity of enteric infection has not been elucidated. Here we show that high blood glucose (i.e. hyperglycemia), independent of obesity, is sufficient to promote mortality during infection with *Citrobacter rodentium*, a diarrhea-causing pathogen in mice. Mortality was caused by dehydration as a result of excessive Wnt/ $\beta$ -catenin signalling. Our findings highlight the importance of glucose lowering and fluid therapy as opposed to immunological dysfunction, gut barrier defects or bacteraemia as modifiers of outcomes from enteric infection during diabetes. Future work should develop a more comprehensive understanding of the molecular changes that connect hyperglycemia, Wnt/ $\beta$ -catenin pathway and fluid balance during infection. We used the most common model to cause diet-induced obesity in mice to study another enteric pathogen. We showed that long- and short-term high-fat diet (HFD) feeding promoted the colonization and expansion of adherent-invasive *Escherichia coli*. Higher pathogen burdens in the intestinal tissues and feces were detected in diet-induced obese mice, which coincided with increased distal gut pathology. Initiating the diet one day prior or after infection was sufficient to promote the expansion of adherent-invasive *E. coli* in the absence of robust weight gain implicating components of diet as a major determinant of pathogen burden. We isolated the dietary factor and found that low fibre content of the high-fat diet was partially responsible for the increased intestinal pathogen burden. Future work should determine how lower fibre alters host and bacterial metabolism in order to promote overgrowth of adherent-invasive *E. coli* in the gut.

## **Acknowledgements**

I would like to thank my supervisor, Dr. Jonathan Schertzer, for his consistently positive attitude and leadership. This was an exciting project for both of us to embark on and I am grateful to him for taking a chance on me. I will always remember his words to me when starting graduate school “Science is just 5% success and slowly building upon that success.” This allowed me to maintain perspective in more trying times and encouraged me to celebrate the little scientific victories. This has been an excellent start to my scientific career. Thank you for cultivating a fantastic learning environment.

I would also like to thank my committee members, Dr. Dawn Bowdish and Dr. Brian Coombes, for their well-rounded scientific guidance and helpful suggestions over the years. Their differing perspectives has helped broaden my scientific knowledge and help me grow as a scientist.

To all members of the Schertzer lab, past and present, thank you for providing a fun and nurturing work environment. Your scientific support and friendship over the years enhanced the grad school experience.

To the Biochemistry and Biomedical Sciences staff, especially Lisa Kush, thank you for helping me navigate the many departmental and scholarship guidelines. Thanks to CIHR for providing scholarship funding throughout this project.

I would like to thank my entire family for their love and support. I am especially grateful to my parents, who raised me to be the person I am today. Rebecca and Gavin, thank you for your constant love and support in not only dealing with my graduate school experience but also with our parents. You two have been just as instrumental as our parents in shaping who I am. You are not only siblings to me but also best friends.

To my friends, thank you for dealing with every up and down I had through grad school. It is true when they say that friends are the family you choose. Thanks for being a constant source of laughs and an endless pool of support.  
#brooklynbunz

To Kevin, who I was lucky to have met just as I was starting this crazy endeavor. I have no idea how I would have gotten through all this without your support. You managed to keep me relatively sane and talked me off the edge quite a few times. I love you and am eternally grateful for you. We've been tested quite a bit throughout this journey, and I don't know what life has next for us, but I am completely confident that we will face any challenge with the same humour, love and teamwork we have before.

## Table of Contents

<b>TITLE PAGE</b>	i
<b>DESCRIPTIVE NOTE</b>	ii
<b>LAY ABSTRACT</b>	iii
<b>ABSTRACT</b>	iv
<b>ACKNOWLEDGEMENTS</b>	v
<b>TABLE OF CONTENTS</b>	vii
<b>LIST OF FIGURES</b>	x
<b>LIST OF ABBREVIATIONS</b>	xiii
<b>DECLARATION OF ACADEMIC ACHIEVEMENT</b>	xv
<b>CHAPTER 1: Introduction</b>	
<b>1.1 Obesity</b>	2
1.1.1 Etiology of obesity	2
1.1.2 Molecular consequences of obesity	5
<b>1.2 Diabetes</b>	9
1.2.1 Diabetes and infection	10
<b>1.3 Intestinal health and maintenance</b>	12
1.3.1 The intestinal microbiota	17
1.3.2 Obesity and intestinal health	20
1.3.3 Diabetes and Wnt Signalling	22
<b>1.4 <i>Citrobacter rodentium</i>: a non-invasive murine model of enteric infection</b>	23
<b>1.5 Adherent-invasive <i>Escherichia coli</i>: a model of enteric infection</b>	26
<b>1.6 Purpose and goals of the dissertation</b>	28
<b>CHAPTER 2: Materials and Methods</b>	
<b>2.1 Animal models</b>	32
<b>2.2 Diet studies</b>	32
<b>2.3 Intraperitoneal glucose tolerance test</b>	33
<b>2.4 <i>In vivo Citrobacter rodentium</i> infection</b>	34
<b>2.5 Insulin pellet insertion</b>	35
<b>2.6 IL-22 treatment</b>	35

<b>2.7 <i>In vivo</i> adherent-invasive <i>Escherichia coli</i> infection</b>	36
<b>2.8 Gene expression analyses</b>	36
<b>2.9 Cytokine quantification</b>	38
<b>2.10 Immunoblotting</b>	38
<b>2.11 FITC-dextran assay</b>	39
<b>2.12 TLR4 assay</b>	40
<b>2.13 Histological evaluation and immunohistochemical evaluation</b>	40
<b>2.14 Immunofluorescence staining</b>	42
<b>2.15 Statistical analysis</b>	42
<b>Chapter 3: Results</b>	
<b>3.1 Hyperglycemia, independent of obesity, worsens outcomes of enteric infections</b>	45
3.1.1 Hyperglycemia predicts mortality during <i>C. rodentium</i> infection	45
3.1.2 Hyperglycemia, independent of obesity, promotes mortality during <i>C. rodentium</i> infection	52
3.1.3 Impaired intestinal barrier function is not responsible for Hyperglycemia-induced mortality during <i>C. rodentium</i> infection	60
3.1.4 IL-22 lowers blood glucose and mitigates severity of enteric infection in obese and diabetic mice	63
3.1.5 Fluid balance regulates mortality during <i>C. rodentium</i> infection in diabetic mice	71
3.1.6 Wnt-inhibition reduces mortality during <i>C. rodentium</i> infection in diabetic mice	77
3.1.7 Hyperglycemia worsens outcomes during a different model of enteric infection	82

<b>3.2 Obesity impairs resolution of adherent-invasive <i>Escherichia coli</i> infection</b>	85
3.2.1 Obesity promotes AIEC expansion and pathology	85
3.2.2 IL-22 promotes AIEC expansion in a diet-induced obesity model	92
3.2.3 Diet and obesity potentiate AIEC expansion in mouse models of obesity	95
3.2.4 Diet, independent of obesity and aging, can promote AIEC expansion	99
<b>3.3 Components of an obesogenic diet promote adherent-invasive <i>Escherichia coli</i> expansion</b>	104
3.3.1 HFD after infection impacts AIEC colonization	104
3.3.2 Low fibre promotes AIEC expansion	105
3.3.3 Short-term diet modification reduces tissue but not fecal burden	111
3.3.4 Cellulose supplementation does not rescue HFD-promoted AIEC expansion	113
<b>Chapter 4 – Discussion</b>	
<b>4.1 Hyperglycemia, independent of obesity, worsens outcomes of enteric infections</b>	117
<b>4.2 Obesity and diet impair the resolution of adherent-invasive <i>Escherichia coli</i> infection</b>	124
<b>4.3 Future Directions</b>	132
<b>Chapter 5 – References</b>	136

## List of Figures

<b>Figure 1</b>	Simplified schematic of the crosstalk between Wnt and Notch signalling in intestinal epithelial cell differentiation	17
<b>Figure 2</b>	Hyperglycemia, independent of obesity, promotes mortality during <i>C. rodentium</i> infection	50
<b>Figure 3</b>	Mortality during <i>C. rodentium</i> infection is not dependent on bacterial burden or dissemination	51
<b>Figure 4</b>	Hyperglycemia is sufficient to promote mortality during <i>C. rodentium</i> infection	54
<b>Figure 5</b>	Pathogen dissemination and overt pathology do not correlate with <i>C. rodentium</i> -induced mortality during diabetes	55
<b>Figure 6</b>	<i>C. rodentium</i> -induced mortality is gender-specific	58
<b>Figure 7</b>	Virulent <i>C. rodentium</i> is required for hyperglycemia-induced mortality	59
<b>Figure 8</b>	Impaired intestinal barrier integrity and overt bacteremia are not detected during <i>C. rodentium</i> -induced mortality of Akita <sup>+/-</sup> mice	62
<b>Figure 9</b>	Exogenous IL-22 supplementation of Akita <sup>+/-</sup> mice rescues mortality during <i>C. rodentium</i> infection and reduces glycemia	68
<b>Figure 10</b>	Exogenous IL-22 supplementation of <i>ob/ob</i> <sup>-/-</sup> mice rescues mortality during <i>C. rodentium</i> infection and reduces glycemia	69
<b>Figure 11</b>	Inflammation does not correlate with <i>C. rodentium</i> -induced mortality in <i>ob/ob</i> <sup>-/-</sup> mice	70
<b>Figure 12</b>	Fluid replenishment rescues hyperglycemia-induced mortality during <i>C. rodentium</i> infection	73
<b>Figure 13</b>	No differences in serum osmolality observed during <i>C. rodentium</i> infection of Akita <sup>+/-</sup> mice	74
<b>Figure 14</b>	Empagliflozin, a diabetic drug, promotes mortality during <i>C. rodentium</i> infection of Akita <sup>+/-</sup> mice	76
<b>Figure 15</b>	Wnt-inhibition rescues hyperglycemia-induced mortality during <i>C. rodentium</i> infection	80

<b>Figure 16</b>	Hyperglycemia does not elevate Rspodin expression or colonic crypt proliferation	81
<b>Figure 17</b>	Akita <sup>+/-</sup> mice have elevated fecal and tissue burdens during adherent-invasive <i>Escherichia coli</i> infection	84
<b>Figure 18</b>	Long-term high fat feeding induces glucose intolerance and increased adiposity	88
<b>Figure 19</b>	Diet-induced obesity promotes adherent-invasive <i>Escherichia coli</i> expansion and colonization in the lower intestinal tract	89
<b>Figure 20</b>	Diet-induced obesity promotes worsened pathology during adherent-invasive <i>Escherichia coli</i> infection	90
<b>Figure 21</b>	Streptomycin pretreatment is required for expansion of adherent-invasive <i>Escherichia coli</i> infection	91
<b>Figure 22</b>	IL-22 exacerbates expansion of adherent-invasive <i>Escherichia coli</i> in diet-induced obese mice	94
<b>Figure 23</b>	An alternative diet-induced obesity model promotes adherent-invasive <i>Escherichia coli</i> infection	97
<b>Figure 24</b>	Body mass does not correlate with bacterial burden during adherent-invasive <i>Escherichia coli</i> infection of murine models of diet-induced obesity	98
<b>Figure 25</b>	Short-term high fat feeding promotes worsened pathology during adherent-invasive <i>Escherichia coli</i> infection	102
<b>Figure 26</b>	High fat feeding, independent of obesity and age, can promote adherent-invasive <i>Escherichia coli</i> expansion	103
<b>Figure 27</b>	Comparison of short-term and long-term high fat feeding models during adherent-invasive <i>Escherichia coli</i> infection	104
<b>Figure 28</b>	Initiation of high fat feeding during adherent-invasive <i>Escherichia coli</i> infection promotes bacterial expansion	105
<b>Figure 29</b>	Short-term feeding with a high fat diet or sucrose and fibre-matched control diet confers similar adherent-invasive <i>Escherichia coli</i> infection kinetics	109
<b>Figure 30</b>	Short-term feeding with a high fat diet or sucrose and fibre-matched control diet confers similar adherent-invasive <i>Escherichia coli</i> infection kinetics	110
<b>Figure 31</b>	Short-term feeding with a low fibre diet promotes adherent-invasive <i>Escherichia coli</i> colonization and expansion	111

<b>Figure 32</b>	Intervention with regular chow diet rescues tissue colonization of adherent-invasive <i>Escherichia coli</i> in a diet-induced obese mouse model	112
<b>Figure 33</b>	Intervention with a high fat diet supplemented with cellulose does not impact adherent-invasive <i>Escherichia coli</i> colonization	114
<b>Figure 34</b>	Long-term feeding with a high fat diet supplemented with cellulose does not prevent obesity-induced expansion of adherent-invasive <i>Escherichia coli</i>	115
<b>Figure 35</b>	Acetate metabolism is not required for obesity-induced expansion of adherent-invasive <i>Escherichia coli</i>	127
<b>Figure 36</b>	Blood glucose indicative of type 2 diabetes is an independent risk factor predicting diarrhea during an <i>Escherichia coli</i> outbreak	135

### Abbreviations

A/E	Attaching and effacing
AREB	Animal review ethics board
BCA	Bicinchoninic acid assay
BMI	Body mass index
cAMP	Cyclic adenosine monophosphate
CD	Crohn's disease
CFU	Colony forming unit
DKK4	Dkkof-4
DM	Diabetes mellitus
DNA	Deoxyribose nucleic acid
EDTA	Ethylenediaminetetraacetic acid
ER	Endoplasmic reticulum
FITC	Fluorescein isothiocyanate
GSK3	Glycogen synthase kinase-3
H & E	Haematoxylin and eosin
HFD	High fat diet
IEC	Intestinal epithelial cell
ISC	Intestinal stem cell
Il-#	Interleukin-#
LB	Luria-burtani media
LEF	Lymphoid enhancer factor
MC4R	Melanocortin 4 receptor
NTP	Nucleotide triphosphate
OB	<i>ob/ob</i> <sup>-/-</sup>
PBS	Phosphate buffered saline

PCR	Polymerase chain reaction
PVDF	Polyvinylidene fluoride
RNA	Ribonucleic acid
RSPOS	Rspondin
SCFA	Short chain fatty acid
T2D	Type 2 Diabetes
TA	Transit-amplifying
TCF	T-cell factor
Th17	T helper cell 17
TNF	Tumour necrosis factor
WT	Wild-type

## Declaration of Academic Achievement

### Co-author peer-reviewed contributions

Chi W, Dao D, Lau TC, Henriksbo BD, Cavallari JF, Foley KP, et al. Bacterial peptidoglycan stimulates adipocyte lipolysis via NOD1. *PLoS One*. 2014 May 14;9(5):e97675.

Henriksbo BD, Lau TC, Cavallari JF, Denou E, Chi W, Lally JS, et al. Fluvastatin causes NLRP3 inflammasome-mediated adipose insulin resistance. *Diabetes*. 2014 Nov;63(11):3742–7.

Denou E, Lolmède K, Garidou L, Pomie C, Chabo C, Lau TC, et al. Defective NOD2 peptidoglycan sensing promotes diet-induced inflammation, dysbiosis, and insulin resistance. *EMBO Mol Med*. 2015 Mar 1;7(3):259–74.

McBride MJ, Foley KP, D’Souza DM, Li Ye, Lau TC, Hawke TJ, et al. The NLRP3 inflammasome contributes to sarcopenia and lower muscle glycolytic potential in old mice. *Am J Physiol Endocrinol Metab*. 2017 Aug;313(2):E222-E232.

Hung CLK, Maiuri T, Bowie LE, Gotesman R, Son S, Falcone M, et al. A patient-derived cellular model for Huntington’s disease reveals phenotypes at clinically relevant CAG lengths. *Mol Biol Cell*. 2018 Nov;29(23):2809-2820.

Breznik JA, Naidoo A, Foley KP, Schulz C, Lau TC, Loukov D, Et al. TNF, but not hyperinsulinemia or hyperglycemia, is a key driver of obesity-induced monocytosis revealing that inflammatory monocytes correlate with insulin in obese male mice. *Physiol Rep*. 2018 Dec;6(23):e13937.

## **Chapter 1 - Introduction**

## **1.1 Obesity**

Obesity is a disease that can be considered a global health epidemic. In 2016, nearly 2 billion adults were overweight and 650 million people were obese worldwide<sup>1</sup>. Body mass index is often used to define obesity and is an indirect measure of body fat, calculated by dividing an individual's weight by the square of their height ( $\text{kg}/\text{m}^2$ )<sup>2,3</sup>. Overweight is defined by a body mass index (BMI) greater than 30. According to the Public Health Agency of Canada, 64% of adults over the age of 18 are overweight or obese. Obesity and its comorbidities have placed a huge economic burden on the healthcare system with direct and indirect costs of over \$6 billion every year in Canada alone<sup>4-6</sup>. Obesity is associated with a lower quality of life and can reduce life expectancy by up to 14 years<sup>7,8</sup>. Obesity is also associated with many comorbidities including an increased risk of Type 2 Diabetes (T2D), cardiovascular disease, non-alcoholic liver disease, and cancer. The rising prevalence of this disease has fostered interest in discerning the molecular causes and potential therapeutic targets to reduce obesity and to directly target its comorbidities.

### **1.1.1 Etiology of Obesity**

Obesity is a multifactorial disease influenced by a combination of biological, environmental, and behavioural factors. In the simplest of terms,

obesity is an energy disbalance with a higher energy intake than energy expenditure. The mechanisms underpinning a skewing of the energy balance towards increased energy storage are very complicated at both the individual and population levels. The prevalence of obesity has risen in countries along with shifts towards more sedentary lifestyles and “Western” diets that are higher in fat and high refined sugar. With technological advances in automation and transportation, there has been a drastic decrease in manual labour and physical activity in recent decades resulting in a decrease in average energy expenditure in daily life<sup>9,10</sup>. Increases in television viewing, and computer and smartphone usage has positively correlated with the incidence of obesity<sup>11–14</sup>.

In regard to energy intake, the rapid industrialization of agriculture has resulted in an environmental shift in terms of food availability and content. The advent of ultra-processed foods, including refined sugars, is associated with the precipitous rise in metabolic disease<sup>15,16</sup>. The typical North American or “Western” diet is calorie dense, high in fat and sugar, and low in fibre. In addition, larger portion sizes and easy accessibility to these foods has exacerbated their health impact<sup>15,17</sup>.

Genetics play a role in predisposing individuals to obesity. A study in monozygotic twins showed significant similarity for obesity within a twin pair, but significant variability across different sets of twins<sup>18</sup>. Although uncommon,

single gene mutations involved in the leptin-melanocortin pathway, including the melanocortin-4 receptor (MC4R) and leptin, have been known to cause obesity<sup>19,20</sup>. However, genetic predisposition cannot fully account for the variability and onset of obesity. Host genetics interact with environmental factors to modify risk of obesity.

One of the biggest environmental factors driving obesity is diet. Currently, dairy products, cereals, refined sugars, refined vegetable oils, and alcohol makeup 72.1% of daily energy intake in the United States whereas these food sources would not have been readily available to our pre-industrialized agricultural ancestors<sup>21</sup>. In the past 40 years, refined sugar consumption has increased by over 30% (specifically sucrose and fructose)<sup>22</sup>. Animal models have been developed to mimic diet-induced obesity using energy dense high fat, high sugar diets. Mice who consume these diets display many characteristics of metabolic syndrome including hyperglycemia, hyperinsulinemia, increased adiposity, and impaired blood glucose control<sup>23,24</sup>. Feeding mice obesogenic diets provides a reductionist model of diet-induced obesity compared to the human population that often eats a varied diet. Diet-induced obesity models can be combined with experiments in monogenic or polygenic mouse models of obesity resulting from hyperphagia. An example of a genetic mouse model of obesity is the leptin-deficient ob/ob (OB) mouse (B6.Cg-Lepob/J) that exhibits hyperphagia and develops obesity independent of changing the diet. This can provide

important proof-of-concept results in mice, since the influence of a single gene in human obesity is relatively small and only can account for a small percentage of obese patients<sup>25,26</sup>.

Certain environmental factors have been found to promote obesity, independent of host genetics. For example, a study in monozygotic twins discordant for obesity found that the microbiota was capable of transmitting features of obesity<sup>27</sup>. The microbiota is essential for nutrient extraction and energy harvest from the ingested diet as germ-free mice are protected from obesity when fed a high fat diet<sup>28</sup>. Conversely, acquisition of commensal microbes (i.e. conventionalization) in germ-free mice resulted in an increase in fat mass and features of prediabetes (i.e. glucose intolerance) despite reductions in food intake<sup>29</sup>. Changes in the microbial composition (dysbiosis) have been reported in obesity<sup>29–32</sup>. In fact, in mouse models, one day of high fat feeding was sufficient to induce alterations in microbial populations<sup>33</sup>. This dysbiosis has been suggested as a potential contributor to obesity and the characteristic underlying inflammation that coincides with obesity.

### **1.1.2 Molecular consequences of obesity**

Obesity is associated with chronic low-level inflammation, including an elevated inflammatory tone in metabolic tissues such as the liver and adipose

tissue, which are key tissues that help control blood glucose. At the onset of obesity, high caloric intake promotes energy storage in adipose tissue and causes hypertrophy of adipocytes. Adipose tissue hypertrophy is associated with adipocyte stress and immune-endocrine alterations that include changes in endocrine signals derived from adipocytes (i.e. adipokines) coincident with the recruitment and expansion of immune cells in adipose tissue. Accumulation of macrophages in adipose tissue has been associated with increased body mass and positively correlated with the development and progression of insulin resistance in mice and humans<sup>34–36</sup>. This macrophage infiltrate can be observed as early as one week after the initiation of a high fat diet in mice<sup>36</sup>. Polarization of these macrophages towards an M1 or pro-inflammatory phenotype have been reported in diet-induced obese mice, marked by elevated production of inflammatory signals, such as interleukin-6 (IL-6) and tumour necrosis factor (TNF), in the local adipose tissue environment<sup>37</sup>. These inflammatory mediators can activate stress kinases (ERK, JNK) that will increase serine phosphorylation of insulin receptor substrate 1 and 2, inhibiting downstream signals of insulin action<sup>20,38,39</sup>. Thus, adipose tissue inflammation lowers the ability of insulin to suppress lipolysis, thereby increasing the lipid load on other tissues. This adipose tissue inflammation and insulin resistance is part of a cascade leading to inflammatory and lipid overload on other tissues, such as liver and skeletal muscle that are major contributors to blood glucose control. In addition to

macrophages, B and T cells have also been implicated in obesity and insulin resistance<sup>40–42</sup>. Proinflammatory CD4<sup>+</sup> (primarily T<sub>h</sub>1 and T<sub>h</sub>17) and CD8<sup>+</sup> T cells have been found to accumulate in the adipose tissue of mice as early as two weeks after the initiation of a high fat diet<sup>42,43</sup>. T-cell accumulation is associated with an increase in interferon (IFN)- $\gamma$ , which promotes the polarization of macrophages towards the M1 subtype and further promotes the secretion of IL-6 and TNF<sup>44</sup>. Treatment of diet-induced obese mice with an anti-CD3 T cell depleting antibody reduced glucose levels and adipose tissue inflammation<sup>44</sup>. B cell infiltration of adipose tissue in diet-induced obese mice precedes T cell infiltration<sup>40,45</sup>. In both obese mice and humans, B cells have been reported to be potent producers of proinflammatory cytokines which play a role in T cell and macrophage activation<sup>46,47</sup>. In fact, high fat fed B cell-deficient mice showed a reduction in T cell proinflammatory cytokine secretion and insulin resistance<sup>41</sup>.

Obesity is also characterized by weakened gut epithelial integrity and poor mucosal host defence. This is often referred to as a “leaky gut”. There appears to be a strong correlation between metabolic disorders and impaired mucosal immunity<sup>48</sup>. As outlined above, obesity has been associated with dysbiosis of the intestinal microbiome that results in increased energy extraction, altered short chain fatty acid (SCFA) production, and the loss of microbial diversity<sup>30,49–51</sup>. These obesity-related changes in the intestinal microbiome composition may also be related to impaired mucosal defence.

However, it is often very difficult to disentangle diet, obesity, and changes to the microbiota or host immunity.

The order of events during obesity and intestinal homeostasis of microbes and immunity is still unclear as it is unknown if dysbiosis or the loss of intestinal barrier integrity occurs first. Nevertheless, these early changes are hypothesized to contribute towards the elevated levels of circulating endotoxin (i.e. metabolic endotoxemia) observed during obesity and high fat feeding, where mouse models clearly show that intestinal microbes are a key source of metabolic endotoxemia<sup>52-54</sup>. Metabolic endotoxemia is one way that the intestinal microbiota can contribute to obesity-induced inflammation by providing a chronic or cyclical load of immune receptor ligands in the form of live or dead bacterial components. Metabolic endotoxemia can promote systemic low-grade inflammation and affect the endocrine and metabolic status of metabolic tissues involved in blood glucose control thereby contributing to insulin resistance during obesity<sup>55-57</sup>.

Specific immune responses associated with obesity-related inflammation can impair insulin action and the resultant insulin resistance precedes and predicts T2D. Inflammation has emerged as a key factor in obesity-driven co-morbidities beyond T2D, including fatty liver disease and cardiovascular disease.

One underlying mechanism for these metabolic diseases is the development of insulin resistance and hyperglycemia.

## **1.2 Diabetes**

Diabetes mellitus (DM) currently affects over 300 million people worldwide and is expected to almost double by 2030<sup>58,59</sup>. DM is a leading cause of death in North America and has placed considerable economic strain on health care systems with estimates of over 245 billion dollars in 2012<sup>58</sup>. There are two main types of DM: insulin-dependent (Type 1 DM) and noninsulin-dependent (T2D). Type 1 DM is usually an auto-immune disorder in which the immune system targets and destroys the pancreatic  $\beta$ -cells. In most cases the etiology of the auto-immune  $\beta$ -cells destruction is not known. Type 1 DM patients are unable to produce enough insulin, but often can effectively respond to it. In contrast, T2D is often preceded and characterized by a state of insulin resistance coupled with relative insulin insufficiency and relative  $\beta$ -cell deficiency or failure. The underlying feature of both types of DM is an inability to properly regulate blood glucose, which can result in cyclical or chronically elevated levels of glucose (i.e. hyperglycemia and high glucose variability). T2D is the most common form, accounting for approximately 90% of DM patients. DM has been

associated with many co-morbidities including cardiovascular disease, neuropathy, retinopathy and elevated risk and severity of infection<sup>60-62</sup>.

### **1.2.1 Diabetes and Infection**

Cohort studies in Canada, Australia and Denmark have found that people with diabetes are at a two-fold greater risk of being hospitalized for infection than non-diabetic patients. People with diabetes have an overall greater risk for contracting most types of infections although the most common are skin and soft tissue, lower respiratory tract, urinary tract, and gastrointestinal<sup>58,63-65</sup>. Even more concerning is that once infected, diabetic patients also have increased severity of infection, including higher risk of mortality<sup>60,61,64,66,67</sup>. Recently, a retrospective study in the UK, found that diabetic patients had elevated risk of contracting and being hospitalized for all types of infection compared to healthy individuals, with bone and joint infections, sepsis, and meningitis amongst the highest. They also found that both Type 2 DM and Type 1 DM patients had approximately 2-fold increased incidence of gastrointestinal infections (incidence rate ratio of 1.70 and 2.04, respectively). This study looked at 361 family practices and tracked the hospital admission of patients from January 2008 to December 2015 and is one of the first clinical studies to separate patients by diabetic type when assessing infection risk<sup>68</sup>. The similar findings for both Type 1

and Type 2 DM groups highlights the possibility of a common underlying feature of DM that modifies risk and/or severity of bacterial infection. Elevated blood glucose or high glucose variability are intriguing possibilities as a common mechanism for infectious risk and outcomes. More recently, admission hyperglycemia, irrespective of diabetic status, has been linked with worsened clinical outcomes including morbidity, mortality, and increased duration of hospital or intensive care unit stays<sup>58,63,69</sup>. For every 1 mmol increase in blood glucose, infection risk is increased by 6-10% and mortality is increased by 33%<sup>66,70</sup>.

One of the earliest cases to identify diabetes as a risk factor for severity of infection was during an enteric infection via a foodborne nosocomial outbreak of *Salmonella enteritidis*<sup>71</sup>. However, since then, most studies have looked at how diabetes impact lower respiratory tract, kidney, and soft tissue infections, but little is known about enteric infections.

Separating the specific physiological factors that cause an increased risk or severity of infection has been difficult. DM is often characterized by immune dysfunction, microvascular alterations and tissue damage<sup>63</sup>. In addition, T2D is strongly linked with obesity, and obesity-induced inflammation is difficult to separate from changes in glycemia, insulin resistance, and other endocrine or immune features inherent to the diabetes-obesity connection. It is also difficult

to discern the effect of diet, which may be particularly relevant to enteric infections given that food can directly interact with enteric pathogens and mucosal defence mechanisms in the gut.

Many of the underlying factors and mechanisms that underpin the relationship between infection, metabolism, and immunity are still poorly defined. Therefore, we aimed to determine how obesity, nutrient excess, different macronutrients or dietary components, and regulation of blood glucose alter the severity, kinetics, and resolution of enteric infection. A primary goal of this thesis is to elucidate the impact of hyperglycemia on enteric infections and to segregate its effects from obesity, a commonly associated confounding variable. Another key goal is to determine if specific dietary components alter the host response to enteric infection. This thesis aims to define these host and dietary factors across multiple models of bacterial infection, including acute diarrhea-causing bacteria and pathogens that can promote chronic infectious colitis in mice.

### **1.3 Intestinal health and maintenance**

The gastrointestinal tract is an integral metabolic site where microbes, immunity, and dietary factors directly interact. The etiology and consequences of impaired intestinal barrier function that is associated with obesity remains

poorly characterized. It is not clear what aspect of the molecular consequences of obesity, if any, contribute to the specific mechanisms of a “leaky gut”. The intestine has a plethora of homeostatic and defence mechanisms to maintain a commensal relationship between the gut-resident microbes and the host. The gastrointestinal tract provides protection from invasive microbes, but it must balance this task with nutrient absorption, and excretion of waste. The intestinal tract is divided into two major compartments, the small (duodenum, jejunum, and ileum) and large (cecum and colon) intestine. The epithelium is arranged into invaginations, known as crypts, and protrusions, known as villi, to increase surface area for nutrient absorption<sup>72-74</sup>. The villi structures are absent in the colon and are replaced by flat sheets of epithelial cells. The primary function of the small intestine is nutrient absorption while the large intestine is responsible for a majority of water absorption from fecal matter. Perturbations in the large intestine, such as those that occur during infectious colitis, can lead to diarrhea. Rodent models are increasingly used for the study of intestinal function and the gut microbiota due to similarities in anatomy and physiology. A major difference between the gastrointestinal tract of humans and mice is the relative size of the cecum, which relative to body mass/size is much larger in mice. A large proportion of fermentation occurs in the cecum and proximal colon of mice whereas the cecum of humans is relatively small and has no known function<sup>75,76</sup>. The murine colon is relatively smooth and lacks any segmentation whereas the

human colon is compartmentalized into haustra with transverse folds present throughout the whole tissue<sup>75</sup>. There are also differences in intestinal cell distribution with goblet cells between humans and mice since goblet cells are abundant from the cecum to rectum in humans but only abundant in the proximal colon of mice<sup>75</sup>.

The intestinal lining is renewed every 3-5 days where tightly regulated, compartmentalized canonical Wnt/ $\beta$ -catenin signalling directs proliferation of intestinal crypt progenitor cells and cellular differentiation<sup>73,77,78</sup>. The intestinal epithelium is composed of absorptive (enterocyte) and secretory (goblet, enteroendocrine, and Paneth cells) cell lineages which originate from a pool of intestinal stem cells (ISCs) at the base of the crypts. Secretory cells, especially goblet and Paneth cells, are important for protection against pathogen invasion. Paneth cells secrete antimicrobial peptides while goblet cells secrete mucins<sup>79,80</sup>. These mucins form the mucous layers on the surface of the epithelium that acts as the primary physical barrier between the luminal bacterial populations and the intestinal epithelium. In the colon, there is an inner and outer mucous layer while the small intestine only contains a single layer. The initial mucous layer is densely packed and adherent to the surface epithelium. It contains a variety of antimicrobial peptides and secreted immune factors, such as REGIII $\beta$  and immunoglobulin (Ig) A. The outer layer is more loosely arranged and provides a habitat for endogenous bacterial populations<sup>80,81</sup>.

All intestinal epithelial cell populations are maintained through a dynamic balance of cell proliferation (Wnt-signalling) and differentiation (Notch) signals. The ISCs give rise to highly proliferative progenitors known as transit-amplifying (TA) cells. As the TA cells rise through the crypt, they receive differentiation signals. Fully mature intestinal epithelium cells (IECs) are found at the villus tip and are eventually shed to counterbalance the continual renewal and proliferation of crypt cells<sup>78,82</sup>. Paneth cells are an exception to this process as during differentiation, they migrate to the base of the crypt<sup>79,83</sup>.

Wnt-signalling is imperative for the initiation and sustainment of this process. There are currently 19 Wnt ligand genes identified in human and murine genomes<sup>84</sup>. The Wnt ligands initiate the Wnt-signalling cascade by binding to two specific co-receptors: the frizzled (Fzd) and low-density lipoprotein-related receptors (LRP)<sup>73,85,86</sup>. This will lead to the nuclear translocation of  $\beta$ -catenin from the cytoplasm and the transcription of developmental and proliferative genes<sup>87</sup>. In the absence of Wnt ligands, cytoplasmic  $\beta$ -catenin is recruited to a destruction complex composed of several components including Axin, adenomatous polyposis coli (APC) and two kinases, casein kinase-1 (CK1) and glycogen synthase kinase-3 (GSK-3). These kinases phosphorylate  $\beta$ -catenin, which targets it for ubiquitination and degradation<sup>77,88</sup>.

When Wnt ligands are present, they bind with Fzd and LRP causing phosphorylation of LRP. This induces a conformational change that recruits the

destruction complex to the membrane. Subsequent newly synthesized  $\beta$ -catenin are no longer ubiquitinated and translocate to the nucleus to bind with T-cell factor (TCF)/lymphoid enhancer factor (LEF). One agonist of Wnt-signalling is the roof plate-specific spondin (R-spondin or Rspod) family which binds to leucine rich repeat containing G protein-coupled receptors (LGRs) and stabilizes the Wnt/Fzd/LRP complex by inactivating Wnt antagonists<sup>89–92</sup>.

Notch signalling is another important component in maintaining intestinal homeostasis. It plays a critical role in the binary intestinal cell fate decision between secretory and absorptive lineages. A downstream Notch target gene, *Hes1*, skews differentiation towards the absorptive cell lineage and is a known repressor of *Math1*, a transcription factor for secretory cell lineage genes. Deletion of *Hes1* results in suppressed proliferation and complete differentiation of intestinal stem cells into secretory cells<sup>93–96</sup>. It has also been reported to be essential for stem cell maintenance, as inhibition of Notch signalling results in the depletion of ISCs and upregulated Wnt signalling<sup>95,97</sup>. In fact, Wnt and Notch signalling are both indispensable for maintaining the stemness of the multipotent cells in the intestinal crypt base, as deletion or blockade of either pathway results in the loss of Lgr5+ (a specific intestinal stem cell marker) expressing cells (**Figure 1**)<sup>78,98,99</sup>.

Bacteria can influence the proliferation and differentiation of intestinal cells. Secretory cell lineage differentiation has been reported to be influenced by

bacterial detection through Myd88-signalling, an adaptor protein of toll-like receptor responses<sup>100,101</sup>. This is one example of how bacterial components can engage host immune receptors in the gut to modify response involved in intestinal health and function.

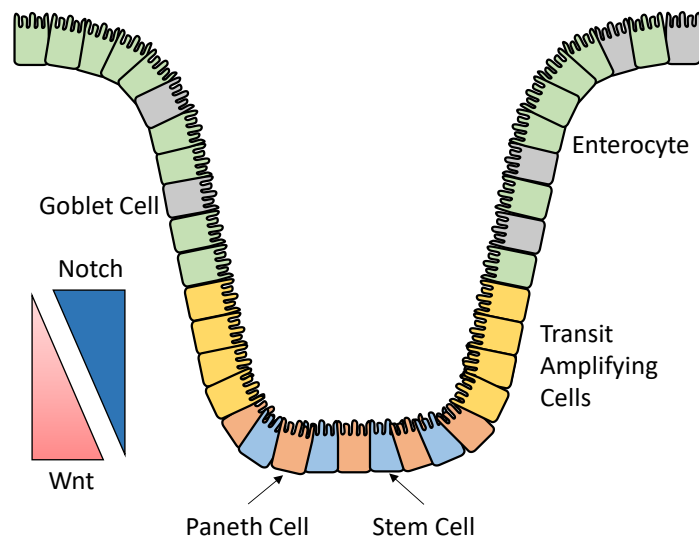


**Figure 1: Simplified schematic of the crosstalk between Wnt and Notch signaling in intestinal epithelial cell differentiation.**

### 1.3.1 The Intestinal Microbiota

In addition to its role in nutrient absorption, the intestinal tract is also home to an intricate bacterial ecosystem. Recent estimates place the number of bacteria to host cells at a 1:1 ratio in humans<sup>102</sup>. These bacteria are commonly found on the intestinal lumen and a majority of the bacteria are referred to as commensals due to their ability to reside on the lumen without damaging the host. Many of these bacteria can process macro- and micro-nutrients and produce metabolites that host cannot synthesize alone. SCFAs are important metabolic signalling molecules produced through microbial digestion of dietary fibres. Certain SCFAs can mitigate the metabolic effects of diet-induced obesity, protect from pathogens, and regulate intestinal barrier integrity<sup>31,103–105</sup>. The primary SCFAs produced by the microbiota are acetate, butyrate, and propionate, which are all absorbable by the host. Microbially derived butyrate is a major nutrient and energy source for colonocytes.

The microbiota plays a role in energy balance that is relevant to metabolic disease evidenced by the fact that germ-free mice are protected from diet-induced obesity. Colonization of germ-free mice confers weight gain and increased adiposity, despite reduced food intake implicating a role for intestinal nutrient extraction facilitated by microbes<sup>29</sup>. In addition, aspects of metabolic disease including adiposity and glucose tolerance, are transmissible via the microbiota<sup>29,33,106</sup>. The intestinal microbiota is also important for protection from

pathogens and immune system development. Commensal bacteria offer colonization resistance through a variety of indirect and direct methods in the gut. Commensal bacteria can colonize specific environmental niches and provide a physical barrier against pathogen colonization. Commensal bacteria can also compete with pathogens for nutrients. For example, the commensal *Bacteroides thetaiotaomicron* is known to compete with pathogenic *Citrobacter rodentium* in the colon by consuming plant-derived monosaccharides that are required for growth<sup>107</sup>. Many bacterial species can also directly inhibit bacterial growth and colonization from other bacterial species (including pathogens) through the secretion of antimicrobials. *Bacillus thuringiensis* from human feces was found to produce a bacteriocin which targets *Clostridium difficile* while some *Bifidobacterium* species can inhibit bacterial growth by secreting antimicrobial acids and peptides, such as defensins, calthelidins<sup>108–110</sup>. The microbiota can also confer colonization resistance indirectly by stimulating the immune system. *B. thetaiotaomicron* colonization has been shown to promote the expression of host antimicrobial peptides, RegIII $\gamma$  and RegIII $\beta$ , which disrupt the cell membrane by forming a membrane-penetrating pore<sup>111,112</sup>.

The close interaction of the microbiota and intestinal immune system helps control the location, amount, and composition of bacterial populations thereby promoting immune tolerance. It is clear that the microbiota (as a whole) plays an important role in intestinal immune development. Germ-free mice are

known to have deficiencies in gut-associated lymphoid tissue development, reduced antibody production, fewer mesenteric lymph nodes and Peyer's patches, and altered intestinal morphology and cell turnover. However, all these features are reversible within a few weeks of exposure to specific pathogen-free, environmental microbes (i.e. conventionalization)<sup>113-115</sup>. It is clear that the microbiota are essential symbionts for metabolism and immunity. Intestinal dysbiosis during obesity is positioned to alter the susceptibility and outcomes of enteric infections. Despite recent interest in the immunometabolism of microbiota and metabolic disease, it is not clear how specific components of diets that promote metabolic disease or specific metabolic disease characteristics influence risk or severity of enteric infection.

### **1.3.2 Obesity and Intestinal Health**

Concurrent with the dysbiosis that occurs in obesity, there is also a change in the intestinal immune response. In contrast to the elevation in systemic inflammation, certain immune responses in specific segments of the intestine can be lower during obesity. In murine models of obesity, Th17 responses were suppressed in the ileum and colon after as little as 30 days of high fat feeding<sup>116,117</sup>. This reduction was related to decreases in specific bacterial species including *Porphyromonas gingivalis*, which is known to induce IL-17 production<sup>117,118</sup>. High fat feeding has also been reported to reduce IL-22

levels in the colon<sup>119,120</sup>. Diet-induced obese mice exhibited lower percentages of IL-22-producing innate lymphoid cells compared to lean mice, which correlated with impaired intestinal barrier integrity and consequent increases in circulating microbial-derived endotoxin<sup>120</sup>. This raises an interesting concept where diet or obesity can suppress immune responses in the intestine, compromise gut barrier function, which then promotes penetration of microbial products that can increase systemic or host tissue inflammation. The timing and causality of intestinal microbes with these compartmentalized immunometabolism responses is important to understand and may alter the risk or severity of enteric infection of the host<sup>116,121</sup>.

IL-22 is an important cytokine for maintaining intestinal barrier integrity by regulating tissue repair and promoting antimicrobial release during acute inflammation. IL-22 is predominantly expressed by T<sub>H</sub>17 and T<sub>H</sub>22 cells and is regulated by the cytokines, IL-23 and IL-12. IL-22 is a unique cytokine as its principal actions are exerted on epithelial cells, as these are the main cell types that express the IL-22 receptor<sup>122–125</sup>. In conjunction with its pro-inflammatory role, IL-22 has also been directly implicated in metabolic regulation<sup>125–127</sup>.

Numerous studies have emerged regarding the potential for exogenous IL-22 as a treatment for obesity. IL-22 has been shown to lower blood glucose, improve glycemic control, reduce liver lipogenic expression, and reduce oxidative and ER

stress, all metabolic improvements that have been associated with improved intestinal barrier function<sup>119,125,128,129</sup>.

Obesity has also been associated with alterations to intestinal structure. Along with the characteristic increase in intestinal permeability, obese humans have been reported to have increased enterocyte mass, which may be the result of increased cellular proliferation rates<sup>130–132</sup>. This process appears to be influenced by diet or nutrient source as caloric restriction is sufficient to decrease the colonic epithelial proliferation rate in obese humans independent of weight loss<sup>133</sup>. Studies in diet-induced obese mice have shown site specific downregulation of Lgr5 in the proximal colon and decreased number of goblet cells compared to mice fed a normal chow diet<sup>134,135</sup>.

### **1.3.3 Diabetes and Wnt Signalling**

Diabetic enteropathy is a common symptom that has been receiving renewed interest as diabetes has recently been linked with an increased risk of colon cancer<sup>136–138</sup>. A connection between diabetes and Wnt signalling has been identified, but it is not yet clear which aspect of diabetes is the potential mechanism linking diabetes, Wnt, and intestinal cancer<sup>136,139</sup>. Studies in diabetic rats have reported increased intestinal proliferation of epithelial cells of the small intestine<sup>140–142</sup>. Streptozotocin-induced diabetic mice have been shown to

have an increase in Lgr5+ cells and increased proliferative rate, which was mitigated with exogenous insulin treatment<sup>143</sup>. This result is interesting since either lowering of glucose mitigated crypt progenitor proliferation or simply provision of insulin suppressed crypt progenitor proliferation. In either case high blood glucose or lack of insulin was the probable causative factor for excessive proliferation of crypt progenitor cells<sup>143</sup>. Glucose has been proposed to influence Wnt signalling through multiple pathways, including cAMP/PKA and increased  $\beta$ -catenin acetylation<sup>144,145</sup>. In an *in vitro* model, high glucose levels were shown to promote Wnt signalling by suppressing the expression of Wnt antagonist, DKK4<sup>146</sup>. Diabetic mouse models have also implicated hyperglycemia with modulating Notch signalling. Diabetic mice have a bias towards Paneth cell differentiation and this was correlated with a downregulation of *Hes1* expression<sup>147</sup>. A recent study comparing a ketogenic diet (that is very low in carbohydrates such as glucose) with a glucose-supplemented diet found that a diet higher in glucose suppressed Notch signalling and skewed differentiation towards secretory cell lines<sup>148</sup>. These data position blood glucose as a key modifier of intestinal cell proliferation and warrant investigation of this relationship in enteric infection during diabetes. Understanding the altered intestinal environment such as changes in the balance of Wnt and Notch signalling as a result of diabetes and metabolic and microbial interactions may be

key to identifying risk factors for enteric infection and identifying potential therapeutic targets.

#### **1.4 *Citrobacter rodentium*: A non-invasive murine model of enteric infection**

*Citrobacter rodentium* is a mouse pathogen related to enteropathogenic and enterohaemorrhagic *Escherichia coli*, which are common diarrhea-causing enteric infections in humans. *C. rodentium* infections are characterized by intestinal crypt hyperplasia, goblet cell depletion and enterocyte shedding. It is a self-limiting infection that primarily localizes in the colon, causes acute diarrhea and is cleared within 2-3 weeks<sup>149–151</sup>. These pathogenic bacteria adhere to the epithelial surface and cause attaching and effacing (A/E) lesions. *Citrobacter rodentium* and these types of pathogens bind to the host enterocyte through an outer cell membrane protein, intimin, which can bind to certain host receptors or the bacterially derived translocated intimin receptor, which are both embedded in the host cell surface<sup>150–153</sup>. *C. rodentium* is a suitable model for studying host-pathogen interactions *in vivo* under physiological conditions, while still allowing for the manipulation of the pathogenic bacteria and/or the host (i.e. mouse). Combined these features of the model allows for investigation of the mechanisms of action of enteric infection<sup>149</sup>. *C. rodentium* infection causes diarrhea but is not fatal in most mouse strains. Only FVB/N and C3H/HeJ mice are susceptible to increased levels of mortality during *C. rodentium* infection

<sup>154,155</sup>. Studies have shown that these “susceptible” mouse strains succumb to *C. rodentium* infection due to excessive diarrhea rooted in severe dehydration and impaired water reabsorption. It was later discovered that this is the result of abhorrent Wnt-signalling<sup>154–156</sup>. These mouse strains that are susceptible to fatal diarrhea have a genetic difference in the *Cri1* locus, which causes abundant and continuous expression of Rspodin-2. Rspodin-2 is a co-activator of canonical Wnt-signalling and promotes  $\beta$ -catenin activity. This excessive activity causes over proliferation and migration of immature enterocytes in the colonic crypts that do not receive the proper differentiation signals. This results in malabsorptive enterocytes or defects in secretory Paneth cells. Ultimately, in the context of *C. rodentium* infection, this culminates as increased mortality due to poor water retention<sup>156</sup>.

Interestingly, a recent study found that leptin-deficient C57BL/6 (*ob/ob*<sup>-/-</sup>, OB) mice have increased mortality during *C. rodentium* infection<sup>157</sup>. Leptin is an endocrine hormone that signals for satiety among other immunological functions<sup>158–160</sup>. OB mice lack function leptin and hence are hyperphagic (i.e. overeat) and develop severe obesity. It is known that OB mice have reduced IL-22 expression in the colon and exogenous IL-22 supplementation rescued these mice from mortality during *C. rodentium* infection<sup>157</sup>. It is also known that IL-22 deficient mice have increased mortality during *C. rodentium* infection. However, a study by *Aychek et al.* showed that mice deficient in *il-23* but not *il-12(p40)*

were susceptible to infection, with complete mortality of *il-23* deficient mice by day 12 post infection, despite similarly reduced levels of IL-22<sup>161</sup>. This result implies that IL-22 deficiency may not be sufficient to promote mortality during *C. rodentium* infection in OB mice, but perhaps the metabolic effects of exogenous IL-22 treatment (i.e. blood glucose reduction) may prevent infection-induced mortality in these OB mice. Another outstanding question is the role of Wnt signalling, which has been implicated in *C. rodentium*-induced mortality, but it is not yet clear how Wnt signals could connect changes in diet and/or aspects of obesity or diabetes to outcomes from enteric infection. It is possible that *C. rodentium*-induced mortality of OB mice or other models of diabetes is associated with Wnt signalling and whether exogenous IL-22 treatment can directly or indirectly impact this pathway through its blood glucose lowering effects. These are key questions addressed in this thesis.

### **1.5 Adherent-invasive *Escherichia coli*: a model of enteric infection**

Adherent-invasive *E. coli* (AIEC) is associated with ileal lesions of Crohn's disease (CD) patients. *E. coli* have been shown to be enriched in CD patients<sup>162-164</sup>. Culturing of *E. coli* isolates from CD patients found that many isolates had unusual adherent and invasive phenotypes. Interestingly, these isolates did not possess toxins or adhesins typically found in pathogenic *E. coli* and lacked a distinctive genetic signature. Thus, these isolates were collectively called

adherent-invasive *E. coli* (AIEC) due to their ability to penetrate the mucosa, adhere and invade epithelial cells, invade macrophages, and stimulate inflammation<sup>163,165–168</sup>. AIEC is considered a pathobiont, a usually benign pathogen that is present in healthy people and CD patients that will rapidly expand during a perturbation, such as those caused by changes in diet or antibiotic treatment<sup>162,168</sup>. Research has focused on the factors promoting colonization and triggers of AIEC pathogenicity. Antibiotic use can potentiate AIEC colonization through dysbiosis and the stimulation of inflammation in the local gut environment<sup>169,170</sup>. A recent study by *Oberc et al.* found that vancomycin use induced mild cecal inflammation and upregulation of *Nos2*<sup>170</sup>. This resulted in the increase of inflammation-derived metabolites (such as nitrates, glucarate, and galactarate) AIEC could selectively use as substrates to expand within the gut. AIEC mutants deficient in metabolic genes for these alternative carbon sources demonstrating similar *in vitro* fitness in nutrient rich media, but impaired competitiveness in antibiotic pretreated mice compared to wild-type AIEC NRG857c strain<sup>170</sup>. These results support the idea that antibiotic treatment is a perturbation that promotes AIEC expansion through the metabolism of alternate carbon sources. This is further supported by the findings of *Spees et al.* showing that streptomycin treatment resulted in inflammation and an upregulation of nitrate metabolites, that supported *E. coli* growth *in vivo*, in the colon<sup>169</sup>. AIEC can also use acetate as an alternative carbon source, which was demonstrated to

be a common host adaptation of many AIEC strains isolated from both chronic long-term murine infection models and human CD patients<sup>171</sup>. In addition to its ability to thrive in an inflammatory environment, AIEC can successfully evade host antimicrobial responses and stimulate further inflammation through invasion of host cells. A study by *McPhee et al.* showed that AIEC contained multiple antimicrobial peptide resistance genes and that loss of these genes impaired colonization and fitness<sup>172</sup>. Due to the lack of a distinct genetic signature and the breadth of AIEC strains, the triggers and mechanism of pathogenicity along with host resolution, have not been well-defined.

## **1.6 Purpose and Goals of the Dissertation**

Obesity and T2D are highly prevalent, interlinked diseases that share many serious comorbidities. Both obesity and T2D have been characterized by altered immune responses, poor intestinal barrier integrity, and intestinal dysbiosis of commensal bacteria. These features play a role in the etiology of metabolic disease, but their impact on enteric infection has not been well-defined. The gut is a key modulator of metabolic health and a large site of immunologic activity. The association between features of diabetes and obesity makes it difficult to segregate the individual effects of each disease on outcomes of enteric infection. A further confounder is diet, where aspects of obesogenic diets can promote diabetes progression. In particular, obesogenic diets are a

commonly used model to study obesity and prediabetes in rodents, but the impact of changes in the macronutrient balance of the diet or specific components of diet on outcomes of enteric infection is poorly understood. The effects should be studied since aspects of the “Western” diet (high fat and sugar, low fibre) can independently impact microbial composition and intestinal health<sup>15,22,30,54,173,174</sup>. The purpose of this study is to elucidate the impact that hyperglycemia, obesity, and diet have on the outcomes of enteric infection.

The hypotheses of this thesis are:

1. High blood glucose worsens the outcomes of enteric infection, independent of obesity in mice
2. High fat content in the diet worsens the outcomes of enteric infection in mice.
3. Host metabolic disease factors (high glucose) and diet (high fat ingestion) will increase intestinal burden of intestinal pathogens in mice

The specific aims of this thesis are:

1. Determine if hyperglycemia, independent of obesity, worsens outcomes of enteric infection during *C. rodentium* infection in mice
2. Determine if IL-22 immunity or Wnt-mediated intestinal homeostasis is involved in the link between hyperglycemia and outcomes of *C. rodentium* infection in mice

3. Determine if obesity promotes adherent-invasive *Escherichia coli* expansion in the intestine of mice
4. Determine which components of an obesogenic diet promote adherent-invasive *Escherichia coli* expansion in the intestine of mice

## **Chapter 2 – Materials and Methods**

## 2.1 Animal models

Breeding and experimental procedures were carried out in accordance with the Canadian Council on Animal Care and approved by the Animal Review Ethics Board (AREB) at McMaster University under Animal Use Protocol #16-06-02. For all studies, mice were 8-10 weeks old before dietary intervention or experiment initiation. Animals were maintained on a 12-hour light/dark cycle, and experiments were performed on multiple cohorts of mice born from different parents at different times of the year. Except where indicated, male mice were used for experiments. Wild-type (WT) C57BL/6J, Akita<sup>+/-</sup> (B6.Ins2 <Akita>/J), and *ob/ob*<sup>-/-</sup> (B6.Cg-Lep<sub>ob</sub>/J) mice were obtained from The Jackson Laboratory (Bar Harbor, ME, USA ; strain 000664, 003548, and 000632, respectively) or from our in-house colony established from C57BL/6J or Akita<sup>+/-</sup> mice received from The Jackson Laboratory. All animals were maintained in a specific pathogen-free facility at McMaster University. Animals were fed a control diet (17% kcal from fat, 29% kcal from protein, 54% kcal from carbohydrate; cat# 8640 Teklad 22/5, Envigo) unless otherwise specified.

## 2.2 Diet studies

For the long-term feeding model, 8-10-week-old C57BL/6J mice were fed 60% high fat, sucrose-matched control, or low fibre control diet (D12492 D12450J, D12450K, respectively; Research Diets) for 16 weeks prior to enteric infection.

For the short-term model, C57BL/6J mice were fed 60% high fat diet, a sucrose-matched control diet, or low fibre control diet (D12492 D12450J, D12450K, respectively; Research Diets) one day prior to infection. For intervention study, 8-10-week-old mice were fed 60% high fat diet (D12492; Research Diets) for 16 weeks prior to initiating a custom diet containing 60% calories from fat that is supplemented with 200 g cellulose (Research Diets) one day prior to infection. For prevention study, 8-10-week-old mice were fed 60% high fat diet (D12492; Research Diets) or custom diet containing 60% calories from fat that is supplemented with 200 g cellulose for 16 weeks prior to infection.

### **2.3 Intraperitoneal glucose tolerance test**

Intraperitoneal glucose tolerance test was performed in 6-hour fasted, conscious mice. D-glucose (0.75 g/kg; Sigma-Aldrich) used is indicated in each figure caption. Blood glucose was measured by tail vein blood sampling using a handheld glucometer (Roche Accu-Check Performa). Area under the curve of blood glucose versus time (with baseline Y set to 0) was calculated using GraphPad Prism 6 software.

#### **2.4 *In vivo Citrobacter rodentium* infection**

*C. rodentium* strain DBS100 was grown overnight in Luria-Bertani (LB) medium shaking at 37°C. Mice were infected by oral gavage of 0.1 ml of phosphate buffered saline solution containing  $\sim 2.5 \times 10^8$  colony forming units (CFUs) of *C. rodentium*. The infectious dose was verified by plating of serial dilutions on brilliant green agar. Body mass and random fed blood glucose levels were measured regularly throughout infection. Fecal pellets were weighed, homogenised in 1 mL PBS (Retsch), serially diluted, and plated onto brilliant agar plates. Plates were incubated overnight at 37°C and colonies were counted to determine colony-forming units (cfu) per gram of feces.

For survival analysis, animals were monitored daily and moribund animals were euthanized by cervical dislocation when clinical endpoints were achieved, according to the AREB standard operating procedures. Upon euthanization, colons were isolated and processed for histological examination, immunostaining, snap-frozen for RNA/protein isolation or plated for bacterial burden. Liver and spleen segments were isolated and plated on brilliant green agar for bacterial burdens. Blood was taken through cardiac puncture or facial bleeding. Blood samples were centrifuged at 7500 rpm at 4°C for 5 minutes to obtain serum for cytokine analysis or were sent to IDEXX Canada for analysis of

dehydration markers on an AU5800 Series Clinical Chemistry Analyzer (Beckman Coulter).

In some experiments, mice were given daily subcutaneous injected with Ringer's Solution (1ml, Fisher Life Sciences) from D3 to D14 after infection. For treatment with LGK-974 (AdooQ Bioscience), mice were orally gavaged with LGK-974 (3 mg/kg) suspended in 0.5% Tween-80, 0.5% methylcellulose from D3 to D14 post infection. For mice treated with empagliflozin, mice were orally gavaged twice daily with Empagliflozin (150 mg/kg).

## **2.5 Insulin pellet insertion**

Mice were anesthetized with isofluorane, a small subcutaneous incision was made with an 18.5-gauge needle and two insulin pellets (LinShin Inc., Toronto, Canada) were inserted. Sham surgery animals were prepared similarly, but pellet was inserted. After surgery, mice were individually housed and monitored daily.

## **2.6 IL-22 treatment**

Mice were injected intraperitoneally with IL-22Fc or IgG control (150 mg; Genentech, San Francisco, USA) three times a week beginning one week prior to infection and throughout the course of infection.

### **2.7 *In vivo* adherent-invasive *Escherichia coli* infection**

AIEC strain NRG857c (serotype O83:H1) was grown overnight in Luria-Bertani (LB) medium shaking at 37°C. Mice were pretreated with streptomycin (2 mg/kg) by oral gavage one day prior to infection. Mice were infected by oral gavage of 0.1 ml of phosphate buffered saline solution containing  $\sim 2 \times 10^9$  colony forming units (CFUs) of AIEC. The infectious dose was verified by plating of serial dilutions on LB agar supplemented with ampicillin and chloramphenicol. Body mass was measured throughout infection. Fecal pellets were weighed, homogenised (Retsch) in 1 mL PBS, serially diluted, and plated onto LB agar plates supplemented with ampicillin (100  $\mu\text{g}/\text{ml}$ ) and chloramphenicol (34  $\mu\text{g}/\text{ml}$ ). Intestinal tissues were harvested into cold PBS at necropsy and were flushed with PBS to remove luminal contents, homogenised with a sterile metal bead, and plated in the same manner as feces. Plates were incubated overnight at 37°C and colonies were counted to determine colony-forming units (cfu) per gram of feces or tissue.

### **2.8 Gene expression analyses**

Total ribonucleic acid (RNA) was obtained from approximately 50 mg of indicated mouse tissues via mechanical homogenization in TRIzol reagent (Cat# 15596018, Thermo Fisher Scientific) at 4.5 meters/second for 30 seconds using a

FastPrep-24 tissue homogenizer (MP Biomedicals) and glass beads, followed by phenol-chloroform extraction. Tissue homogenate was centrifuged at 12 000 x g for 10 minutes at 4°C, the supernatant was added to a new tube containing chloroform at half the volume of supernatant, and the solution was mixed and centrifuged at 12 000 x g for 10 minutes at 4°C. The aqueous upper phase was then added to an equal volume of isopropanol, mixed, incubated at room temperature for 20 minutes, and centrifuged at 12 000 x g for 10 minutes at 4°C. Precipitated RNA pellets were washed twice with a 75% ethanol/ultrapure water solution. RNA pellets were suspended in ultrapure water and incubated at 55°C for 15 minutes. Subsequently, cDNA was prepared using 1000 ng total RNA. Briefly, RNA was treated with DNase I (Cat# 18068015, Thermo Fisher Scientific) and incubated at room temperature for 15 minutes. Random hexamer primers and dNTPs were added to RNA. Solutions were incubated at 95°C for 10 minutes to inactivate DNase, followed by incubation at 55°C for 10 minutes to allow primers to anneal RNA strands. cDNA was prepared by adding SuperScript III Reverse Transcriptase (Cat# 18080044, Thermo Fisher Scientific) to RNA-primer solutions, followed by incubation at 55°C for 50 minutes, and 70°C for 15 minutes. cDNA was diluted 1/25 with ultrapure water. Transcript expression was measured using TaqMan Gene Expression Assays (Thermo Fisher Scientific) with AmpliTaq Gold DNA polymerase (Cat# 4311818, Thermo Fisher Scientific). Briefly, cDNA was incubated with polymerase and TaqMan assays and placed in a

Rotor-Gene Q real-time PCR cycler (QIAGEN). Samples completed 45 cycles of: incubation at 95°C for 5 seconds, and incubation at 58°C for 10 seconds. Target genes were compared to *Rplp0* housekeeping gene using the  $\Delta\Delta CT$  method. A list of all probes used in this thesis are provided in **Table 1**.

## **2.9 Cytokine quantification**

Tissues removed at necropsy on day 4 and 10 following infection *C. rodentium* and were washed with cRPMI (10% fetal bovine serum, 1% L-glutamine and 50 µg/mL gentamicin), cut into pieces, placed in 1 mL of cRPMI and incubated overnight at 37°C, 5% CO<sub>2</sub>. Supernatants were removed after incubation and levels of cytokines and chemokines were determined using the Mouse 32-Plex Discovery Assay by Eve Technologies (Calgary, AB).

## **2.10 Immunoblotting**

For protein analysis, colon tissues were lysed in ice-cold lysis buffer containing 250 mM NaCl, 5 mM EDTA, 0.5% deoxycholate, 0.1% SDS, 1% NP40, and 50 mM Tris-HCl (pH 8.0). Protein concentration was measured using a bicinchoninic acid (BCA) assay kit (Pierce, Rockford, IL, USA). Western blotting was performed as described previously<sup>175</sup>. Briefly, lysates were denatured, separated by SDS-PAGE, transferred to polyvinylidene fluoride (PVDF) membranes. Membranes were

blocked and immunoblotted with  $\beta$ -actin (1:5000) and non-phosphorylated  $\beta$ -catenin (1:2000) antibodies.

**Table 1: List of TaqMan probes used for gene expression analysis.**

Probe	Target	Assay ID
Rplp0	Ribosomal protein, large, P0	Mm00725448_s1
Il17a	Interleukin 17a	Mm00439618_m1
Il22	Interleukin 22	Mm01226722_g1
Il23a	Interleukin 23, alpha subunit p19	Mm00518984_m1
Rspo1	R-spondin 1	Mm00507077_m1
Rspo2	R-spondin 2	Mm00555790_m1
Rspo3	R-spondin 3	Mm01188251_m1

\*All probes were ordered from ThermoFisher Scientific.

### 2.11 FITC-dextran assay

On the day of the assay, 4 kDa fluorescein isothiocyanate (FITC)-dextran was dissolved in phosphate buffered saline (PBS) to a concentration of 80 mg/ml.

Mice were fasted for 4 hours prior to gavage with 150  $\mu$ l FITC-dextran. Tail vein

blood was collected 4 hours after injection, centrifuged at 1,000 x g for 10 min at 4°C. Serum was collected and fluorescence was quantified at an excitation wavelength of 485 nm and emission wavelength of 535 nm.

### **2.12 TLR4 assay**

HEK-Blue™ mTLR4 (InvivoGen, San Diego, CA) cells were cultured in DMEM medium supplemented with 10% FBS and HEK-Blue™ Selection (InvivoGen) at 37 °C according to the supplier's instructions. To determine TLR4 activation,  $2 \times 10^4$  HEK-Blue™ mTLR4 cells were suspended in 200 µL/well HEK-Blue™ detection medium adding 4 µL/well testing blood serum (2% v/v), and plated in a 96-well plate for 8 h at 37 °C. The production of secreted SEAP was assessed by reading the absorbance at 620 nm (Molecular Devices, San Jose, CA).

### **2.13 Histological evaluation and immunohistochemical (IHC) analysis**

At day 7 and 10 post infection, the distal colon was collected and fixed in buffered 10% formalin for 96 hours, paraffin-embedded, sectioned into 5-µm slices and then stained with haematoxylin and eosin (H&E) by Histology Services (McMaster University, Hamilton, ON). A minimum of 5 views per section were analyzed for each sample and scored according to previously defined criteria<sup>176</sup>. Crypt length measurements and goblet cell quantification were done using

ImageJ software on a Nikon microscope with at least five well-oriented crypts measured per field. Pathology scoring was scored according to the following criteria (scores are given in parentheses after each category):

i) **Lumen.** Necrotic epithelial cells (empty, 0; scant, 1; moderate, 2; dense, 3), polymorphonuclear (PMN) leukocytes (empty, 0; scant, 1; moderate, 2; dense, 3), and lymphocytes (empty, 0; scant, 1; moderate, 2; dense, 3).

ii) **Surface epithelium.** Epithelial sloughing (yes, 1), desquamation (patchy, 1; diffuse, 2), presence of PMN leukocytes (yes, 1), ulceration (yes, 1), and lymphocyte infiltration (scant, 0; moderate, 1; severe, 2).

iii) **Mucosa.** Loss of crypts (rare, <15%, 1; moderate, 15-20%, 2; abundant, >50%, 3), monocytic infiltration (1 small aggregate, 0; >1 aggregate, 1; large aggregates plus single cells, 2), crypt hyperplasia (yes, 1), loss of goblet cells (yes, 1), presence of granulation tissue (yes, 1), and lymphocytic infiltration (scant, <10 cells, 0; moderate, 50-100 cells, 1; dense, >100 cells, 2).

iv) **Submucosa.** Mononuclear cell infiltrate (1 small aggregate, 0; >1 aggregate, 1; large aggregates plus single cells, 2), PMN leukocyte infiltrate (no extravascular PMNs, 0; single PMNs, 1; PMN aggregates, 2), lymphocyte infiltrate (scant, <10 aggregates, 0; moderate, <50 aggregates, 1; severe, >50 aggregates, 2), and edema (mild, 1; moderate, 2; severe, 3).

#### **2.14 Immunofluorescence staining**

Colon samples were extensively washed and fixed and 4% paraformaldehyde. Samples were washed, paraffin-embedded and sectioned. Paraffin sections were de-paraffinized and antigen-retrieved in 10 mM sodium citrate, pH 6. Samples were incubated in PBS containing 20% (v/v) normal horse serum and 0.2% (v/v) Triton X-100 for 1 h; and then incubated over-night with mouse anti-Ki-67 (Cell Signaling 9449) and Alexa fluor-350 phalloidin (Invitrogen A22281) primary antibodies. Sections were washed and incubated for 1 hour with Alexa 488-conjugated donkey anti-mouse antibody and imaged on a Nikon A1+ confocal system attached to a TiEclipse inverted microscope.

#### **2.15 Statistical analysis**

Data was assessed for normal distribution using the D'Agostino-Pearson normality test. For normally distributed data sets, statistical significance was determined by unpaired two-tailed *t*-test, one-way ANOVA with Tukey post hoc multiple comparison analyses, or two-way ANOVA with Sidak post hoc multiple comparison analyses. For non-normally distributed data sets, statistical significance was determined by Mann-Whitney *U* test or Kruskal-Wallis test. One-way ANOVA with Tukey post-test was performed using a 95% confidence interval to determine difference among infection groups. Kaplan-Meier survival curves were analyzed with the log-rank test. All analyses were performed using

Graph Prism 6.0 (GraphPad Software Inc. San Diego, CA). A P-value of 0.05 or less was considered significant.

## **Chapter 3 - Results**

### **3.1 Hyperglycemia, independent of obesity, worsens outcomes of enteric infections**

#### **3.1.1. Hyperglycemia predicts mortality during *C. rodentium* infection**

Data on the infectious risk in people with diabetes has been documented, with numerous studies reporting a two-fold or greater risk of contracting infection compared to people without diabetes<sup>69,177,178</sup>. However, the data linking obesity or increased adiposity and risk of enteric infection is not yet clear. As diabetes and obesity are positively correlated, the initial aim of this thesis was to parse out the effects of obesity and hyperglycemia on infectious colitis. To do so, we first tested obese mice that were discordant for blood glucose using leptin deficient C57BL/6J OB mice of different ages. OB mice have a mutation in the leptin gene. Leptin is an endocrine hormone responsible for neural (i.e. hypothalamic) control of appetite and energy expenditure. OB mice are leptin deficient, hyperphagic, hyperlipidemic, and hyperinsulinemic<sup>179,180</sup>. During the first 3-5 months of life, OB mice are hyperglycemic, but after this period, the blood glucose levels gradually drop with increasing age due to the expansion of insulin-producing pancreatic  $\beta$ -cells, which is thought to be a temporary compensatory increase in insulin secretion to compensate for obesity-induced insulin resistance<sup>179-182</sup>. It is important to note that although OB mice are insulin resistant, metabolic syndrome in these mice does not progress to complete  $\beta$ -cell destruction and unregulated diabetes in the time frame and ages of mice tested in this thesis<sup>179</sup>. An initial pilot experiment using 12- and 15-week-old OB

mice was conducted with former lab member Dr. Joseph McPhee to assess the kinetics of *C. rodentium* infection during obesity. Interestingly, after 14 days of infection we observed 100% mortality only in the 12-week-old OB group but no mortality in the 15-week-old OB group or WT control mice ( $p < 0.05$ ; **Fig. 2A**). In this initial experiment we tested OB mice that had similar body masses (data not shown), but only differed in age at the time of the infection. Blood glucose measurements were not taken during this experiment, however, based on their age discrepancy we hypothesized that an age-related difference in blood glucose may have been responsible for the mortality observed. Younger OB mice have higher blood glucose and we hypothesized that the relative hyperglycemia was the factor responsible for increased mortality in only this group of OB mice. To assess the role of hyperglycemia, independent of diet and obesity status in the context of obesity during *C. rodentium* infection, we infected 10-week and 22-week-old OB mice with *C. rodentium* as these mice have different blood glucose levels, with the 10-week-old OB mice having relative hyperglycemia, whereas the 22-week-old mice are within the age range of mice that have  $\beta$ -cell compensation and lower blood glucose despite profound obesity. Age-matched wild-type C57Bl/6J (WT) mice were used as controls while high fat fed C57Bl/6J (HFD) mice (that do not develop overt hyperglycemia) were used to control for body mass. These mice were all infected with *C. rodentium* and their body mass, random-fed blood glucose, and fecal burdens were regularly collected, and we

only tested until 10 days post infection which is in the midst of infection-induced mortality in hyperglycemic OB mice. The results show that only 40% of the 10-week-old OB group survive *C. rodentium* infection while 80% of the 22-week-old OB group survive up to 10 days after infection (**Figure 2B**). There was no mortality observed in all other groups of WT mice, despite the body mass of HFD-fed WT mice being similar to that of the 10-week-old OB mice. It is noteworthy that there was ~20% mortality observed in the older (22-week-old) cohort of OB mice infected with *C. rodentium*, which may be attributed to leptin deficiency rather than changes in blood glucose. In addition to its role in feeding behaviour, leptin has also been implicated in immune regulation and OB mice have shown resistance to dextran sulfate sodium (DSS)-induced (i.e. chemical-induced) intestinal colitis with reduced proinflammatory cytokine secretion and lower immune cell infiltration<sup>183</sup>. These immunological effects were reversible with leptin supplementation. Leptin levels have also been reported to rise in human and rodent models of infection<sup>184–186</sup>. OB mice are known to have an attenuated immune response during *Klebsiella pneumoniae* infection<sup>187</sup>.

At the onset of infection, as expected, the 22-week-old OB mice had the highest body mass (average, 58.9 grams,  $p < 0.05$ ), while the 10-week-old OB mice and the HFD-fed WT mice had similar body masses (44.7 vs. 47.1 grams, respectively) indicating that body mass was unlikely to be the cause of mortality (**Fig. 2C**). Both age-matched WT control diet-fed groups of mice had significantly

lower body masses compared to all other groups but were not different from each other (31.7 vs. 30.8 grams, 10- and 22-week-old WT mice, respectively). In terms of blood glucose, the 10-week-old OB mice had significantly higher blood glucose levels compared to all other groups at the onset of infection (23.6 vs. 8.6 vs. 9.0 vs. 8.7 vs. 10.7 mmol glucose/litre for OB [10 w], WT [10 w], WT [22 w], HFD [22 w], and OB [22 w], respectively,  $p < 0.05$ ; **Fig. 2D**). Increased blood glucose was evident in 10-week-old OB mice until day 6 post-*C. rodentium* infection, after this point of enteric infection a survivorship effect confounded blood glucose measurement during enteric infection. Stratifying all of the obese mice (inclusive of the 10-week and 22-week-old OB mice, and HFD) into groups by survivorship, we observed that blood glucose, but not body mass prior to infection was a strong predictor for mortality from infectious colitis during *C. rodentium* infection (**Fig. 2E-F**). Both 10- and 22-week-old cohorts of OB mice had higher burdens of *C. rodentium* in the colon (day 7: 8.3 vs. 7.9 vs. 5.8 vs. 5.2 vs. 6.2 log cfu/g; day 10: 8.2 vs. 8.9 vs. 6.2 vs. 7.0 vs. 6.9 log cfu/g, OB [10 w], OB [22 w], HFD [22 w], WT [10 w], and WT [22 w], respectively;  $p < 0.05$ ), liver (day 7: 6.8 vs. 6.8 vs. 4.3 vs. 5.1 vs. 5.9 log cfu/g; day 10: 7.2 vs. 6.6 vs. 4.3 vs. 5.5 vs. 5.2 log cfu/g, OB [10 w], OB [22 w], HFD [22 w], WT [10 w], and WT [22 w], respectively;  $p < 0.05$ ), and spleen (day 7: 6.3 vs. 6.0 vs. 4.1 vs. 3.8 vs. 5.0 log cfu/g; day 10: 5.5 vs. 6.1 vs. 4.1 vs. 4.2 vs. 4.2 log cfu/g, OB [10 w], OB [22 w], HFD [22 w], WT [10 w], and WT [22 w], respectively;  $p < 0.05$ ) compared to all

other groups of WT mice (**Fig. 3A-D**). However, it is critical that there was no difference in bacterial burdens between 10- and 22-week-old OB mice OB mice. This is important because only the 10-week-old OB mice showed a profound increase in mortality, indicating that neither bacterial burden nor bacterial dissemination was associated with hyperglycemia and increased mortality during *C. rodentium* infection (**Fig. 3A-D**).

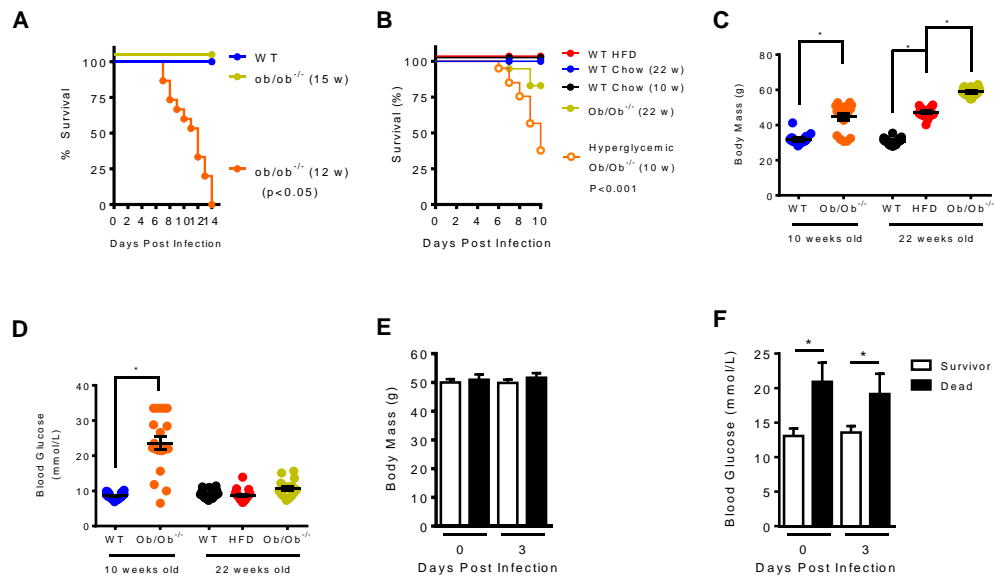


**Figure 2: Hyperglycemia, independent of obesity, promotes mortality during *C. rodentium* infection.** Initial pilot experiment with Dr. Joseph McPhee in which 12-week-old *ob/ob*<sup>-/-</sup> mice and WT controls were infected with *Citrobacter rodentium* (n=10/group). A, Survival curve of genetically induced obese mice and WT C57Bl/6 mice during *C. rodentium* infection. A follow-up experiment in which 10- and 22-week-old *ob/ob*<sup>-/-</sup> mice, long-term high fat diet (HFD)-fed, and age-matched chow-fed mice were infected with *C. rodentium* (n=8-12/group). B, Survival curve of diet-induced and genetically induced obesity mouse models during *C. rodentium* infection. Log-rank test was conducted to determine significance. C, D Initial body mass and blood glucose measurement. One-way ANOVA was conducted to determine significance. E, F, Correlation of body mass and blood glucose to mortality, respectively. Student's unpaired t-test was conducted to determine significance. Values are presented as mean ± SEM. \*p<0.05.

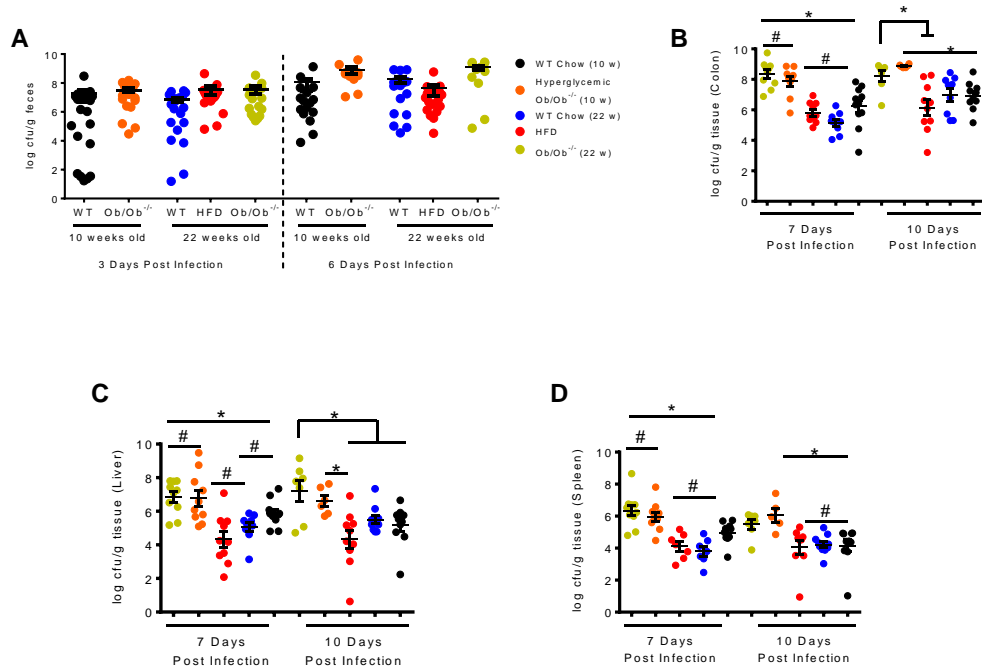


**Figure 3: Mortality during *C. rodentium* infection is not dependent on bacterial burden or dissemination.** 10- and 22-week-old *ob/ob*<sup>-/-</sup> mice, long-term high fat diet (HFD)-fed, and age-matched chow-fed mice were infected with *Citrobacter rodentium*. A, Fecal burdens of diet-induced and genetically induced obesity mouse models during *Citrobacter rodentium* infection (n=8-10/group). One-way ANOVA was conducted to determine significance. B, C, D tissue burdens at day 7 and 10 post infection of colon, liver and spleen, respectively (n=6-8/tissue/group). One-way ANOVA was conducted to determine significance. Values are presented as mean ± SEM. \*p<0.05; # indicates the lack of significant difference.

### 3.1.2. Hyperglycemia, independent of obesity, promotes mortality during *C. rodentium* infection

The results in OB mice show that higher blood glucose was associated with an increased risk of mortality during *C. rodentium* infection in obese mice. We next questioned if obesity was required for these outcomes from enteric infection. Also, while the OB mice provide some insight into high blood glucose and increased adiposity, their leptin deficiency is a considerable confounding factor. To focus on the sole impact of hyperglycemia, we applied our *C. rodentium* infection model to a murine model of Type I diabetes. Akita<sup>+/-</sup> mice are lean, diabetic mice in a C57Bl/6J background<sup>188</sup>. They have a mutation that alters the conformation of insulin 2 rendering it non-functional; this ultimately results in early loss of pancreatic  $\beta$ -cells, as an accumulation of misfolded proinsulin induces apoptosis<sup>188,189</sup>. Male Akita<sup>+/-</sup> mice develop hyperglycemia shortly after weaning, when a 71% decrease of  $\beta$ -cell mass can be observed. Consequently, insulin levels drop and the Akita<sup>+/-</sup> mice develop a persistent state of hypoinsulinemia and hyperglycemia<sup>188</sup>. Akita<sup>+/-</sup> mice develop other diabetes-related health complications with age (~20 weeks old) such as retinopathy, nephropathy, and neuropathy<sup>63</sup>.

Concordant with our earlier results, 100% mortality was observed in Akita<sup>+/-</sup> mice during *C. rodentium* infection compared to 0% mortality in littermate WT mice ( $p < 0.05$ ; **Fig. 4A**). Remarkably, mortality during *C. rodentium*

infection in Akita<sup>+/-</sup> mice was completely prevented with insulin pellet implantation ( $p < 0.05$ ; **Fig. 4A**). At the onset of infection, Akita<sup>+/-</sup> mice with or without insulin had a lower body mass compared to littermate WT mice (23.1 vs. 22.5 vs. 25.5 grams, Akita<sup>+/-</sup> with and without insulin versus WT mice, respectively;  $p < 0.05$ ). Akita<sup>+/-</sup> mice had higher random-fed blood glucose compared to WT littermate mice (31.7 vs. 10.2 mmol glucose/litre, Akita<sup>+/-</sup> and WT mice, respectively) and insulin pellet implantation lowered blood glucose levels in Akita<sup>+/-</sup> mice to a similar level to WT mice (10 mmol glucose/litre,  $p < 0.05$ ; **Fig. 4B-C**). Akita<sup>+/-</sup> mice that did not receive insulin pellets had slightly higher fecal burden at 3 days post infection than all other groups (6.6 vs. 5.8 vs. 5.8 log cfu/gram feces, Akita<sup>+/-</sup> with and without insulin and WT mice, respectively;  $p < 0.05$ ), but no differences in fecal pathogen burden were observed 6 days post infection (7.2 vs. 7.2 vs. 6.6 log cfu/gram feces, Akita<sup>+/-</sup> with and without insulin and WT mice, respectively; **Fig. 5A**). Our results suggest that mortality during *C. rodentium* infection was not dependent on intestinal bacterial burden or dissemination to host tissues as only insulin-treated mice had higher splenic burdens (4.8 vs. 4.3 vs. 4.2 log cfu/gram tissue, Akita<sup>+/-</sup> with and without insulin and WT mice, respectively), but there were no differences in pathogen burden in the colon (3.8-4.2 log cfu/gram tissue) or liver (4.8-5.0 log cfu/gram tissue; **Fig. 5B**). No differences in tissue pathology were observed between groups (**Fig. 5C**). This result indicates that susceptibility of diabetic mice

to mortality during *C. rodentium* infection cannot be traced to typical measurements of intestinal pathogen burden or pathology.

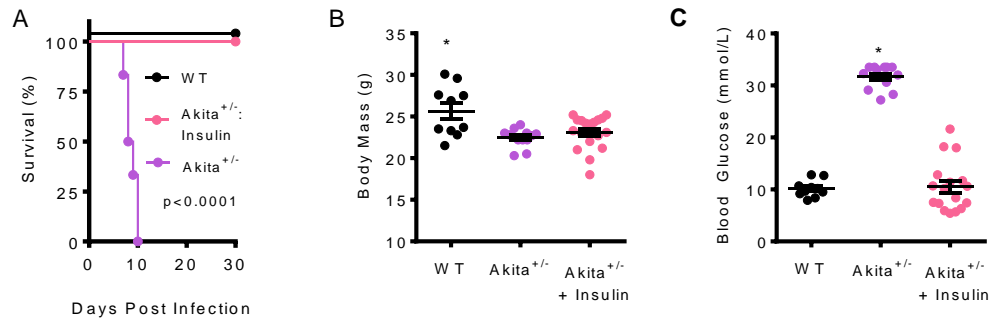


**Figure 4: Hyperglycemia is sufficient to promote mortality during *C. rodentium* infection.** 10-week-old Akita<sup>+/-</sup> mice underwent subcutaneous implantation of insulin or sham surgery and age-matched WT littermates were infected with *Citrobacter rodentium* (n=12-15/group). A, Survival curve of non-obese, diabetic Akita<sup>+/-</sup> mouse with or without insulin supplementation during *C. rodentium* infection. Log-rank test was conducted to determine significance. B, C, Initial body mass and blood glucose measurement. One-way ANOVA was conducted to determine significance. Values are presented as mean  $\pm$  SEM. \* $p < 0.05$ .

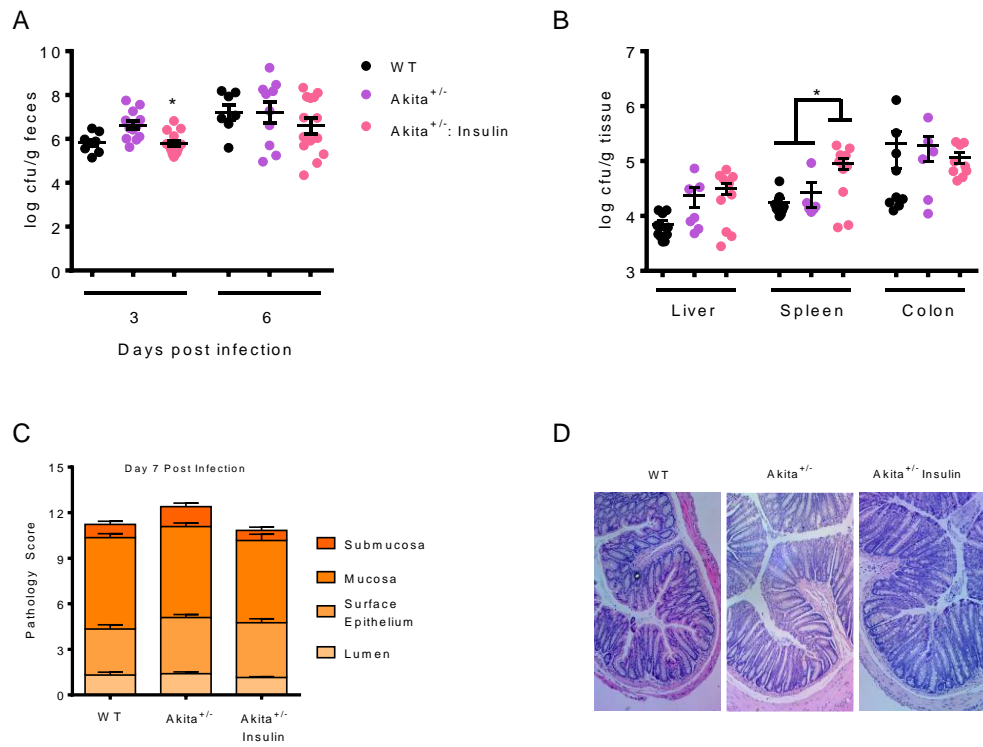


**Figure 5: Pathogen dissemination and overt pathology do not correlate with *C. rodentium*-induced mortality during diabetes.** 10-week-old Akita<sup>+/-</sup> mice underwent subcutaneous implantation of insulin or sham surgery and age-matched WT littermates were infected with *Citrobacter rodentium*. A, Fecal burdens at day 3 and 6 post infection (n=8-11/group). B, Organ burdens at day 7 post infection (n=6-8/group). C, Colonic pathology score at day 7 post infection (n=7-8/group). D, Representative H & E stained colon sections at day 7 post infection. One-way ANOVA was conducted to determine significance. Values are presented as mean  $\pm$  SEM. \*p<0.05.

We next wanted to observe whether mortality during *C. rodentium* infection was dependent on the sex of the mice. We infected 10-week-old female Akita<sup>+/-</sup> mice and WT littermate mice with *C. rodentium*. No mortality was observed over the course of infection in 10-week-old female Akita<sup>+/-</sup> mice (**Fig. 6A**). No differences in body mass were observed over the course of infection, and similar to male Akita<sup>+/-</sup> mice, female Akita<sup>+/-</sup> had significantly higher blood glucose levels throughout the course of infection (**Fig. 6B-C**). However, the magnitude of hyperglycemia is lower in female Akita<sup>+/-</sup> mice compared to the male Akita<sup>+/-</sup> mice (~12-17 mmol/L vs. ~27-33 mmol/L, respectively). These data on blood glucose demonstrate the potential for a threshold glucose concentration to promote mortality from *C. rodentium* infection. Also, sex-specific regulation immunity and intestinal homeostasis should be considered as a modifier of the severity of *C. rodentium* infection. Again, similar to male mice, no overt differences in fecal burden were observed between female Akita<sup>+/-</sup> and littermate WT mice (**Fig. 6D**).

To determine if mortality was dependent on the virulence of *C. rodentium* or was just the result of an oral gavage of a bacterial bolus, we infected Akita<sup>+/-</sup> mice with an avirulent, Type 3 secretion system knock-out strain of *C. rodentium* ( $\Delta escn$ ). The Type 3 secretion system is essential for *C. rodentium* virulence as it is required for the translocation of bacterial effector proteins into the host cell<sup>151,190-192</sup>. The  $\Delta escn$  strain did not promote mortality in

Akita<sup>+/-</sup> mice (**Fig. 7A**), despite the Akita<sup>+/-</sup> mice having expectedly higher blood glucose levels (**Fig. 7B**) and lower body mass (**Fig. 7C**) compared to littermate WT control mice throughout the course of infection. The  $\Delta escn$  strain was unable to successfully infect and persist in the gastrointestinal tract of mice the  $\Delta escn$  strain was only detectable in the feces at day 3 post infection, but not day 7 or 9 (**Fig. 7D**).

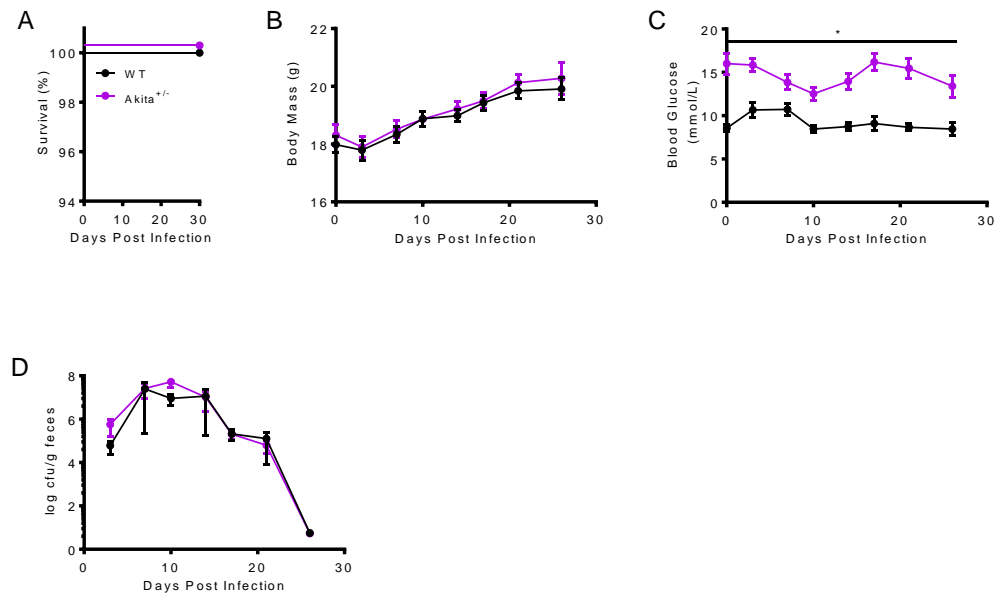


**Figure 6: *C. rodentium*-induced mortality is gender-specific.** 10-week-old female WT and Akita<sup>+/-</sup> mice were infected with *Citrobacter rodentium* (n=8-9/group). A, survival curve of female WT and Akita<sup>+/-</sup> mice infected with *C. rodentium*. B, C, Body mass and blood glucose during the course of infection, respectively. D, Fecal burden during the course of infection. Student's unpaired t-test was conducted to determine significance. Values are presented as mean  $\pm$  SEM. \*p<0.05.

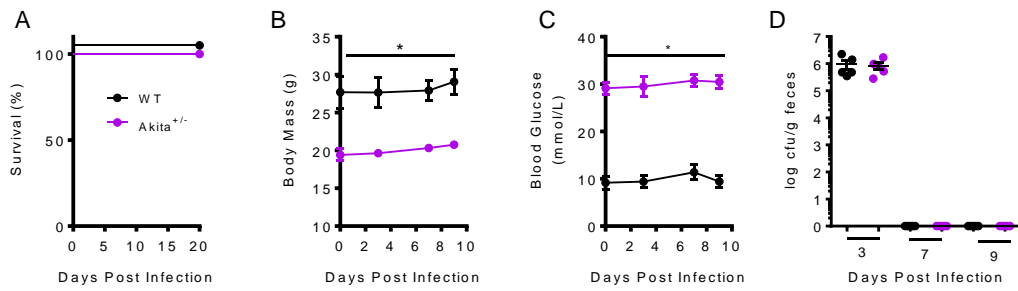


**Figure 7: Virulent *C. rodentium* is required hyperglycemia-induced mortality.** A, survival curve of WT and Akita<sup>+/-</sup> mice infected with  $\Delta$ escn *Citrobacter rodentium* strain (n=6/group). B, C, body mass and blood glucose during the course of infection, respectively. D, fecal burdens at days 3, 7, and 9 post infection. Values are presented as mean  $\pm$  SEM.

### **3.1.3. Impaired intestinal barrier function is not responsible for hyperglycemia-induced mortality during *C. rodentium* infection**

We next assessed if hyperglycemia in Akita<sup>+/-</sup> compromised intestinal barrier function. We assessed intestinal permeability by gavaging FITC-dextran and found no differences between naïve (uninfected) Akita<sup>+/-</sup> and WT mice (2207 vs. 3362 absorbance units (AU); **Fig. 8A**). As an additional indirect measure of intestinal permeability during infection, we used a TLR4-HEK reporter cell line to quantify any differences in circulating endotoxin. It is known that TLR4 ligands such as LPS are derived from the intestinal microbiota during metabolic endotoxemia, which equates to chronic, low level increases in endotoxin load during diet-induced obesity and diabetes in mice<sup>53,185,193</sup>. However, very little is known about hyperglycemia and metabolic endotoxemia during enteric infection. Our results show that at day 9 post *C. rodentium* infection, no differences in circulating/serum TLR4 ligands were observed between Akita<sup>+/-</sup> mice with or without insulin and WT mice (**Fig. 8B**). To determine whether *C. rodentium* infection promoted dissemination of other bacteria to cause mortality, we cultured bacteria from the blood, liver and spleen of Akita<sup>+/-</sup> mice with or without insulin and WT mice at day 9 post infection on four different agar mediums/conditions. We detected no bacterial growth in the blood from many mice (data not shown). We found no statistical differences in total dissemination between Akita<sup>+/-</sup> mice and Akita<sup>+/-</sup> mice treated with insulin, indicating that hypoglycemia and mortality from infection was not associated

with bacterial dissemination. We consistently found higher bacterial burdens in the liver and spleen between Akita<sup>+/-</sup> mice treated with insulin compared to WT mice in all plating conditions ( $p < 0.05$ ; **Fig. 8C-F**). Given that insulin promoted survival during enteric infection in Akita<sup>+/-</sup> mice, our results showed no evidence of impaired intestinal barrier function as an underlying cause for hyperglycemia-induced mortality from enteric infection. Rather, these results indicate that hyperglycemia, independent of obesity, is sufficient for *C. rodentium*-induced mortality. The increased risk of mortality from enteric infection in diabetic mice was not associated with overt intestinal pathology or bacteremia.

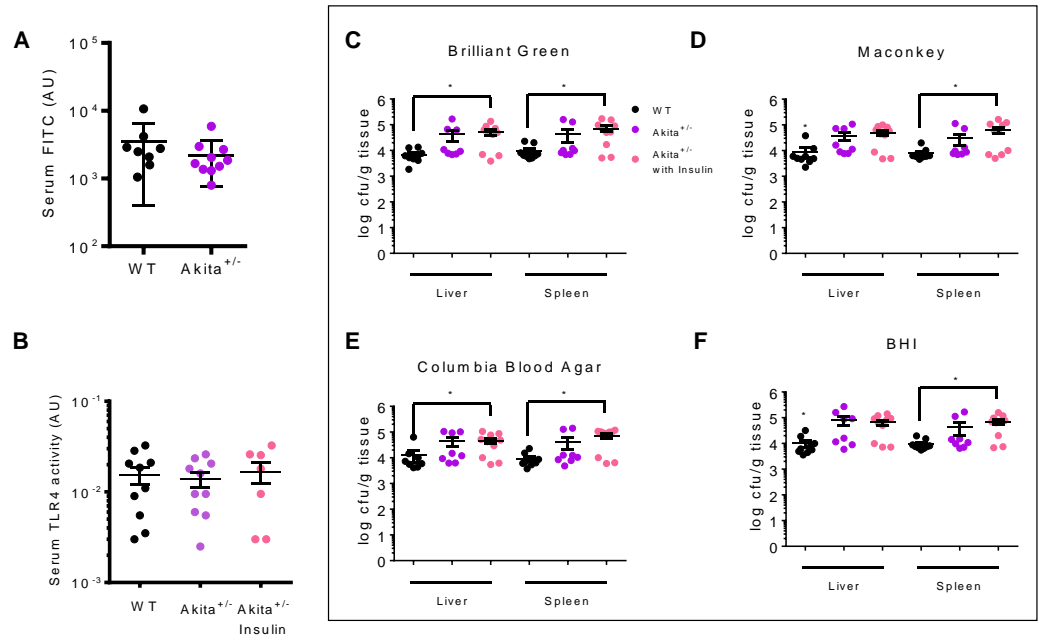


**Figure 8: Impaired intestinal barrier integrity and overt bacteremia are not detected during *C. rodentium*-induced mortality of Akita<sup>+/-</sup> mice.** A, FITC-dextran assay of WT and Akita<sup>+/-</sup> mice prior to infection (n=8-10/group). B, Quantification of serum endotoxin levels of WT and Akita<sup>+/-</sup> with or without insulin at day 9 post infection (n=7-9/group). Livers and spleens of WT and Akita<sup>+/-</sup> with or without insulin, were plated on different media conditions: C, brilliant green; D, blood-heart infusion (BHI); E, Columbia blood agar; F, Maconkey, to assess dissemination of *C. rodentium* and commensals (n=8-10/group). Values are presented as mean ± SEM. \*p<0.05

### **3.1.4. IL-22 lowers blood glucose and mitigates severity of enteric infection in obese and diabetic mice**

In support of our results, a recent study conducted by *Wang et al.* found that OB mice and *db/db*<sup>-/-</sup> mice that lack the leptin receptor are both obese mouse strains that have increased mortality after *C. rodentium* infection<sup>119</sup>. The OB and *db/db*<sup>-/-</sup> mice used in this study were infected at an age that would be hyperglycemic<sup>119</sup>. Intriguingly, this study also found that HFD-fed, obese mice did not have increased mortality from *C. rodentium* infection, but the authors could not explain this effect as the premise of testing appeared to be on age or obesity status, rather than blood glucose. However, this study made a fascinating connection to IL-22-related immunity. OB mice were found to have reduced IL-22 expression in the colon, during *C. rodentium* infection which correlated with increased mortality infection. They detected similar numbers of IL-22<sup>+</sup> innate lymphoid cells and T cells but found that during infection, induction of IL-22 was impaired in OB mice compared to wild-type (WT) controls. As IL-23 is known to regulate IL-22 expression, this study used a hydrodynamic tail vein injection of an IL-23 containing plasmid, three days prior to infection, which improved survival of OB mice and rescued IL-22 expression at day 4 post infection. The researchers then gave OB mice exogenous IL-22 supplementation, using an IL-22-Fc antibody, and rescued OB mice from *C. rodentium*-induced mortality. In their HFD-induced obesity model, these authors also found reduced levels of IL-22 without any mortality, which they suggested was a result of the older age in mice. To assess

the metabolic effects of IL-22, the authors treated HFD-fed WT mice with exogenous IL-22. IL-22 supplementation reduced weight gain, improved glucose tolerance and insulin sensitivity, and lowered blood glucose levels; however, these metabolic parameters were never measured in IL-22 treated OB mice before or during *C. rodentium* infection<sup>157</sup>. In summary, this seminal paper suggested a link between obesity, and IL-22-mediated intestinal mucosal barrier function during obesity, but the cause of mortality during enteric infection was not well-defined. It remained possible that exogenous IL-22 treatment lowered blood glucose, which was a key factor for mortality risk during *C. rodentium* infection.

IL-22 is an important cytokine for maintaining intestinal barrier integrity by regulating tissue repair and promoting antimicrobial release during acute inflammation. IL-22 is predominantly expressed by T<sub>H</sub>17 and T<sub>H</sub>22 cells and is regulated by the cytokines, IL-23 and IL-12. IL-22 is a unique cytokine as its main actions are exerted primarily on epithelial cells, as these are the main cell types that express the IL-22 receptor<sup>122-125</sup>. In conjunction with its inflammatory role, IL-22 has also been recently implicated in metabolic regulation, including lowering blood glucose<sup>125-127</sup>. Numerous studies have shown that exogenous IL-22 can improve metabolic status during obesity. IL-22 has been shown to lower blood glucose, body mass, and adiposity; improve glycemic control, intestinal

barrier function, reduce liver lipogenic expression, and reduce oxidative and ER stress<sup>119,125,128,129</sup>.

While it is well-known that IL-22 deficient mice have increased mortality during *C. rodentium* infection, a study by *Aychek et al.* showed that mice deficient in *il-23* but not *il-12(p40)* succumbed to *C. rodentium* infection by day 15 post infection, despite similarly reduced levels of IL-22<sup>161</sup>. Critically, the OB mice used in the study by *Wang et al.* were 5-6 weeks of age, which is known to be within the hyperglycemic stage of OB mouse development. We hypothesized that IL-22 supplementation promoted survival of obese, hyperglycemic mice infected with *C. rodentium* through the glucose lowering and metabolic actions of IL-22. To assess this, we treated both OB and Akita<sup>+/-</sup> mice with the same IL-22-Fc antibody and tracked survival, body mass, and blood glucose.

We first tested if Akita<sup>+/-</sup> mice (which all die from *C. rodentium* infection) had different levels of IL-22 or related cytokines in the colon during infection. We found that *C. rodentium* infection increased IL-22 transcript levels in the colons of both WT and Akita<sup>+/-</sup> mice, but no differences in IL-22 expression were observed between WT and Akita<sup>+/-</sup> mice at days 0, 5, and 9 post infection (**Fig. 9A**). We assessed other intestinal inflammatory markers in the IL-22 pathway (IL-17 and IL-23) but found no differences between Akita<sup>+/-</sup> and WT mice at days 0, 5, or 9 post infection (**Fig. 9A**). Importantly, while IL-22Fc injection reduced

mortality of Akita<sup>+/-</sup> mice from *C. rodentium*-induced mortality (p=0.0019), IL-22Fc injection coincidentally reduced body mass (p<0.05) and blood glucose levels (p<0.05; **Fig. 9B-C**).

We were able to repeat the findings of Wang et al. by showing complete rescue of OB mice from *C. rodentium*-induced mortality (p=0.0019) by injecting the IL-22Fc compound, but we also observed significantly reduced body mass (p<0.05) and blood glucose levels (p<0.05; **Fig. 10A-C**). We were also able to reproduce the results of Wang et al, showing lower IL-22 transcript levels in the colon during *C. rodentium* infection in OB mice (**Fig. 10**). However, we also tested OB mice discordant for hyperglycemia at 2 different ages. Quantifying IL-22 gene expression in the colons from OB mice discordant for hyperglycemia (which are discordant for risk of mortality) showed that 10-week and 22-week-old OB mice had similarly reduced levels of IL-22 compared to WT controls at days 6 and 10 post infection (**Fig. 10D**). Since both OB mice had similarly reduced levels of IL-22 and our Akita<sup>+/-</sup> mice showed no changes in IL-22 levels from WT, our results suggest that blood glucose lowering rather than the immunological actions of IL-22 promote survival from enteric infection. In order to further probe the relationship of inflammation/immunity and mortality from infection, we next assessed a panel of circulating markers of inflammation in OB mice that may indicate or predict mortality. We found no indicators of overt inflammation or predictors of mortality in serum/circulating inflammatory factors. Compared to

WT mice at day 4 and 10 post infection, 10-week-old OB mice had significantly lower il-9 (16.32 vs. 60.88 pg/ml) at day 4 and significantly higher IL-6 (123.40 vs. 54.98 pg/ml), IL-15 (89.55 vs. 60.93 pg/ml), IL-17 (16.94 vs. 5.52 pg/ml), and TNF $\alpha$  (35.54 vs. 8.28 pg/ml) at day 10 post infection (all  $p < 0.05$ ; **Fig. 11A-B**). Overall, these data result support our hypothesis that hyperglycemia, not IL-22 deficiency, nor overt systemic inflammation promotes mortality during *C. rodentium* infection. IL-22Fc was a potent glucose lowering agent in models of diabetes and obesity.

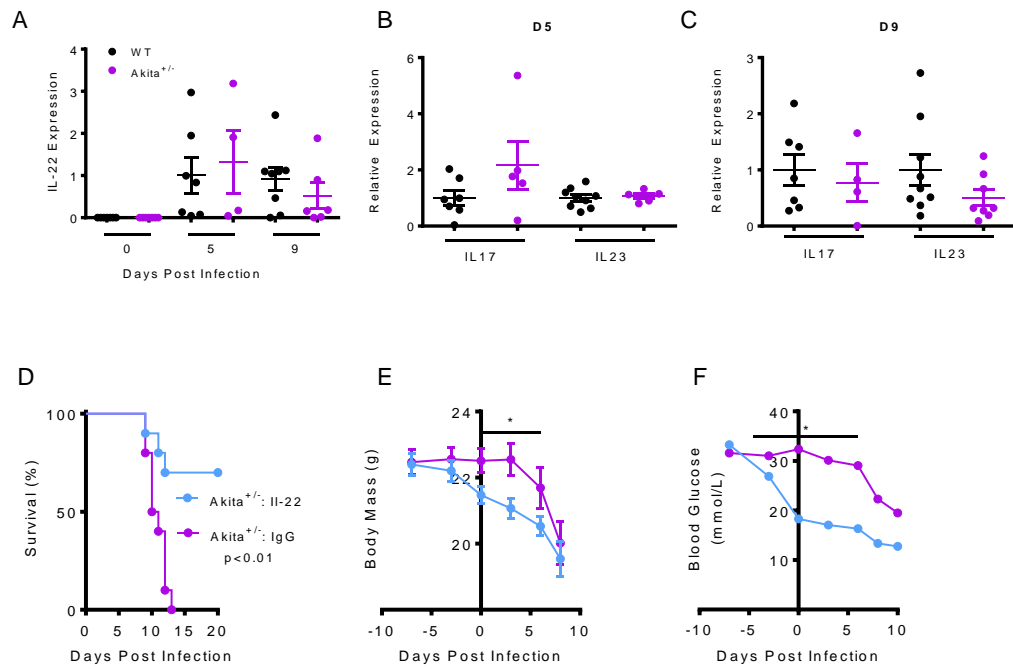


**Figure 9: Exogenous IL-22 supplementation of Akita<sup>+/-</sup> mice rescues mortality during *C. rodentium* infection and reduces glycemia.** A, IL-22 gene expression at day 0, 5 and 9 post infection (n=7-8/group). IL-17 and IL-23 gene expression at B, day 5 and C, 9 post infection (n=5-7/group). D, Survival curve of Akita<sup>+/-</sup> mice treated with IL-22Fc or control supplementation during *Citrobacter rodentium* infection. Log-rank test was conducted to determine significance. E, F, Body mass and blood glucose level during the course of treatment (n=8-10/group). Student's unpaired t-test was conducted to determine significance. Values are presented as mean ± SEM. \*p<0.05.

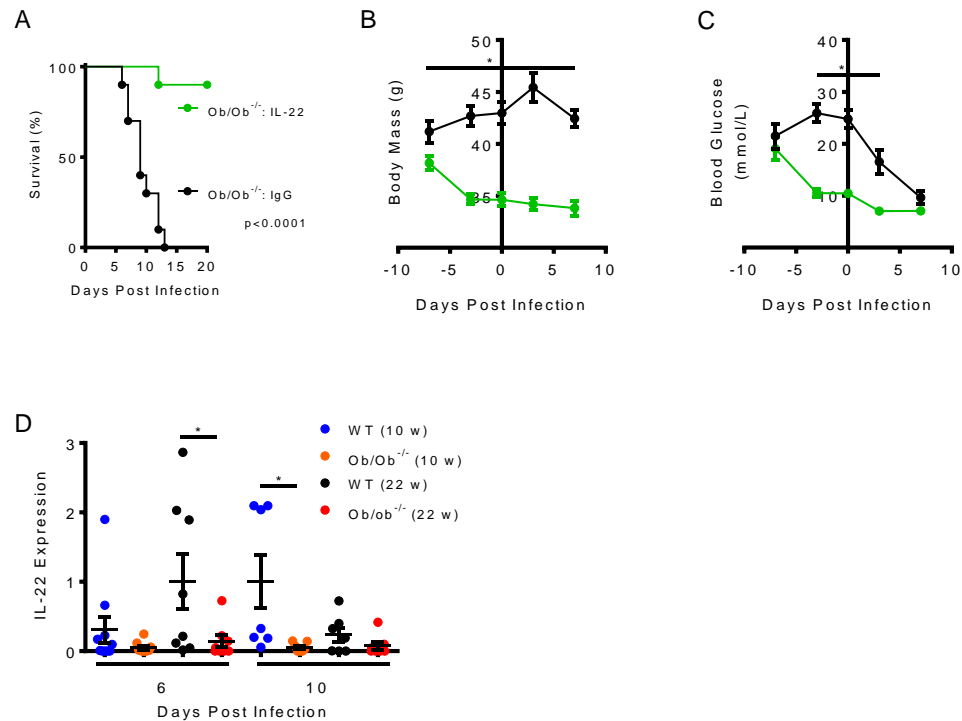


**Figure 10: Exogenous IL-22 supplementation of *ob/ob*<sup>-/-</sup> mice rescues mortality during *C. rodentium* infection and reduces glycemia.** A, survival curve of 10-week-old, *ob/ob*<sup>-/-</sup> mice treated with IL-22Fc or control supplementation during *Citrobacter rodentium* infection. Log-rank test was conducted to determine significance. B, C, Body mass and blood glucose level during the course of treatment (n=10/group). D, IL-22 gene expression at day 6 and 10 post-infection (n=6-8/group). Student's unpaired t-test was conducted to determine significance. Values are presented as mean ± SEM. \*p<0.05.

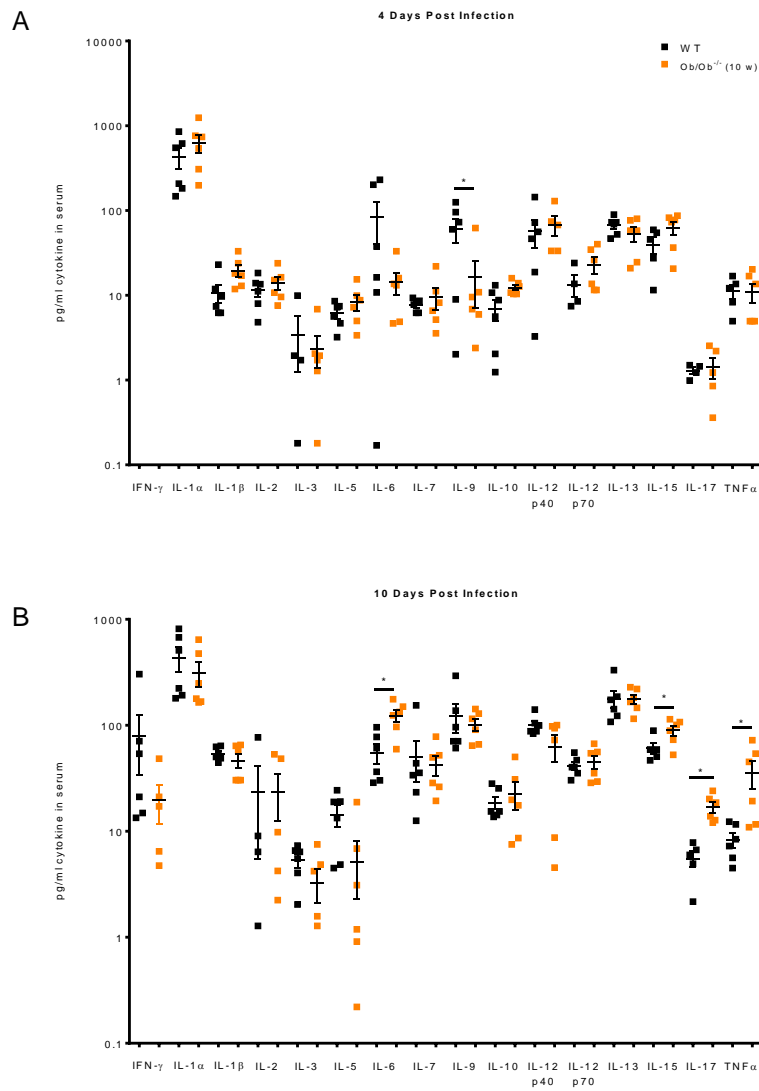


**Figure 11: Inflammation does not correlate with *C. rodentium*-induced mortality in *ob/ob*<sup>-/-</sup> mice.** Quantification of serum cytokines using ELISA-immunoabsorbant assay at A, day 4 and B, day 10 post infection (n=5-8/group). Student's unpaired t-test was conducted to determine significance. Values are presented as mean  $\pm$  SEM. \*p<0.05.

### 3.1.5. Fluid balance regulates mortality during *C. rodentium* infection in diabetic mice

Despite the sufficiency for hyperglycemia, the underlying cause of mortality remained unclear in our enteric infection model during diabetes. As previously mentioned, of the known mouse strains susceptible to *C. rodentium*-related mortality, fluid imbalance due to dysregulated Wnt-signalling was primarily responsible for the risk of mortality during enteric infection.

First, to determine if dehydration was responsible for mortality, we provided fluid replenishment with Ringer's solution, an isotonic solution consisting of sodium chloride, potassium chloride, and sodium bicarbonate, throughout *C. rodentium* infection. Mice were given a daily subcutaneous injection of 1 ml of Ringer's solution at the onset and throughout the course of infection. Fluid replacement completely prevented Akita<sup>+/-</sup> mice from *C. rodentium*-induced mortality (**Fig. 12A**). There were no differences between the treated and untreated groups in initial body mass (23.2 vs. 24.2 grams, respectively) or blood glucose (31.4 vs. 32.6 mmol glucose/litre, respectively), a trend that continued throughout the course of infection (**Fig. 12B-C**). It was striking that hyperglycemic Akita<sup>+/-</sup> mice all survived the enteric infection, if mice were given fluid therapy. There were also no differences in fecal burden at days 3 or 6 of infection and no differences in organ burdens at day 9 between fluid treated and untreated Akita<sup>+/-</sup> mice and WT control (**Fig. 12D**). To assess the

level and nature of dehydration in mice, we quantified serum osmolality but found no differences in protein or ion levels between groups (**Fig. 13**). This may be the result of physiological adaptations to chronic dehydration, as studies have shown that acute water deprivation, but not prolonged water restriction, show alterations in osmolality<sup>194,195</sup>. In response to this deprivation, intracellular volume is decreased to maintain body fluid volume while ion reabsorption in the kidneys is reduced<sup>194</sup>. In our model, diarrhea onset was observed as early as 3 days post infection and coupled with the polyuric behaviour of Akita<sup>+/-</sup> mice, may have induced a state of chronic dehydration. Additionally, as water consumption was not monitored during infection, osmolality differences may also be masked by polydipsia of Akita<sup>+/-</sup> mice<sup>188,196</sup>.

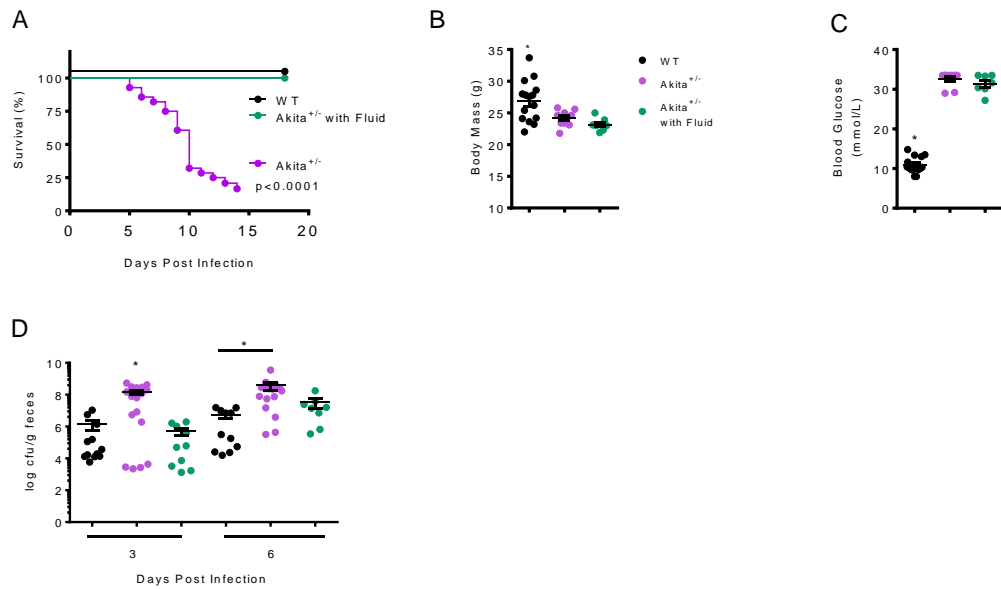


**Figure 12: Fluid replenishment rescues hyperglycemia-induced mortality during *C. rodentium* infection.** A, survival curve of non-obese, diabetic Akita<sup>+/+</sup> mouse with daily subcutaneous injections of Ringer's solution (1 ml) during *Citrobacter rodentium* infection. Log-rank test was conducted to determine significance. B, C, Initial body mass and blood glucose measurement (n=7-15/group). D, Fecal burdens at days 3 and 6 post-infection (n=6-12/group). One-way ANOVA was conducted to determine significance. Values are presented as mean  $\pm$  SEM. \* $p < 0.05$ .

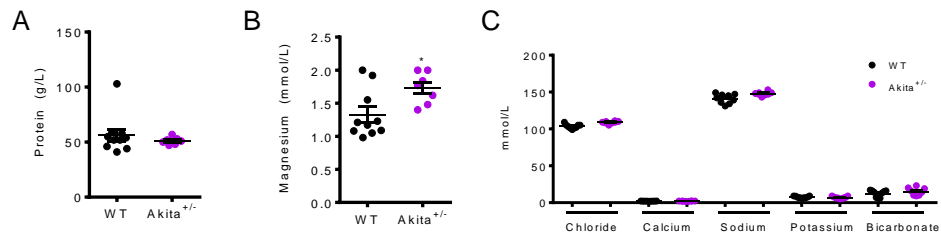


**Figure 13: No differences in serum osmolality observed during *C. rodentium* infection of Akita<sup>+/-</sup> mice.** Serum concentration of: A, protein; B, magnesium; C, chloride, calcium, sodium, potassium, and bicarbonate taken at endpoint (n=6-9/group). Student's unpaired t-test was conducted to determine significance. Values are presented as mean ± SEM. \*p<0.05.

While these studies were conducted in mice, the results indicate the potential for diabetics to be at an increased susceptibility to dehydration during diarrhea-causing acute gastrointestinal colitis which is of concern when current clinical trials are looking to sodium-glucose transport inhibitors (SGLTs) as treatment for diabetes. This drug class works by selectively inhibiting SGLT-2, a glucose transporter in the kidney that is responsible for 90% of glucose reabsorption from urine<sup>197–199</sup>. As a result of this inhibition, glucose is constantly excreted through urination, which promotes lowering of blood glucose levels but increases the risk of dehydration. Hence, we tested Empagliflozin, an SGLT-2 inhibitor that is currently used in humans. We found that Empagliflozin-treated Akita<sup>+/-</sup> mice had an increased mortality rate during *C. rodentium* infection, despite marginally improved glucose levels before infection (31 vs. 21.5 mmol glucose/litre, untreated vs. treated,  $p < 0.05$ ), but no differences in fecal pathogen burden (**Fig. 14A-C**).

Our data showing that Akita<sup>+/-</sup> mice given fluid replenishment had lower mortality despite similarly high blood glucose levels indicates that hyperglycemia is necessary, but not sufficient to promote mortality during *C. rodentium* infection in mice. Fluid balance is a key factor in risk of mortality during enteric infection in diabetic mice.

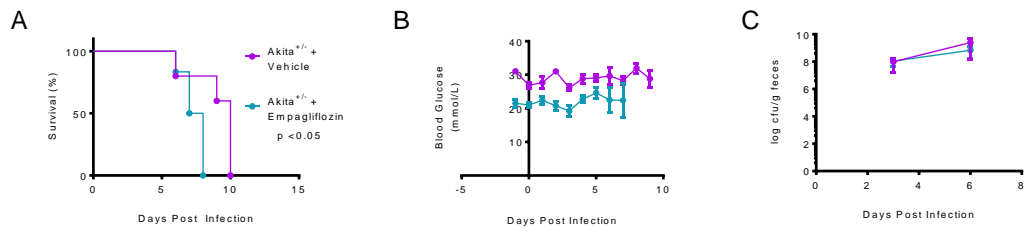


**Figure 14: Empagliflozin, a diabetic drug, promotes mortality during *C. rodentium* infection of Akita<sup>+/-</sup> mice.** A, Survival curve of non-obese, diabetic Akita<sup>+/-</sup> mouse with daily oral gavage of empagliflozin (150 mg/kg) during *Citrobacter rodentium* infection. Log-rank test was conducted to determine significance. B, Blood glucose during the course of infection (n=6-8/group). C, Fecal burden during the course of infection (n=5/group). Student's unpaired t-test was conducted to determine significance. Values are presented as mean  $\pm$  SEM.

### 3.1.6. Wnt-inhibition reduces mortality during *C. rodentium* infection in diabetic mice

Next, we inhibited Wnt-signalling with LGK-974 during enteric infection. LGK-974 is a newly developed, orally available compound that is currently being tested as an anti-tumour drug. It impairs Wnt-signalling by inhibiting porcupine, whose post-translational modification of Wnt is necessary for secretion<sup>90,97,200</sup>. LGK-974 (3 mg/kg) or 1% methylcellulose vehicle control was gavaged three times a week into Akita<sup>+/-</sup> mice beginning one week prior and throughout the course of infection. To verify our hypothesis that Wnt-signalling is involved in *C. rodentium*-induced mortality, we attempted to determine if LGK treatment inhibited markers of Wnt-signalling in the colon. We quantified the amount of active  $\beta$ -catenin in the colon using Western blotting (**Fig. 15A**). There was a significant increase in active  $\beta$ -catenin (i.e. de-phosphorylated  $\beta$ -catenin) in the colons of untreated Akita<sup>+/-</sup> group compared to littermate WT mice (**Fig. 15B**). LGK-974 treatment and insulin pellets prevented the increase in active  $\beta$ -catenin in the colons of Akita<sup>+/-</sup> mice (**Fig. 15B**). Importantly, LGK-974 treatment also lowered mortality in Akita<sup>+/-</sup> mice during *C. rodentium* infection. These data implicate Wnt-signalling involvement in hyperglycemia-induced mortality (**Fig. 15C**). There were no differences in initial body mass [23.1 (LGK) vs. 23.3 (untreated) grams] or blood glucose [26.8 (LGK) vs. 29.4 (untreated) mmol glucose/litre] between treated and untreated groups, a trend that continued throughout the course of infection (**Fig. 15D-E**). There were also no differences in

fecal burden at days 3 or 6 of infection and no differences in organ burdens at day 9 (**Fig. 15F**).

We next measured regulators of Wnt activity known to be involved in *C. rodentium* responses. We quantified the expression levels of R-spondins (*rspos*) 1-3 prior to infection and at day 7 post infection in the colons of mice (**Fig. 16A-C**). R-spondins are important regulators of the canonical Wnt-signalling pathway and have been shown to be differentially regulated during *C. rodentium* infection, with *Rspos2* being significantly elevated in susceptible mouse strains<sup>87,201,202</sup>. We did not measure *rspos4*, as expression levels were consistently below the limit of detection during *C. rodentium* infection, levels<sup>202</sup>. Expression of *rspos1* was significantly higher in the colons of Akita<sup>+/-</sup> mice supplemented with insulin compared to untreated Akita<sup>+/-</sup> mice; however, no difference was observed compared to WT littermate mice. No differences in *rspos2* and *rspos3* were observed between groups at baseline or day 7 post infection. Therefore, we find that transcript levels of R-spondins do not biomark or correlate with Wnt-activity or risk of mortality in our model of enteric infection during diabetes in mice.

Next to assess the level of proliferation in the intestinal crypts, we stained for Ki-67 and active  $\beta$ -catenin in paraffin-embedded colon sections collected at day 9 post infection (**Fig. 16D-E**). Distance of Ki-67 detection from the up the

base of crypt to the villi was used as a measurement of proliferation and taken as a ratio of total crypt length. Overall, no significant difference was observed in Ki67 (a marker of cellular proliferation) or total crypt length (**Fig 16F**). Overall, from these results we show that hyperglycemia worsens the outcome of enteric infection with *C. rodentium* by promoting mortality via fluid imbalance and increased Wnt signalling in the distal gut, but it was unclear if this effect extends to other types of enteric infections.

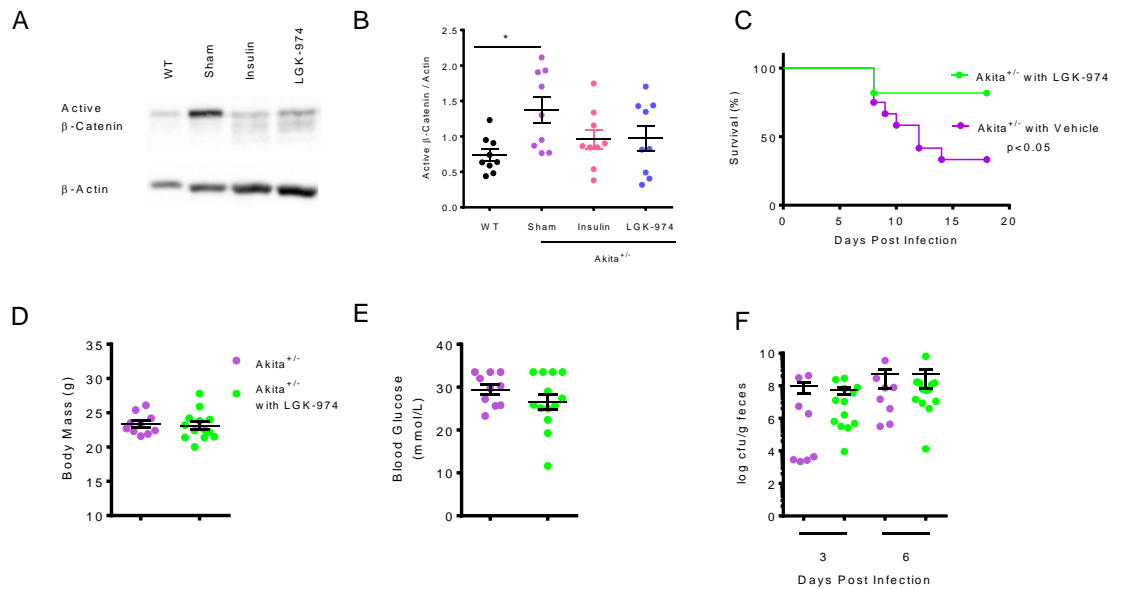


**Figure 15: Wnt-inhibition rescues hyperglycemia-induced mortality during *C. rodentium* infection.** A, Representative Western blot of  $\beta$ -catenin and  $\beta$ -actin levels. Representative image is of 10 samples for each group. B, Quantification of Western blot images for colonic protein concentrations of active, non-phosphorylated  $\beta$ -catenin, normalized to  $\beta$ -actin levels (n=8-12/group). C, survival curve of non-obese, diabetic Akita<sup>+/-</sup> mouse with daily oral gavage of LGK-974 (3 mg/kg) during *Citrobacter rodentium* infection. Log-rank test was conducted to determine significance. D, E, Initial body mass and blood glucose measurement (n=11-13/group). F, Fecal burdens at days 3 and 6 post infection (n=9-11/group). Student's unpaired t-test was conducted to determine significance. Values are presented as mean  $\pm$  SEM. \*p<0.05.

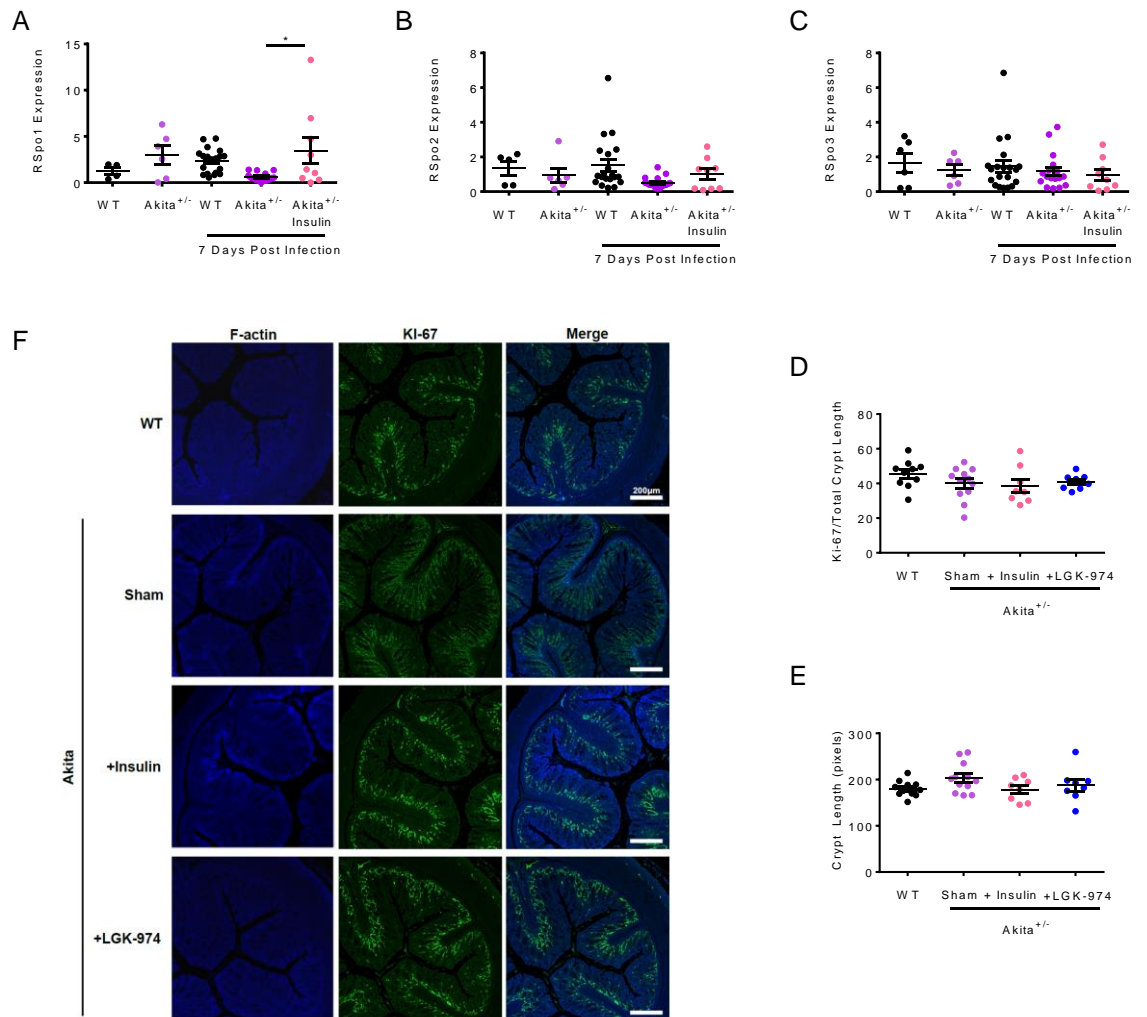


**Figure 16: Hyperglycemia does not elevate Rpondin expression or colonic crypt proliferation.** Gene expression of uninfected and at day 7 post infection of A, *rspos1*, B, *rspos2*, and C, *rspos3* (n=6-8/group). D, Measurement of Ki-67 as a ratio of crypt length. E, Total crypt length. F, representative immunofluorescent images taken at 10x objective using a Nikon A1+ confocal system attached to a TiEclipse inverted microscope (n=8-11/group). One-way ANOVA was conducted to determine significance. Values are presented as mean ± SEM. \*p<0.05.

### 3.1.7. Hyperglycemia worsens outcomes during a different model of enteric infection

Next, we used another model of enteric infection, adherent-invasive *Escherichia coli* (AIEC), to assess whether hyperglycemia would impact outcomes of AIEC infection. AIEC has gained recent interest for its association with Crohn's disease (CD). *E. coli* have specifically been shown to be enriched in CD patients<sup>162–164</sup>. Culturing of *E. coli* isolates from Crohn's disease patients found that many isolates had unusual adherent and invasive phenotypes. Interestingly, these isolates did not possess toxins or adhesins typically found in pathogenic *E. coli*; thus, they were collectively called adherent-invasive *E. coli* for their ability to penetrate the mucosa, adhere and invade epithelial cells, and stimulate inflammation<sup>163,165–168</sup>. AIEC is considered a pathobiont, a usually benign pathogen that will rapidly expand during a perturbation, as it is found in CD patients and healthy individuals<sup>162,168</sup>.

No mortality was observed when male Akita<sup>+/-</sup> mice were infected with AIEC (**Fig. 17A**). Compared to WT littermate mice, Akita<sup>+/-</sup> mice had significantly lower body mass ( $p < 0.05$ ; **Fig. 17B**) and higher blood glucose levels ( $p < 0.05$ ; **Fig. 17C**) at the onset of infection. Compared to WT littermate mice, Akita<sup>+/-</sup> mice had significantly higher fecal AIEC burdens at Day 7-17 post AIEC infection (**Fig. 17D**). Compared to WT littermate mice, Akita<sup>+/-</sup> mice had higher bacterial

burdens of AIEC in all segments of the lower intestinal tract ( $p < 0.05$ ), but no differences in dissemination were observed since tissue burdens were similar to WT littermate mice (**Fig. 17E**). We next questioned if blood glucose was the key factor regulating outcomes from AIEC function and focused on bacterial burdens of AIEC in diet-induced obesity and metabolic disease models in mice.

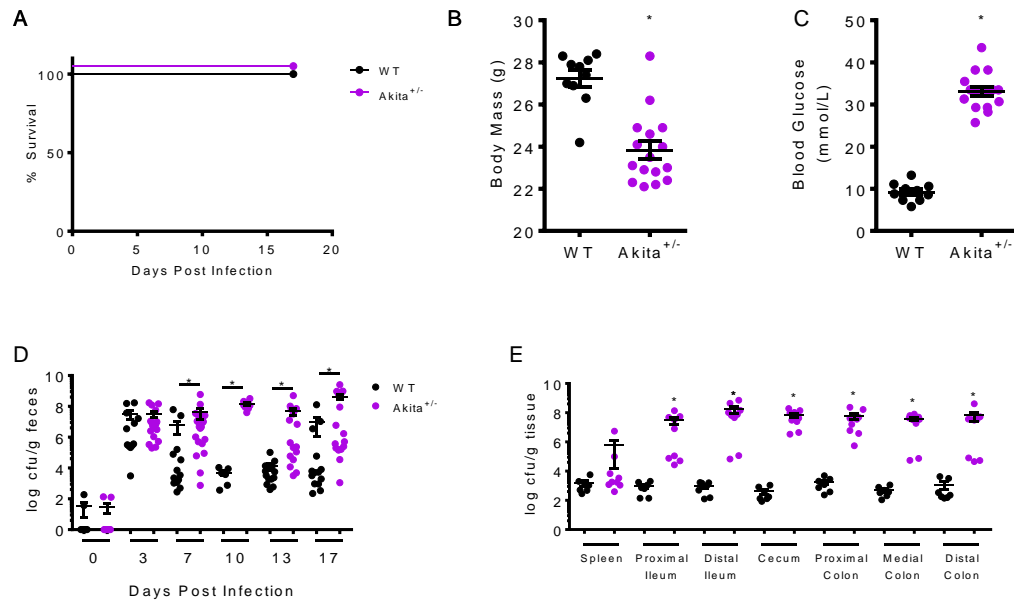


**Figure 17: *Akita*<sup>+/-</sup> mice have elevated fecal and tissue burdens during adherent-invasive *E. coli* infection.** A, Survival curve of non-obese, diabetic *Akita*<sup>+/-</sup> mice during infection. Log-rank test was conducted to determine significance. B, C, Initial body mass and blood glucose measurement. D, Fecal burdens during the course of infection. E, Tissue burdens at day 17 post infection (n=7-9/group). Student's unpaired t-test was conducted to determine significance. Values are presented as mean ± SEM. \*p<0.05.

## **3.2. Obesity impairs resolution of adherent-invasive *Escherichia coli* infection**

### **3.2.1. Obesity promotes AIEC expansion and pathology**

Susceptibility to AIEC and subsequent expansion have been linked with dysbiosis and inflammation, both characteristics associated with obesity<sup>52,53,116,170,174,203–206</sup>. HFD has also been implicated in altering the composition of the microbiome, possibly potentiating an immune response or enabling a specific pathogen, such as adherent and invasive *E. coli* (AIEC) to flourish in mice<sup>52,207</sup>. In fact, a recent study by *Agus et al.*, found that a high fat/high sugar diet perturbed the microbiota of mice which lead to increased susceptibility to AIEC infection and that this phenotype was microbiota-dependent as fecal transfers from high fat/high sugar fed mice to germ-free mice conferred the same susceptibility<sup>174</sup>. A study by *Small et al.* looked at the impact of secondary infections with *S. typhimurium* and *C. rodentium* after a primary infection with AIEC and found that following secondary infections, AIEC expansion occurred only in the presence of intestinal inflammation<sup>203</sup>. Obesity has many characteristics that make it a good candidate as a potentiator of AIEC infection, including low-grade chronic inflammation, altered mucosal immunity, and impaired intestinal barrier integrity<sup>208–211</sup>. However, the impact of diet components versus obesity on AIEC infection outcomes has not been clearly defined.

To assess the impact of obesity on AIEC infection, we subjected male C57Bl/6J mice to long-term 60% HFD (for 16-18 weeks) before and throughout AIEC infection. We pre-treated with 2 mg/g streptomycin one day prior to infection with  $\sim 2 \times 10^9$  colony forming units (CFU) of AIEC. Feces were collected throughout the course of infection to track bacterial burden and the small and large intestine and spleen were collected and plated on day of sacrifice to observe dissemination.

We characterized the metabolic status of these long-term HFD-fed mice to confirm obesity. Compared to chow fed mice, HFD mice were glucose intolerant (**Fig. 18A**) and had higher fasting blood glucose ( $p < 0.05$ ; **Fig. 18B**). The HFD group also had significantly larger body mass ( $p < 0.05$ ; **Fig. 18C**) and higher levels of adiposity (**Fig. 18D**) prior to infection. During AIEC infection, minimal weight loss was observed, and the HFD-fed mice maintained their higher body mass compared to chow-fed mice (**Fig. 19A**). Starting from day 1 until day 30 post infection, there were significantly higher fecal burdens of AIEC in the HFD-fed mice (**Fig. 19B**). The elevated fecal burdens corresponded with elevated tissue burdens when tested at day 17 post infection. Higher AIEC CFUs were observed in the ileum, cecum, and colon but no difference in dissemination was observed, evidenced by the lack of countable AIEC colonies from spleen homogenates in either the chow- or HFD-fed groups of mice (**Fig. 19C**). At day 9 post AIEC infection, worsened pathology and crypt elongation was observed in

the cecum of HFD mice compared to chow-fed mice (**Fig. 20A-C**). Tissues were scored on the severity of crypt hyperplasia, immune cell infiltration, epithelial cell loss, and edema. By day 17 post AIEC infection, crypt elongation was observed in the ileum, cecum, and colon but overall pathology was only significantly elevated in the colon of HFD mice compared to chow-fed mice (**Fig. 20D-F**).

Antibiotics are known potentiators of AIEC infection and it was not clear if they were required for the exacerbated AIEC outgrowth observed in our HFD-feeding model<sup>170</sup>. We infected long-term HFD mice with AIEC without streptomycin pre-treatment and did not observe any differences in AIEC colonization between HFD- and chow-fed mice, despite differences in body mass (**Fig. 21A-B**). Hence, we conclude that antibiotics interact with obesity and/or HFD-feeding to exacerbate AIEC infection characteristics.

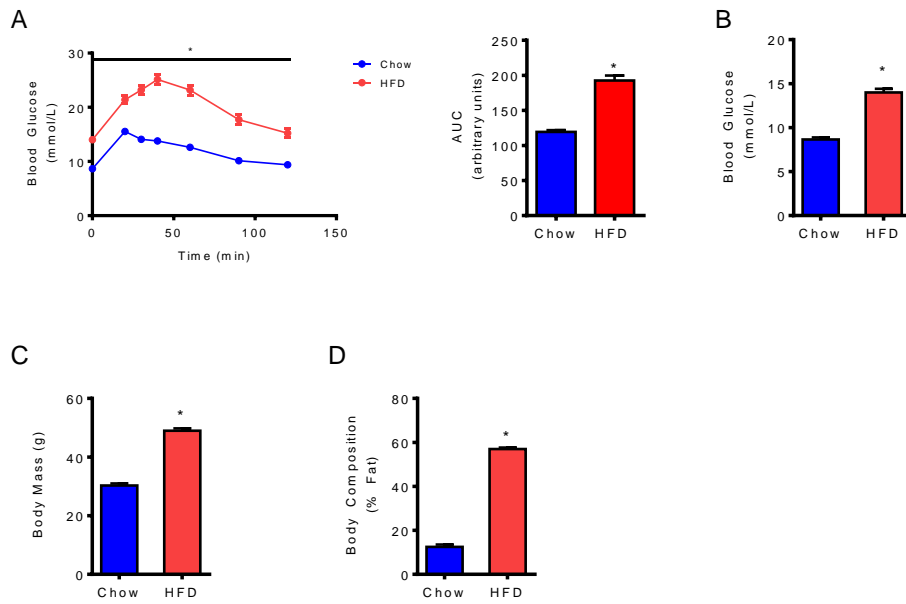


**Figure 18: Long-term high fat feeding induces glucose intolerance and increased adiposity.** C57BL/6 mice (8-10 weeks old) were fed a 60% high fat diet (HFD) for 16 weeks (n=18-22/group). A, Intraperitoneal glucose (0.75 g/kg) tolerance test and area under the curve (AUC) quantification. B, Fast blood glucose measurement. C, D, Body mass and adiposity measurement. Student's unpaired t-test was conducted to determine significance. Values are presented as mean  $\pm$  SEM. \*p<0.05.

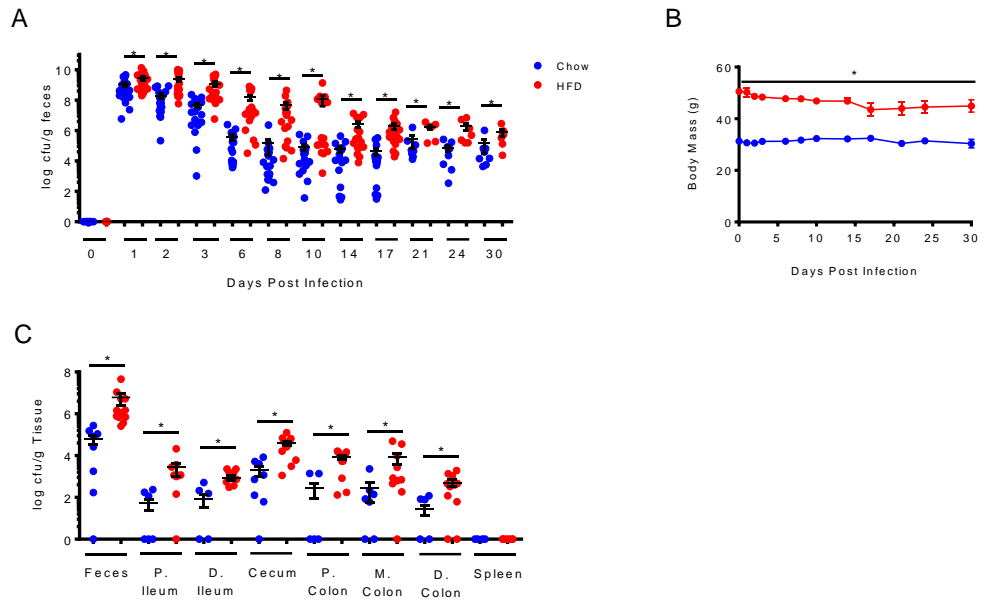


**Figure 19: Diet-induced obesity promotes adherent-invasive *Escherichia coli* expansion and colonization in the lower intestinal tract.** C57BL/6 mice (8-10 weeks old) were fed a 60% high fat diet (HFD) for 16 weeks and pretreated with streptomycin (2 mg/mouse) one day prior to infection with adherent-invasive *Escherichia coli* (AIEC). A, Fecal burdens during the course of infection (n=16-19/group). B, Body mass during the course of infection. C, Tissue burdens at day 17 post infection (n=10-12/group). Student's unpaired t-test was conducted to determine significance. Values are presented as mean  $\pm$  SEM. \*p<0.05.

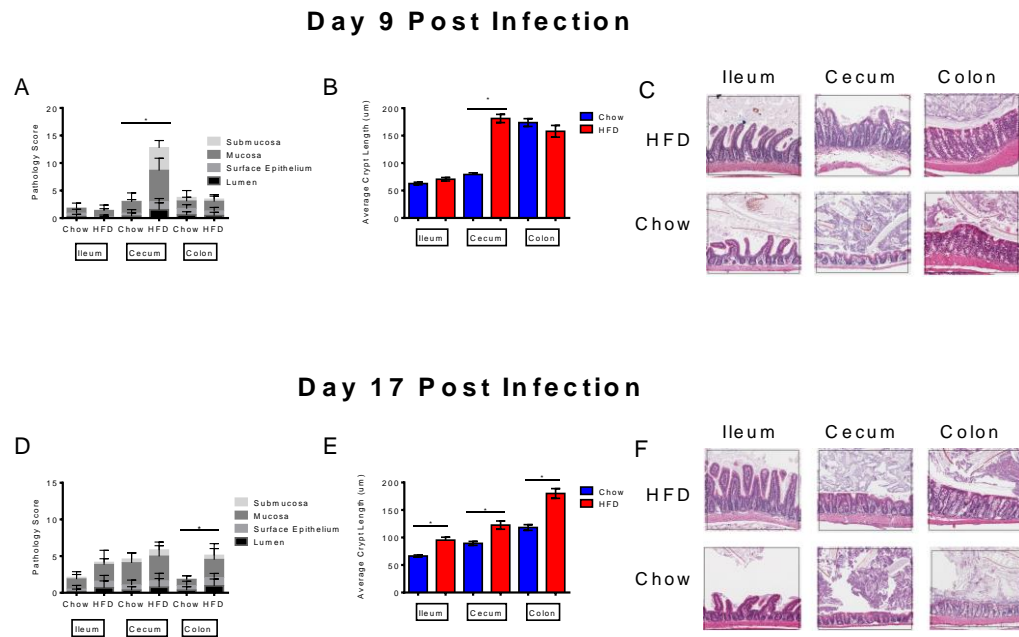


**Figure 20: Diet-induced obesity promotes worsened pathology during adherent-invasive *Escherichia coli* infection.** C57BL/6 mice (8-10 weeks old) were fed a 60% high fat diet (HFD) for 16 weeks and pretreated with streptomycin (2 mg/mouse) one day prior to infection with adherent-invasive *Escherichia coli* (AIEC). Overall pathology, crypt length measurements, and representative images of the ileum, cecum, and colon of AIEC-infected mice at A, B, C, day 9; and D, E, F, day 17 post infection, respectively (n=5 mice/group; 5 images/mouse). Student's unpaired t-test was conducted to determine significance. Values are presented as mean  $\pm$  SEM. \*p<0.05.

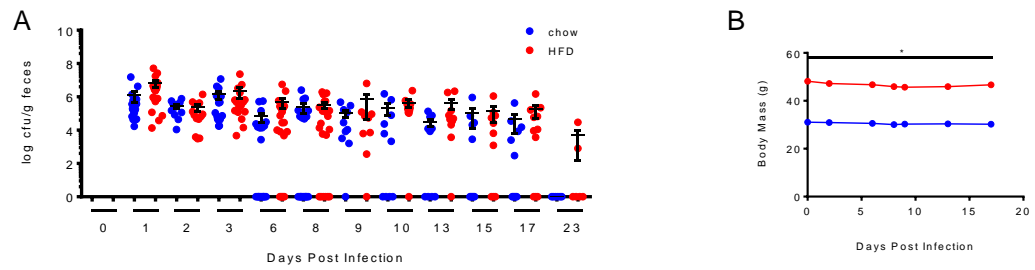


**Figure 21: Streptomycin pretreatment is required for expansion of adherent-invasive *Escherichia coli* in diet-induced obese mice.** C57BL/6 mice (8-10 weeks old) were fed a 60% high fat diet (HFD) for 16 weeks prior to infection with adherent-invasive *Escherichia coli* (n=8-10/group). A, Fecal burdens during the course of infection. B, Body mass during the course of infection. Student's unpaired t-test was conducted to determine significance. Values are presented as mean  $\pm$  SEM. \*p<0.05.

### 3.2.2. IL-22 promotes AIEC expansion in a diet-induced obesity mouse

Our lab has previously showed that during long-term HFD, IL-17 and IL-22 are lowered in the ileum and colon, respectively<sup>212</sup>. These cytokines are important for maintaining intestinal barrier integrity and mucosal immunity and have been implicated in the resolution of AIEC-mediated inflammation<sup>213–217</sup>. Since AIEC was found in elevated levels in the proximal and distal ileum, cecum and colon, we hypothesized that this may be the result of impaired intestinal immune response<sup>212</sup>. Furthermore, we found that IL-22Fc administration lower body mass and blood glucose and improved outcomes from *C. Rodentium* infection in OB and Akita<sup>+/-</sup> mice. Hence, we treated long-term HFD mice with an IL-22Fc compound. Interestingly, our findings showed that IL-22Fc *exacerbated* AIEC expansion compared to HFD mice treated with control IgG, an effect that began at day 2 post infection and persisted until day 17 post AIEC infection (**Fig. 22A**). IL-22 treated HFD mice had significant weight loss but marginal reductions in blood glucose levels (**Fig. 22B-C**). The small effect on blood glucose is likely rooted in the fact that HFD-feeding does not promote overt hyperglycemia in C57Bl/6J mice. The elevated fecal burdens after IL-22Fc treatment also correlated with large increase in tissue burdens at day 17 post infection, but no differences in dissemination (**Fig. 22D**). We assessed IL-22 expression at day 8 post infection, which is when the largest separation in fecal AIEC burden occurs between chow- and HFD-fed mice. There was a significant reduction in the ileum

of HFD mice, but no appreciable/measurable levels of IL-22 transcript in the colon (**Fig. 22E**). Our data showing that IL-22 supplementation increased AIEC expansion may be the result of IL-22's role in promoting antimicrobial peptide secretion. A recent study by *McPhee et al.* showed that AIEC strain NRG857c contained a plasmid-encoded genomic island that conferred resistance to  $\alpha$ - and  $\beta$ -defensins<sup>218</sup>. The ability of AIEC to induce and flourish under host inflammation and antimicrobial responses may allow this strain to expand as bacteria competing for similar resources are eliminated.

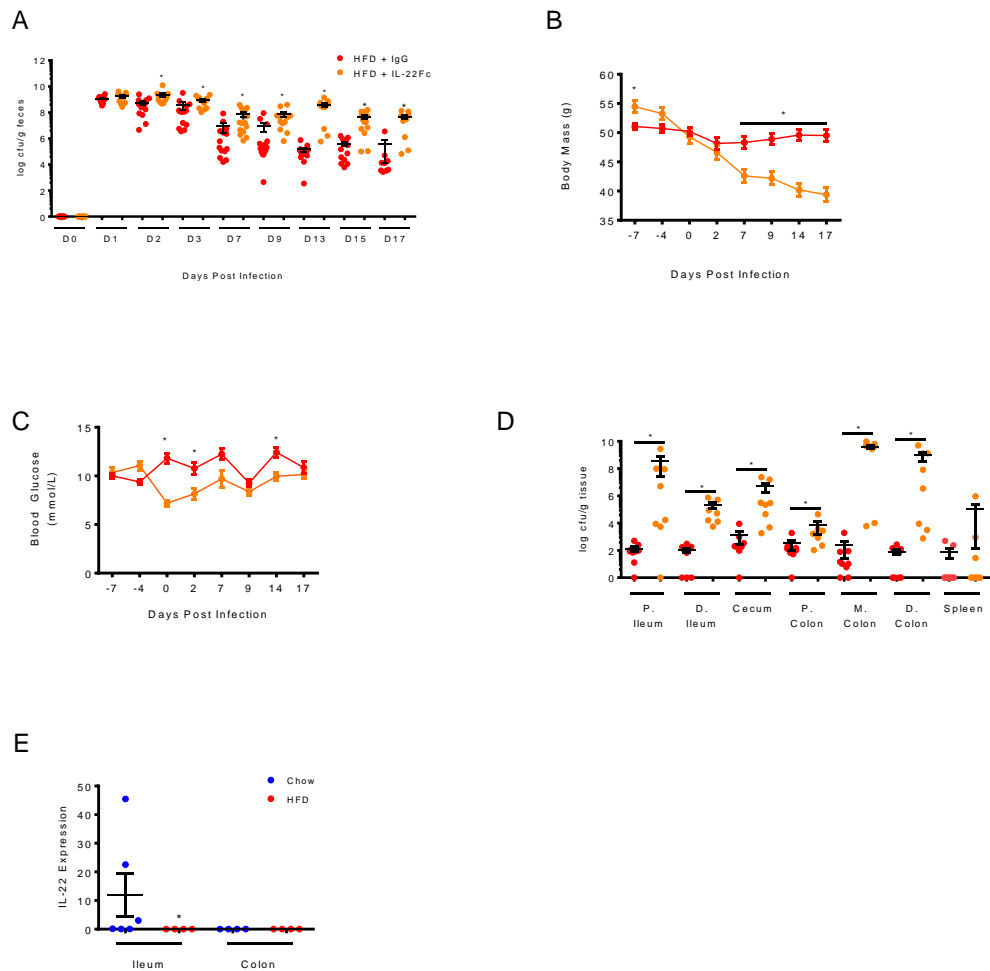


**Figure 22: IL-22 exacerbates expansion of adherent-invasive *Escherichia coli* in diet-induced obese mice.** C57BL/6 mice (8-10 weeks old) were fed a 60% high fat diet (HFD) for 16 weeks and pretreated with streptomycin (2 mg/mouse) one day prior to infection with adherent-invasive *Escherichia coli* (AIEC). Mice were given IL-22Fc or control IgG (150 ug/mouse) three times a week starting one week prior to infection and continuing throughout (n=12-15/group). A, Fecal burdens during the course of infection. B, C, Body mass and blood glucose during the course of infection. D, Tissue burdens at day 17 post infection. E, *il22* gene expression in the ileum and colon at day 8 post infection (n=7-8/group). Student's unpaired t-test was conducted to determine significance. Values are presented as mean  $\pm$  SEM. \*p<0.05.

### **3.2.3. Diet and obesity potentiate AIEC expansion in mouse models of obesity**

To determine if the impaired resolution of AIEC was specific to the 60% HFD or shared with other diets that are widely used to model diet-induced obesity, we tested a long-term 45% HFD (feeding for 16 weeks) in the same AIEC colitis model over the course of 30 days. As expected, mice fed a 45% HFD for 16 weeks had significantly higher body mass compared than their chow-fed control mice (**Fig. 23A**). In agreement with our other results using a 60% HFD, mice fed a 45% HFD had elevated fecal burdens from day 1 until day 17 post infection with AIEC (**Fig. 23B**).

We next compared fecal burdens of mice fed either a 60% or a 45% HFD at days 8, 13, 17, and 24 days post infection to determine what relation, if any, body mass may have to fecal burden during diet-induced obesity (**Fig. 24A-D**). This provides some scope to find if the level of obesity influences infectious colitis since 45% HFD mice were approximately 10 grams lighter than 60% HFD mice. We found no correlation at days 8, 13, 17 and 24 between body mass and fecal burden between either HFD group (**Fig. 24A-D**). The 45% HFD mice had significantly lower fecal burdens of AIEC at day 17 and 24 ( $3.3 \times 10^6$  vs.  $2.0 \times 10^5$  cfu/g feces;  $2.0 \times 10^6$  vs.  $1.2 \times 10^5$  cfu/g feces, respectively;  $p < 0.05$ ). As some mice in both HFD groups had similar body masses, it appears that body mass or

obesity status is not the key factor, but rather these data indicate that diet composition may be a driving factor promoting AIEC burden. However, it was unclear if the high fat content or another dietary component of these obesogenic diets was contributing to the expansion of AIEC. Overall, these findings reveal that diet-induced obesity potentiates AIEC expansion in the gut, but within an obese state, body mass is not a major predictor of AIEC burden. These data position diet components as drivers of AIEC burden in the gut.

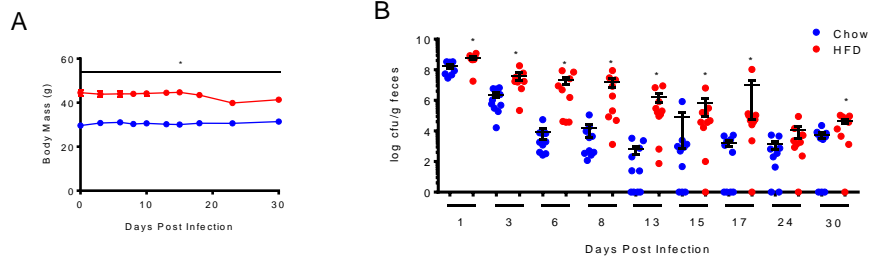


**Figure 23: An alternative diet-induced obesity model promotes adherent-invasive *Escherichia coli* expansion.** C57BL/6 mice (8-10 weeks old) were fed a 45% high fat diet (HFD) for 16 weeks and pretreated with streptomycin (2 mg/mouse) one day prior to infection with adherent-invasive *Escherichia coli* (n=8-10/group). A, Body mass during the course of infection. B, Fecal burdens during the course of infection. Student's unpaired t-test was conducted to determine significance. Values are presented as mean  $\pm$  SEM. \*p<0.05.

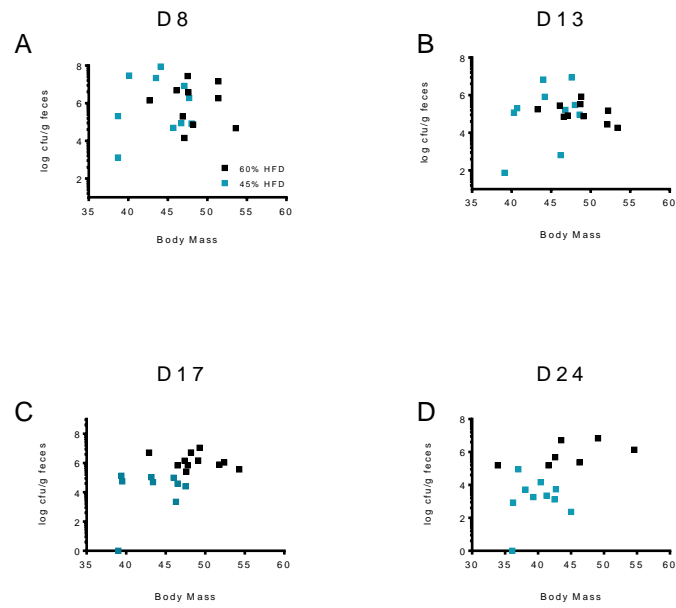


**Figure 24: Body mass dose not correlate with bacterial burden during adherent-invasive *Escherichia coli* infection of murine models of diet-induced obesity.** Comparison of fecal burden data from 45% and 60% high fat diet (HFD)-fed mice infected with adherent-invasive *Escherichia coli* at A, 8; B, 13; C, 17; and D, 24 post infection.

### **3.2.4. Diet, independent of obesity and aging, can promote AIEC expansion**

To parse out the effects of obesity from diet, we implemented a short-term HFD protocol in which mice are switched to 60% HFD one day prior to AIEC infection and remain on either the HFD or chow diet throughout the course of infection. There were no initial differences in body weight at the onset of diet, but body mass was slightly higher in HFD-fed mice during infection (**Fig. 25A**). Fecal burdens were significantly higher in the HFD-fed group from days 3-9 (**Fig. 25B**). At day 9, differences in organ burdens were only observed in the cecum and the proximal colon, where HFD-mice had higher AIEC burdens (**Fig. 25C**). These results indicate that the constituents of the HFD may be a major factor responsible for AIEC outgrowth, independent of overt obesity. However, our data does not completely rule out a role for obesity, since even short term HFD fed mice had higher body mass and adiposity compared to chow-fed mice. Further, by comparing the data we collected on long-term and short-term HFD, we observed that long-term HFD had significantly higher fecal AIEC burdens compared to short-term HFD and chow controls from day 1 to 9 post infection while short-term HFD had significantly higher burdens than chow-fed control mice from day 3 to 9 post infection. Critically, while the short-term HFD group had elevated AIEC burdens, the body mass of short term HFD-fed mice was significantly lower than the long-term chow-fed control group of mice. This is

very important because despite lower body mass, short-term-HFD fed mice, still had significantly higher burdens compared to chow-fed (long-term, control) mice that were older indicating that diet, independent of body mass, may play an important role in the regulation of AIEC infection. It is interesting to speculate that long-term HFD feeding and the physiological adaptations associated with obesity may be required for augmented colonization in the ileum and medial and distal colon.

As a major difference between the short- and long-term experiments is the age of mice, we conducted another short-term HFD experiment with mice age-matched to the long-term cohorts to assess the impact that age may have on the observed phenotype of increased AIEC burdens. Similar to obesity, aging has been associated with a chronic low-grade inflammatory state and a recent study by *Thevaranjan et al.* implicated age-related dysbiosis with increased intestinal permeability impaired intestinal barrier integrity and circulating pro-inflammatory cytokines<sup>219–223</sup>. Similar to our short-term HFD experiment, we observed a delayed onset of AIEC expansion occurring at day 3 post infection, lasting until day 15 (**Fig. 26A**), concurrently with an increase in body mass (**Fig. 26B**). Comparing the short- and long-term feeding experiments, we observed that the level of bacterial burden in the short-term HFD cohort, while significantly different from chow-fed controls starting at day 3 post infection, still did not reach the high levels of AIEC burden seen in long-term HFD-fed mice (**Fig.**

**27A)** indicating that while diet can promote AIEC expansion, there may be some underlying physiologic changes that occur in long-term feeding that may further exacerbate AIEC colonization or resolution. Further confirming diet as a major component in promoting AIEC expansion was our finding that the short-term HFD mice did not differ in body mass from long-term chow-fed controls after 3 days post infection, despite significantly higher fecal burdens (**Fig. 27B**). As expected, the long-term HFD cohort had significantly higher adiposity compared to all other groups (**Fig. 27C**).

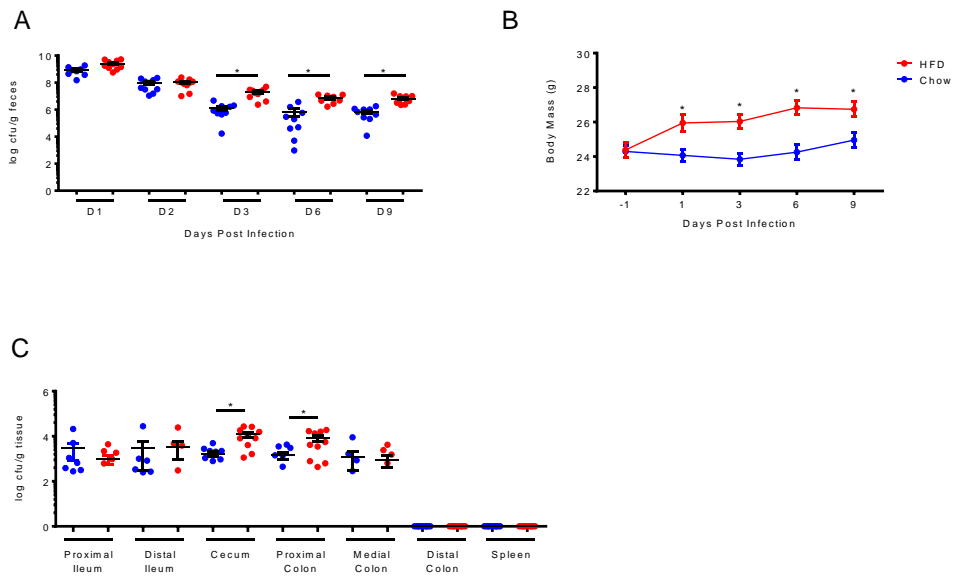


**Figure 25: Short-term high fat feeding promotes adherent-invasive *Escherichia coli* expansion.** C57BL/6 mice (8-10 weeks old) were pretreated with streptomycin (2 mg/mouse) and started on a 60% high fat diet (HFD) one day prior to infection with adherent-invasive *Escherichia coli* (n=8-10/group). A, Fecal burdens during the course of infection. B, Body mass during the course of infection. C, Tissue burdens at day 9 post infection. Student's unpaired t-test was conducted to determine significance. Values are presented as mean  $\pm$  SEM. \* $p < 0.05$ .

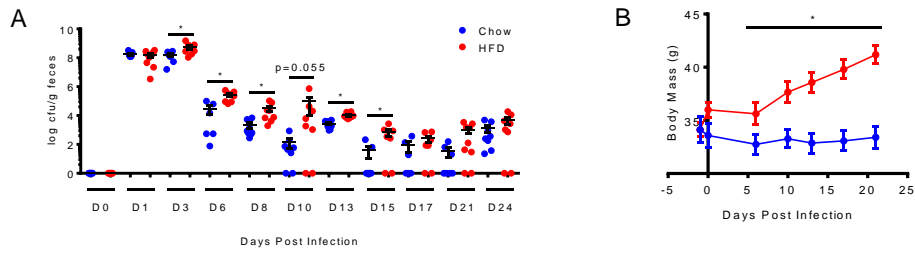


**Figure 26: High fat feeding, independent of obesity and age, can promote adherent-invasive *Escherichia coli* expansion.** C57BL/6 mice (24 weeks old) were pretreated with streptomycin (2 mg/mouse) and started on a 60% high fat diet (HFD) one day prior to infection with adherent-invasive *Escherichia coli* (n=9-12/group). A, Fecal burdens during the course of infection. B, Body mass during the course of infection. Student's unpaired t-test was conducted to determine significance. Values are presented as mean  $\pm$  SEM. \*p<0.05.

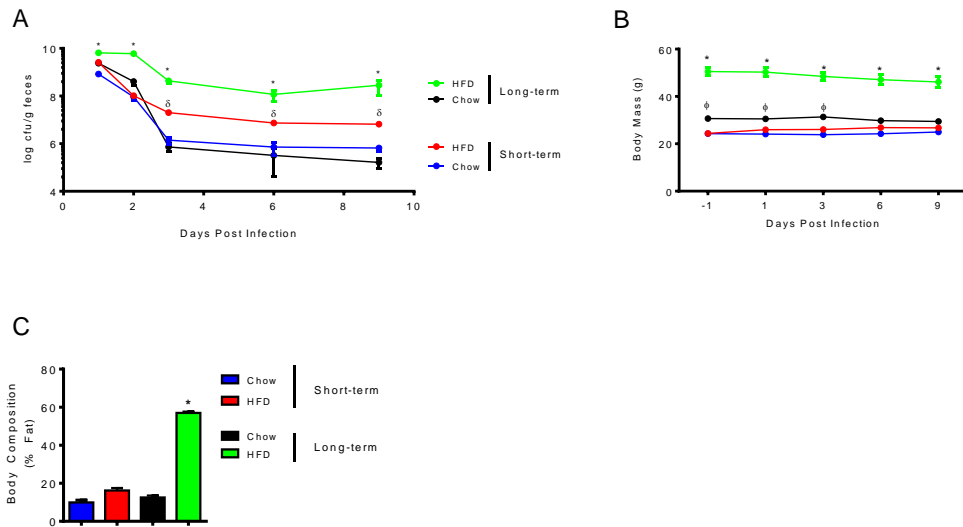


**Figure 27: Comparison of short-term and long-term high fat feeding models during adherent-invasive *Escherichia coli* infection.** Comparison of fecal burden and body mass from mice fed a long-term or short-term 60% high fat diet (HFD) and age-matched chow-fed controls. A, Fecal burdens during the course of infection. B, Body mass during the course of infection. C, Adiposity measurements prior to infection. One-way ANOVA was conducted to determine significance. Values are presented as mean  $\pm$  SEM. Significance was set at  $p < 0.05$ . \*denotes difference from all groups.  $\delta$  denotes difference from chow-fed controls.  $\Phi$  denotes difference from short-term HFD- and chow-fed mice.

### 3.3. Components of an obesogenic diet promote adherent-invasive *Escherichia coli* expansion

#### 3.3.1. HFD after infection impacts AIEC colonization

We next tested the impact of changing the timing of dietary changes on AIEC colonization. We infected C57BL/6J mice with AIEC and started HFD feeding one day after infection. We observed statistically higher fecal burdens at day 3, 8, 10, and 17 post infection when HFD was initiated after AIEC infection (**Fig. 28A**) and differences in body mass starting at day 13 post infection (**Fig. 28B**).

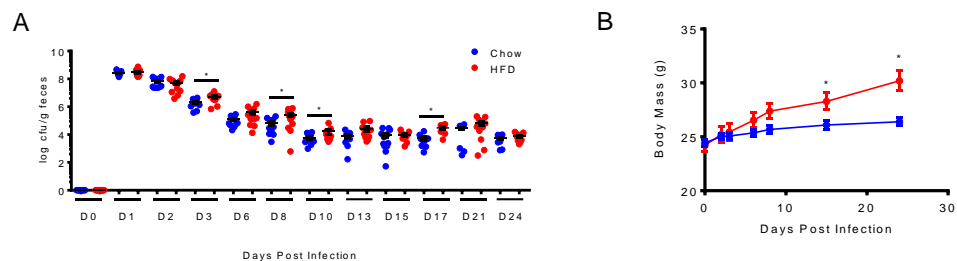


**Figure 28: Initiation of high fat feeding during adherent-invasive *Escherichia coli* infection promotes bacterial expansion.** C57BL/6 mice (8-10 weeks old) were pretreated with streptomycin (2 mg/mouse) one day prior to infection with adherent-invasive *Escherichia coli* (AIEC) and started on a 60% high fat diet (HFD) one day after (n=8-10/group). A, Fecal burdens during the course of infection. B, Body mass during the course of infection. Student's unpaired t-test was conducted to determine significance. Values are presented as mean  $\pm$  SEM. \* $p < 0.05$ .

### **3.3.2. Low fibre promotes AIEC expansion**

Next, we wanted to determine what component of the diet may be responsible for AIEC expansion. In conjunction with the high fat content of the 60% HFD, the diet formula is also comprised of higher sucrose content and lower fibre content. As many studies look at the impact of Western diet on metabolic syndrome and other diseases, a major confounding variable is the fact that in comparison with typical (and highly variable) “chow” diets the HFD diets used are typically also comprised of higher levels of sugars (in our case, sucrose) and lower levels of fibre in conjunction with the high fat content. Each of these components have been individually associated with intestinal health. A study looking at the impact of high fat (without high sugar) diet in mice showed that high fat feeding exacerbated DSS-induced colitis with elevated colonic levels of TNF- $\alpha$  and interferon- $\gamma$ <sup>224</sup>. Another study looking at high sugar diets in mice saw a similar exacerbation of DSS-induced colitis as a result of reduced short chain fatty acids (SCFAs) and increased intestinal permeability<sup>225</sup>. Fibre content has been a major area of interest because of their influence on microbiota composition and SCFA production. Diets low in fibre have been associated with decreased levels of butyrate as well as loss of mucosal barrier integrity<sup>226,227</sup>. Conversely, diets high in fibre have shown to be protective from DSS-induced colitis and development of metabolic disease<sup>213,228–230</sup>. So, it is unclear whether

there is a specific component or combination of components of the diet that promotes AIEC expansion during high fat feeding.

We utilized defined control diets as comparators for the 60% HFD. There are two main control diets for the 60% HFD: a sucrose-matched diet which has the same sucrose and fibre content as the 60% HFD but with reduced fat level; a fibre-matched diet that has the same amount of fibre but has a reduced fat level and no sucrose. These diets contain the same ingredients in similar proportions except a majority of the fat and sucrose content has been substituted with corn starch and maltodextrin. To test the impact that fat content has on the AIEC infection, we used the high sucrose, low fibre-matched diet (HSLF). We used both the short-term and long-term feeding models with this control diet.

From short-term experiments, we first made the important observation that fat content was not the key factor driving AIEC burden. Our data show that AIEC burden were similar in HFD-fed mice and mice fed a HSLF (low in fat but matched to the HFD in sucrose and fibre content). The fecal burdens of AIEC were the same in HFD and the HSLF fed mice (**Fig. 29A**). There was a significant difference in body mass starting at day 8 post infection, with the HFD mice expectedly more obese (**Fig. 29B**). Interestingly, the HFD mice have significantly higher adiposity than the HSLF-fed mice (16.6% vs. 8.5%, respectively; **Fig. 29C**), with the HSLF mice having similar adiposity to age-matched chow-fed mice (8.5%

vs. 9.3%). This finding supports the idea that differences in adiposity or body mass do not solely account for differences in AIEC colonization. We also did not observe any differences in tissue burdens at day 17 post infection in HFD-fed mice and HSLF-fed mice (**Fig. 29D**). Similar to the short-term study, we saw no significant differences in fecal burden (**Fig. 30A**), despite the HFD group being significantly heavier throughout infection (**Fig. 30B**). Again, no differences in tissue burden or dissemination were observed at day 17 post infection in long-term (16 week) HFD-fed mice and HSLF-fed mice (**Fig. 30C**).

To assess the influence of low fibre, we used the low fat, no sucrose, low fibre control diet (NSLF) in our short-term feeding model. We compared this to the regular chow diet as a comparison of high vs. low fibre. We observed elevated fecal burdens from day 1-15 post infection in the NSLF mice compared to chow-fed mice (**Fig. 31A**) despite no differences in body mass (**Fig. 31B**). We also observed higher tissue burdens in the distal ileum, cecum, and proximal colon at day 17 post infection (**Fig. 31C**). This finding would suggest that the low fibre content in the diet may play a role in promoting AIEC expansion. However, one confounding variable in all three diets is the presence of maltodextrin. A recent *in vitro* study showed that maltodextrin, irrespective of chain length, promoted AIEC growth and biofilm formation<sup>205</sup>. This study also found that sucrose did not confer a growth advantage to AIEC, which supports our hypothesis that the low fibre content, not high sucrose in the diet can promote

AIEC growth. However, it is currently unclear if the phenotype we observe is the result of maltodextrin in the diet and it is recommended that future experiments control for maltodextrin quantity.

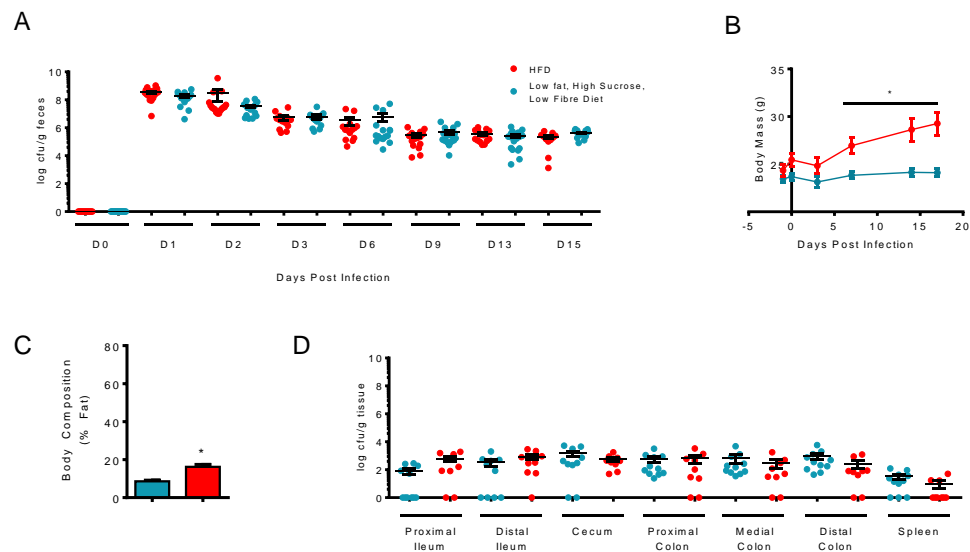


**Figure 29: Short-term feeding with a high fat diet or sucrose and fibre-matched control diet confers similar adherent-invasive *Escherichia coli* infection kinetics.** C57BL/6 mice (8-10 weeks old) were pretreated with streptomycin (2 mg/mouse) and started on a 60% high fat diet (HFD; n=9) or control diet (low fat, high sucrose, low fibre; n=13) one day prior to infection with adherent-invasive *Escherichia coli*. A, Fecal burdens during the course of infection. B, Body mass during the course of infection (n=8-10/group). C, Tissue burdens at day 17 post infection (n=9-13/group). Student's unpaired t-test was conducted to determine significance. Values are presented as mean  $\pm$  SEM. \*p<0.05.

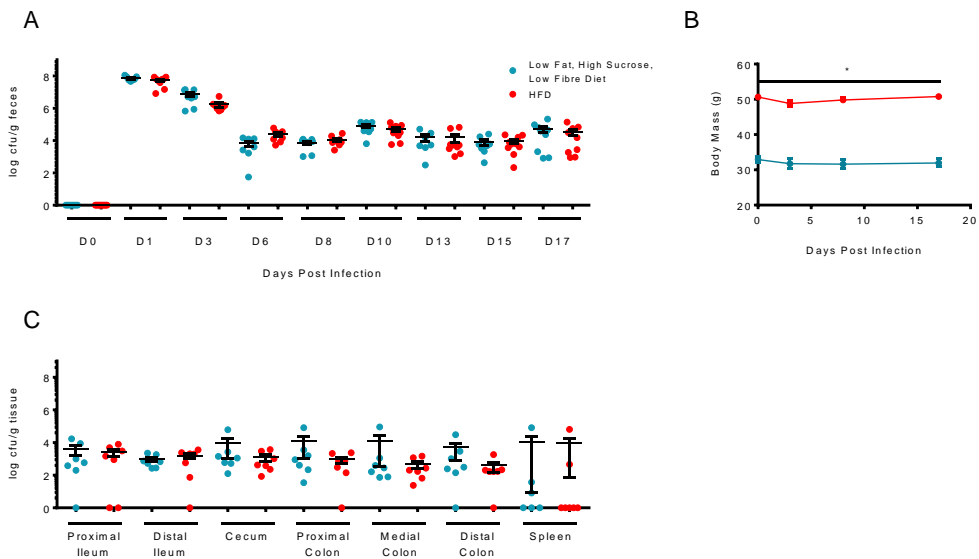


**Figure 30: Long-term feeding with a high fat diet or sucrose and fibre-matched control diet confers similar adherent-invasive *Escherichia coli* infection kinetics.** C57BL/6 mice (8-10 weeks old) were fed a 60% high fat diet (HFD; n=8) or control diet (low fat, high sucrose, low fibre; n=9) for 16 weeks and pretreated with streptomycin (2 mg/mouse) one day prior to infection with adherent-invasive *Escherichia coli* (AIEC). A, Fecal burdens during the course of infection (n=6-9/group). B, Body mass during the course of infection. C, Tissue burdens at day 17 post infection (n=8-9/group). Student's unpaired t-test was conducted to determine significance. Values are presented as mean  $\pm$  SEM. \*p<0.05.

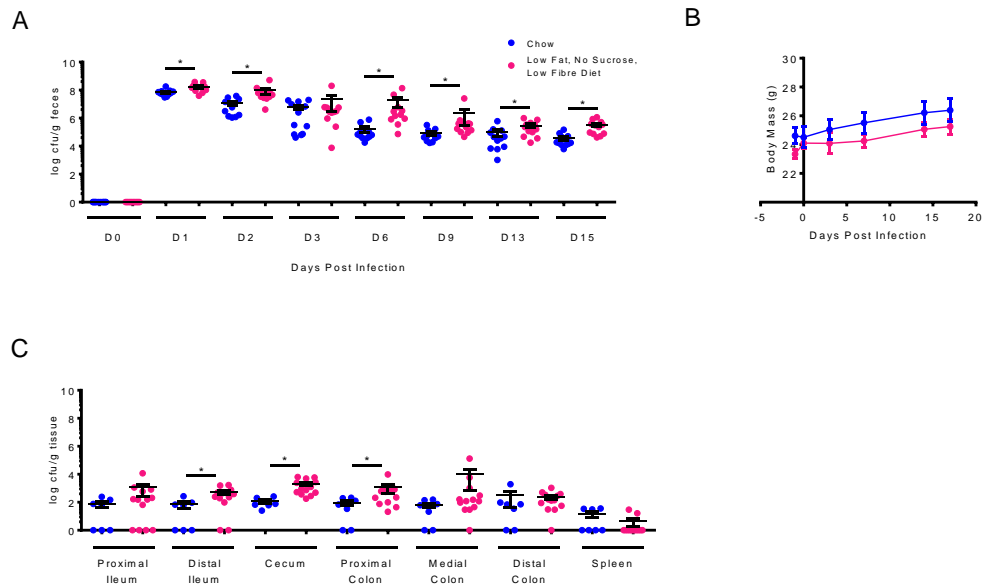


**Figure 31: Short-term feeding with a low fibre diet promotes adherent-invasive *Escherichia coli* expansion and colonization.** C57BL/6 mice (8-10 weeks old) were pretreated with streptomycin (2 mg/mouse) and started on a low fibre control diet one day prior to infection with adherent-invasive *Escherichia coli* (n=7-13/group). A, Fecal burdens during the course of infection. B, Body mass during the course of infection. C, Tissue burdens at day 17 post infection. Student's unpaired t-test was conducted to determine significance. Values are presented as mean  $\pm$  SEM. \*p<0.05.

### 3.3.3. Short-term diet modification reduces tissue but not fecal burden

Next, we wanted to assess whether intervention with dietary fibre could rescue the HFD-promoted expansion of AIEC. We hybridized our long- and short-term feeding models for the intervention study and started long-term HFD mice on regular chow diet one day prior to infection. As expected, the long-term HFD -> chow mice were significantly heavier than chow-fed controls but underwent relatively rapid weight loss over the course of infection (**Fig. 32A**). The long-term HFD -> chow-fed mice still had significantly higher fecal burdens from day 3 to 9 post infection (**Fig. 32B**) but at day 9, only the medial colon showed a significant elevation in the long-term HFD -> chow-fed mice (**Fig. 32C**). The elevated fecal burdens, in this case, may not correlate with increased colonization but may be the result of increased AIEC shedding.

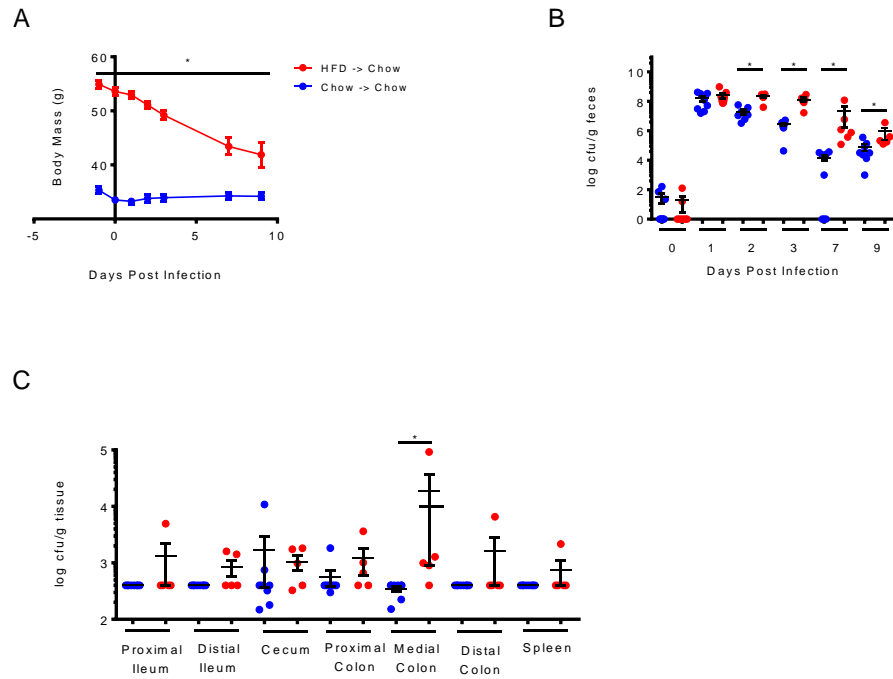


**Figure 32: Intervention with regular chow diet rescues tissue colonization of adherent-invasive *Escherichia coli* in a diet-induced obese mouse model.** C57BL/6 mice (8-10 weeks old) were fed a 60% high fat diet (HFD) for 16 weeks and pretreated with streptomycin (2 mg/mouse) and started on a regular chow diet one day prior to infection with adherent-invasive *Escherichia coli* (n=8-9/group). A, Body mass during the course of infection. B, Fecal burdens during the course of infection (n=7-9/group). C, Tissue burdens at day 9 post infection (n=8-9/group). Student's unpaired t-test was conducted to determine significance. Values are presented as mean  $\pm$  SEM. \*p<0.05.

### **3.3.4. Cellulose supplementation does not rescue HFD-promoted AIEC expansion**

While the switch from HFD to chow was able to mitigate aspects of worse AIEC colonization, it was a dramatic change in diet composition. To more directly assess the impact of fibre, we tested the effectiveness of cellulose (the fibre component of HFD) in intervention and prevention feeding models.

We provided long-term HFD-fed mice with HFD supplemented with 200 grams of cellulose one day prior to infection. There were no differences in fecal burden (**Fig. 33A**) but we observed significant weight loss in the HFD supplemented with cellulose group (**Fig. 33B**). For our prevention model, mice were fed a chow diet, HFD, or HFD supplemented with 200 grams of cellulose for 16 weeks prior to infection. We observed that cellulose transiently increased AIEC fecal burden at 9 days post infection but saw no major differences at later time points (**Fig. 34A**). Long-term HFD-fed mice were significantly heavier than all other groups, while mice fed HFD supplemented with cellulose were significantly heavier than chow-fed controls (**Fig. 34B**). Mice fed HFD supplemented with cellulose had significantly higher AIEC colonization in the distal ileum, but no other differences were observed at day 17 post infection ( $4.2 \times 10^7$  vs. 28579 vs. 4960 log cfu/g tissue, HFD supplemented with cellulose, HFD, and chow-fed control, respectively;  $p < 0.05$ ; **Fig. 34C**). A confounder in this

long-term prevention study was the barbering activity of the mice. Multiple mice had skin lesions prior to infection.

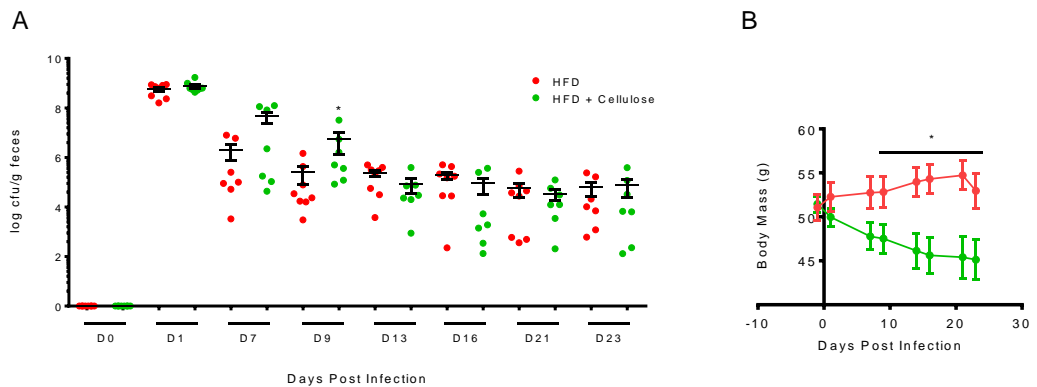


**Figure 33: Intervention with a high fat diet supplemented with cellulose does not impact adherent-invasive *Escherichia coli* colonization** C57BL/6 mice (8-10 weeks old) were fed a 60% high fat diet (HFD) for 16 weeks and pretreated with streptomycin (2 mg/mouse) and started on a high fat diet supplemented with cellulose (200 grams) one day prior to infection with adherent-invasive *Escherichia coli* (n=8-9/group). A, Body mass during the course of infection. B, Fecal burdens during the course of infection. Student's unpaired t-test was conducted to determine significance. Values are presented as mean  $\pm$  SEM. \*p<0.05.

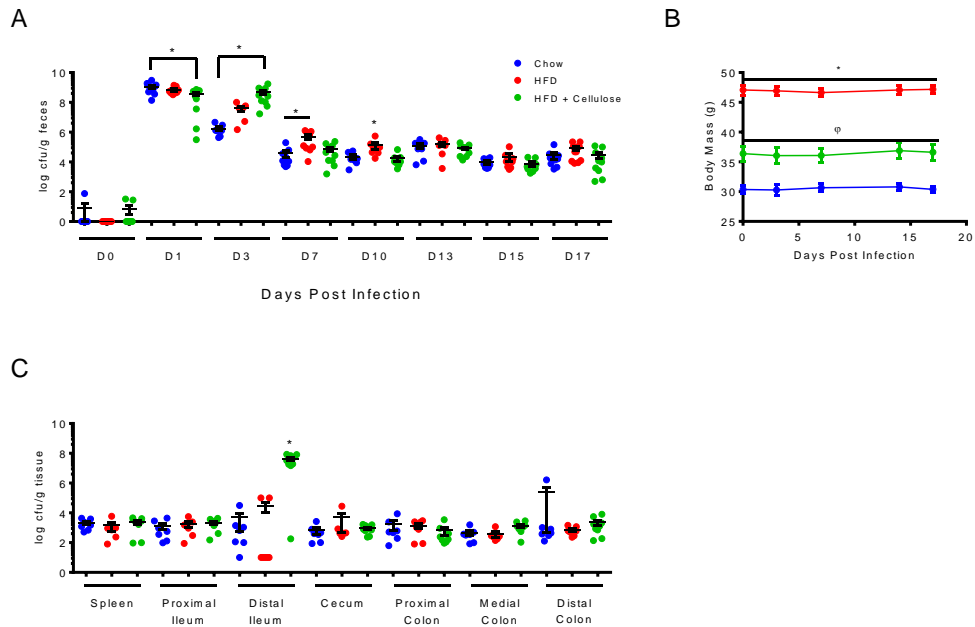


**Figure 34: Long-term feeding with high fat diet supplemented with cellulose does not prevent obesity-induced expansion of adherent-invasive *Escherichia coli*.** C57BL/6 mice (8-10 weeks old) were fed a 60% high fat diet (HFD) or 60% HFD supplemented with cellulose (200 grams) for 16 weeks and pretreated with streptomycin (2 mg/mouse) one day prior to infection with adherent-invasive *Escherichia coli* (n=8-10/group). A, Body mass during the course of infection. B, Fecal burdens during the course of infection. C, Tissue burdens at day 17 post infection. One-way ANOVA was conducted to determine significance. Values are presented as mean  $\pm$  SEM. Significance was set at  $p < 0.05$ . \*denotes difference from all groups.  $\Phi$  denotes difference chow-fed controls.

## **Chapter 4 - Discussion**

Obesity is a rapidly growing global health concern that affects tens of millions of people worldwide. It is a major predictor of T2D in addition to a wide range of other co-morbidities such as cardiovascular disease and non-alcoholic liver disease. Obesity has been associated with numerous physiological changes including insulin resistance, low-grade inflammation in metabolic tissues, impairment of the intestinal barrier, and changes in intestinal microbial composition. Importantly, insulin resistance and the low-grade metabolic inflammation contribute towards the gradual development of T2D. People with diabetes share many of the comorbidities of obese patients but have also been shown to be at an increased risk of contracting multiple types of bacterial infections and suffering worsened outcomes.

#### **4.1 Hyperglycemia, independent of obesity, worsens outcomes of enteric infections**

This is one of the first reports to parse out the independent effects of obesity and hyperglycemia on enteric infection in mice. We have shown that hyperglycemia, independent of obesity, promotes mortality during enteric infection with *C. rodentium*. This effect is caused by dehydration and can be rescued with insulin treatment or Wnt-inhibition. This study further strengthens the burgeoning connections between glucose concentration and Wnt signalling.

Similar to other reports, our experiments using OB mice demonstrated that OB mice *can* have increased mortality during *C. rodentium* infection. Previous studies suggested that IL-22 deficiency and increased pathogen dissemination are responsible for mortality, this was not consistent with our findings. By infecting 10- and 22-week-old OB mice, we showed that 10-week-old hyperglycemic mice succumb to infection, whereas 22-week-old OB mice do not show profound hyperglycemia or mortality. Both groups of OB mice had similar levels of bacterial pathogen dissemination, indicating that loss of intestinal barrier integrity was not responsible for mortality. By using a HFD mouse model, we were able to control for body mass as these mice were of similar weight to the 10-week-old OB mice but did not succumb to infection and did not have elevated fecal or tissue burdens of *C. rodentium*. The mortality rate of 60% by 10 days post infection of the 10-week-old OB mouse group in this experiment differed from those we observed in our initial pilot experiment and those previously reported<sup>157,231</sup>. This was most likely due to the fact that the infection was terminated at day 10 rather than tracked for a longer period where complete mortality was observed at day 14 post infection in our pilot experiment. In the study by Wang *et al.*, 5- to 8-week-old female OB and leptin receptor-deficient (*db/db*<sup>-/-</sup>) mice were used<sup>157</sup>. The majority of the mortality observed in OB mice occurred between days 10-13 post infection. These mice would have been within the hyperglycemic age range, but blood glucose

measurements were not taken or reported for these infection studies. Also, *db/db*<sup>-/-</sup> mice are known to have more severe hyperglycemia and diabetic complications than OB counterparts<sup>180,232</sup>. As mentioned previously, leptin has numerous physiological roles in addition to its regulation of satiety. This may partially account for the mortality observed in the older OB mouse group.

To address the confounding factor of leptin-deficiency and understand if obesity plus hyperglycemia was required for increased mortality during enteric infection, we utilized the Akita<sup>+/-</sup> mouse model of T1D. Our findings using Akita<sup>+/-</sup> mice showed that hyperglycemia was sufficient for mortality during *C. rodentium* infection, which was caused by dehydration, but not related to increased pathogen dissemination. Similar to the study by *Thaiss et al.*, we showed that insulin supplementation rescued diabetic mice from succumbing to *C. rodentium* infection; in addition, however, we found that fluid replenishment and Wnt inhibition could also rescue these diabetic mice from dying during *C. rodentium* infection<sup>231</sup>. These findings indicate that dehydration was responsible for hyperglycemia-mediated mortality. We did not find any overt differences in fecal or tissue burdens between treated (insulin, fluid therapy, LGK-974) and untreated Akita<sup>+/-</sup> or WT mice. *Thaiss et al.* primarily used a streptozotocin-induced diabetic mouse model, which may account for some of the differences<sup>233</sup>. Streptozotocin is a broad spectrum antibiotic that was first isolated from *Streptomyces acromogenes*<sup>234,235</sup>. It is one of the most widely used

chemicals for the induction of diabetes in experimental animal models due to its  $\beta$ -cell toxicity<sup>234–237</sup>. However, it has also been shown to cause non-organ specific toxicity and dose-dependent mortality in mice and rats<sup>238,239</sup>. Streptozotocin is a cytotoxic glucose analogue and DNA alkylating agent that is able to enter cells through the GLUT2 transporter and inhibit DNA synthesis<sup>240–242</sup>. While GLUT2 is abundantly expressed in pancreatic  $\beta$  cells, it is also expressed by other tissues such as the liver, kidney, and intestinal epithelium<sup>235,240,243–246</sup>. Therefore, it is possible that the elevated levels of dissemination may be the result of streptozotocin toxicity on the intestinal epithelium, causing the loss of barrier integrity. Gender specific responses have also been observed with streptozotocin treatment, with males displaying a larger response<sup>247</sup>. Multiple low dose ( $\leq 45$  mg/kg) treatments have been recommended over the commonly used single high dose ( $\geq 100$  mg/kg) treatment for faster induction of hyperglycemia and reduction in toxicity<sup>234,235,239</sup>. In the study by *Thaiss et al.*, diabetes was induced through a daily intraperitoneal injection of streptozotocin (100 mg/kg) over two days<sup>231</sup>. Mice were used within 2-3 weeks of injection, but no comment was made regarding the gender of mice used or any off-target complications caused by streptozotocin. While Akita<sup>+/-</sup> mice were used in this study, only elevated tissue burdens were presented with no mention on survival rate<sup>233</sup>.

Similar to *Wang et al.*, we showed that exogenous IL-22 was able to rescue both OB and Akita<sup>+/-</sup> mice from *C. rodentium*-induced mortality<sup>248</sup>.

However, we found no differences in IL-22 expression in Akita<sup>+/-</sup> mice during infection. We also showed that exogenous IL-22 drastically reduced body mass and lowered blood glucose levels. We hypothesize that it is the metabolic effects, specifically the glucose-lowering capability, of IL-22 that confer protection from *C. rodentium*-induced mortality.

While *C. rodentium* is primarily considered a self-limiting model of intestinal colitis, it has been shown to cause mortality in three strains of mice (C3H, C3O, FVB)<sup>154,156,249</sup>. It was determined that these mice succumbed to *C. rodentium* infection as a result of dehydration<sup>155,249</sup>. Work by the Gruenheid lab determined this process to be the result of a genetic predisposition towards excessive Rspodin expression during *C. rodentium* infection<sup>156,202</sup>. Rspodins are Wnt-mediators that stabilize Wnt-receptor complexes to facilitate signalling<sup>90</sup>. Our finding that Wnt inhibition was able to rescue diabetic mice from *C. rodentium*-induced mortality implicates the involvement of the Wnt signalling cascade in the susceptibility of diabetic mice to outcomes from enteric infection. However, we were unable to observe any differences in gene expression of Rspodins at day 7 post infection or differences in intestinal cell proliferation at day 9 post infection. It is possible that there is a cell-specific dysregulation in Rspodin production or that the timing of tissue collection was not appropriate. Future studies should further verify Rspodin involvement through time course studies and cell-specific secretion assays. In conjunction

with our finding that fluid replenishment can also rescue from mortality and the lack of differences in crypt hyperplasia and Wnt mediators implies a potential defect in differentiation of intestinal cells responsible for water reabsorption or fluid balance rather than simply unregulated cell proliferation. Our data also strengthens the growing connection between high glucose levels and Wnt activation. However, there has been some controversy into the exact mechanism through which hyperglycemia and canonical Wnt signalling interact.

Hyperglycemia has been associated with an increased risk of colon cancer through the priming of Wnt/ $\beta$ -catenin signalling<sup>136-144</sup>. Recently, a study conducted by Min *et al.*, looked at the impact of hyperglycemia on the proliferation and differentiation of intestinal crypt cells in streptozotocin-induced diabetic mice. They found that the efficacy of Notch signalling was impaired in diabetic mice. Transcript analysis of the small intestine showed elevated levels of Msi1, an upstream transcription factor of Notch that is also Wnt-regulated. However, Notch, itself, and other downstream effectors such as Hes1, were lower in diabetic mice compared to the controls indicating that Notch activity is impaired<sup>147</sup>. Notch signalling is essential for intestinal stem cell maintenance as well as differentiation towards absorptive cell lineage<sup>250-253</sup>. Deletions of Notch or Hes1 have resulted in the loss of Lgr5+ intestinal stem cells as well as skewing intestinal cell fate towards a secretory cell lineage<sup>93,96,251,252</sup>. A study by Tian *et al.* investigating the roles of Wnt and Notch signalling in

intestinal homeostasis found that Notch inhibition increased the number of lysozyme (a Paneth cell marker)-expressing cells, indicating a biased differentiation towards Paneth cells, but Wnt inhibition was able to rescue this phenotype<sup>95</sup>. This study also found that in the presence of Notch blockade, there was an increase in Wnt signalling, evidenced by increases in downstream Wnt targets, *Axin2* and *Sox9*, and Wnt expression<sup>95</sup>. A study by *Cheng et al.* found that 3-hydroxy-3-methylglutaryl-Coa synthase 2, a key enzyme in ketosis, was a key regulator of intestinal stem cell differentiation through the production of  $\beta$ -hydroxybutyrate<sup>148</sup>. Mice given a low-carbohydrate, ketogenic diet had improved intestinal stem cell function and post-injury regeneration but those given glucose-supplemented drinking water for 2-4 weeks had markedly reduced Lgr5+ stem cell population and increased populations of Paneth and goblet cells. The glucose-mediated response could be rescued with a single bolus of  $\beta$ -hydroxybutyrate. In our model, hyperglycemia may be facilitating Wnt-signalling while concurrently, impairing proper Notch function. This could allow for elevated Wnt levels and the resulting initial rapid proliferation of the crypts with a bias towards secretory cell differentiation. With impaired Notch signalling, the initial proliferative burst during *C. rodentium*-induced colitis, could deplete the stem cell reservoir potentially explaining the lack of difference in crypt lengths at the time points measured. As the turnover of intestinal crypts is 3-5 days, this may explain why mortality is observed after 9-10 days post infection. Therefore,

in our system, hyperglycemia may be suppressing Notch signalling and causing a defect in differentiation resulting in impaired absorption and through Wnt inhibition, we were able to rescue the diabetic mice. To confirm this, future studies must assess the level of Notch signalling in Akita<sup>+/-</sup> mice prior to and during infection.

It may be interesting to test either  $\beta$ -hydroxybutyrate or a ketogenic diet in our Akita<sup>+/-</sup> mouse model to assess whether this mechanism of Notch-inhibition plays a role in the observed *C. rodentium*-induced mortality in diabetic mice. The ketogenic diet is especially interesting, as our experiments with insulin have shown that internal regulation of glucose levels could rescue from mortality, but it is unclear if intestinal luminal regulation or concentrations of glucose also have an impact on outcomes from enteric infection. This can also be tested by giving glucose-supplemented drinking water to WT mice to see if it can promote mortality or worsen pathology during *C. rodentium* infection.

#### **4.2. Obesity and diet impair the resolution of adherent-invasive *Escherichia coli* infection**

Our study is one of the first to look at the individual contributions of diet versus obesity on enteric infection with a pathobiont such as AIEC. We showed that long-term HFD feeding promotes AIEC colonization and worsened pathology

in mice. Short-term HFD initiated just before or just after AIEC infection can also promote pathogen colonization, but to a lesser extent.

Since diet-induced obesity showed sustained fecal levels of AIEC 30 days post infection, future experiments should track the infection over a longer period to determine if these higher levels correlate with chronic infection and continued worsened pathology. *Small et al.* showed that chronic infection with AIEC induced chronic inflammation, sustained pathology, and fibrosis<sup>176</sup>. We only evaluated pathology and intestinal burdens at day 17 post infection, so it may be interesting to determine whether later time points show similar tissue burdens and pathology.

Many physiological changes occur as the result of HFD feeding, including weight gain, metabolic inflammation, glucose intolerance, and insulin resistance<sup>30,185,254,255</sup>. HFD feeding also changes in the composition of the intestinal microbiota<sup>24,29</sup>. In fact, as early as one day after the initiation of a high fat diet has been reported to transiently alter microbial populations with long-term feeding associated with a new sustained microbial composition<sup>33,256,257</sup>. The finding that exacerbated AIEC expansion induced by HFD-feeding only occurs when combined with the use antibiotics would imply a role for the microbiota in this process. The microbiota is a link between diet and host physiology. The microbiota modifies (and promotes) energy harvest from food and is at the crossroads of diet and intestinal immunity. The microbiota can ferment dietary

components, specifically non-digestible fibres, that escape digestion in the upper gastrointestinal tract into SCFAs (most commonly acetate, propionate, and butyrate). Butyrate is a primary energy source for colonocytes and is the most widely studied of the SCFAs for its beneficial effects on dysbiosis, weight gain, and inflammation<sup>258–260</sup>. During obesity, there is a bias towards acetate production in multiple body sites, including the intestine<sup>261</sup>. A study by *Perry et al.* determined that intestinal acetate levels were elevated in a HFD-fed rodent model and the elevated intestinal acetate levels were transmissible through fecal transplantation and ablated with antibiotics<sup>261</sup>. As AIEC is known to use acetate as alternative carbon source, we hypothesize that elevations in intestinal acetate in our long-term HFD model promote the colonization of AIEC. A pilot experiment was conducted using a mutant strain of AIEC ( $\Delta asc\Delta ack-pta::Gm$ ) attained from the laboratory of Dr. Coombes lab. We tested an AIEC strain ( $\Delta asc\Delta ack-pta::Gm$ ) that has attenuated growth in acetate-rich media. It was hypothesized that if acetate levels were elevated in our HFD model, impaired colonization of this mutant strain would be observed because it could not capitalize on augmented acetate levels to promote AIEC colonization. However, no difference in colonization was observed between WT AIEC and  $\Delta asc\Delta ack-pta::Gm$  AIEC in long-term HFD mice (**Fig. 35**). It is recommended that future studies quantify the levels of SCFAs in the cecum to assess the level of fermentation. It has been reported that bacterial fermentation is another

process that confers pathogen resistance as the production of SCFAs lowers the pH of cecum and colon<sup>262</sup>. It may be that there is a decrease in fermentation that produces a more favourable environment for AIEC expansion.

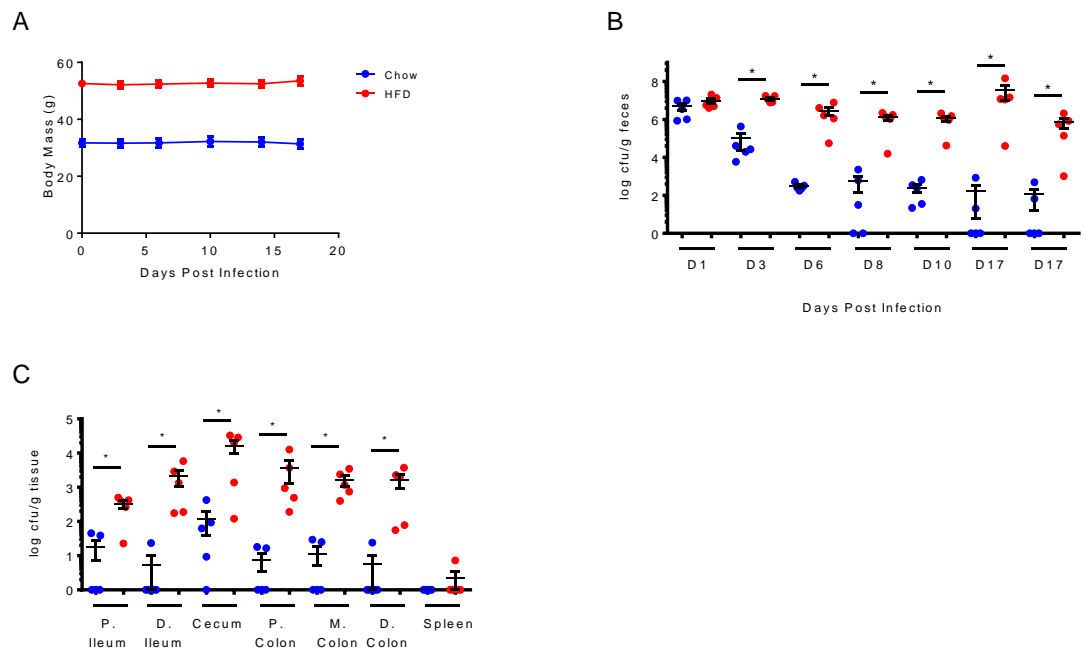


**Figure 35: Acetate metabolism is not required for obesity-induced expansion of adherent-invasive *Escherichia coli*.** C57BL/6 mice (8-10 weeks old) were fed a 60% high fat diet (HFD) for 16 weeks and pretreated with streptomycin (2 mg/mouse) one day prior to infection with adherent-invasive *Escherichia coli* ( $\Delta asc\Delta ack-pta::Gm$ ; n=8-10/group). A, Body mass during the course of infection. B, Fecal burdens during the course of infection. C, Tissue burdens at day 17 post infection. Mann-Whitney was conducted for statistical analysis. Values are presented as mean  $\pm$  SEM. \*p<0.05.

Obesity and HFD-feeding are often intertwined in mice. Our findings show that the exacerbation of AIEC infection is partially diet-regulated while the role of obesity is not yet clear. To further evaluate the impact of obesity, genetic murine models should be used to avoid the confounder of diet. While OB mice are commonly used for this purpose, the immunodeficiencies associated with leptin-deficiency may mask the effects of obesity. Leptin is a known mediator of metabolism for the activation and proliferation of T cells<sup>160,263</sup>. OB mice are known to have reduced thymic cellularity and reduced CD8+ T cell populations, which have been reported to be important in C57BL/6 mice for controlling AIEC infection<sup>176,264</sup>. Mice depleted of CD8+ T cells showed higher fecal burdens and worsened pathology during persistent AIEC infection<sup>176</sup>. OB mice may show an elevated AIEC burden which would be confounded by T cell deficiency and obesity. Therefore, an alternative model of genetically induced obesity, the melanocortin-4-receptor (MC4R) knock out mouse model, should be used in future experiments to segregate the impact of obesity and diet on AIEC infection. Melanocortin receptors are primarily expressed in the central nervous system and are important for regulating food intake and body weight<sup>265–267</sup>. Specifically, the melanocortin-4 receptor has been found to regulate leptin signalling in the hypothalamus<sup>268</sup>. Therefore, this model can induce hyperphagia in mice fed a “chow” diet without the loss of peripheral leptin function. Using this model, we

can determine the impact of obesity and adiposity independent of diet on AIEC colonization and pathology.

A major strength of the series of studies on diet and AIEC was the use of multiple defined control diets to assess the impact of specific dietary components. A majority of studies using animal models of diet-induced obesity compare well-defined and controlled HFDs with a “regular chow” diet<sup>269</sup>. “Regular chow” diets exhibit large inter-batch variability, lack a defined composition, and vary in their ingredient sources<sup>262,269,270</sup>. One of the major differences between “regular chow” diet and defined diets is the fibre content, with insoluble cellulose as the main source in defined diets while “regular chow” is considered a fibre-rich diet<sup>262</sup>. Fibre type and quantity are known to affect intestinal development and microbial populations which may confound metabolic research comparing defined diets to ‘regular chow’ diets<sup>226,230,271–273</sup>. In a study by *Dalby et al.*, they found that low- and high-fat refined diets caused similar changes to the microbial populations and SCFA concentrations indicating that these features were independent of dietary fat content or obesity<sup>274</sup>. If the low-fat refined diet were not used, these differences may have been attributed to the high fat percentage and increased weight gain. While our diets were well controlled, one confounding variable in all three diets is the presence of maltodextrin. Maltodextrin is a resistant starch, which is defined as the portion of starch that escapes digestion in the small intestine<sup>275</sup>. Because of this,

resistant starches physiologically act similar to dietary fibre and are commonly considered as part of the dietary fibre content of foods<sup>275,276</sup>. A recent *in vitro* study showed that maltodextrin, irrespective of chain length, promoted AIEC growth and biofilm formation<sup>205</sup>. This study also found that sucrose did not confer a growth advantage to AIEC, which supports our hypothesis that the low fibre content, not high sucrose in the diet can promote AIEC growth. However, it is currently unclear if the phenotype we observed is the result of maltodextrin in the diet and it is recommended that future experiments control for maltodextrin quantity.

With regards to the fibre content, there are two main types of fibre: soluble (i.e. inulin) and insoluble (i.e. cellulose)<sup>273</sup>. Soluble fibres can be fermented by the microbiota into SCFAs while insoluble fibres provide bulk for waste disposal<sup>256,270</sup>. There have been numerous regarding dietary fibre supplementation as a potential therapeutic for obesity and metabolic disease. A study by *Zou et al.* showed that HFD supplemented with inulin had increased mucosal immunity and restored microbial diversity compared with a non-supplemented HFD or one supplemented with cellulose<sup>277</sup>. Interestingly, while HFDs supplemented with inulin or cellulose reduced body mass, only the diet supplemented with inulin showed improved glucose and insulin tolerance<sup>277</sup>. Another study found that inulin and oligofructose improved intestinal immunity and resistance to *Candida albicans*, an intestinal pathogen<sup>278</sup>. They also found

that inulin, and to a lesser extent oligofructose, improved survival during a systemic *Salmonella typhimurium* infection<sup>278</sup>. These findings may explain why cellulose supplementation of the HFD had minimal effects. It may be that the type of fibre (soluble vs. insoluble) plays a larger role than the amount. To first test this, cellulose should be replaced with an equal amount of inulin. Further studies regarding the type and amount of fibre in the diet and their impact on AIEC colonization is required to further our understanding of this opportunistic pathobiont. A comprehensive study conducted by the Faith lab, utilized over 40 custom diets consisting of different proportions of macronutrients to assess their impact on resolution of DSS-induced colitis. Of the macronutrients they tested, they found that high protein diets resulted in worsened outcomes while high fibre diets were protective. Furthermore, they narrowed it down to casein (protein) and psyllium (fibre) as having the strongest effects<sup>229</sup>. A high casein diet exacerbated DSS-induced colitis with much more severe weight loss, higher levels of fecal lipocalin-2 and colonic TNF and IL-6, and much more severe pathology. A psyllium enriched diet had the opposite effect with minimal weight loss during DSS treatment, lower levels of colonic inflammatory markers and no observable pathology. Cellulose and inulin had milder effects but were still able to reduce DSS-induced pathology. Casein comprises the largest protein component in both the HFD and control diets and it may be interesting to adjust the proportions to observe what impact that may have on AIEC colonization.

DSS-induced intestinal colitis is commonly used as a model of human inflammatory bowel disease<sup>279–281</sup>. This chemical compound causes the rapid onset of epithelial degradation with concomitant weight loss and bloody diarrhea, common markers of human inflammatory bowel disease<sup>280</sup>. However, the mechanism through which DSS induces intestinal epithelial damage is currently unclear but it is known that variations in molecular weight, dosage, and the gender and strain of mice used can vary the severity and duration of colitis<sup>282</sup>. HFD has shown to worsen the severity of DSS-induced colitis marked by much greater weight loss and colonic epithelial degradation compared to chow-fed controls<sup>279</sup>. Overall, our findings clearly indicate the importance of diet in regulating the progression and outcomes of enteric infection.

#### **4.3 Future Directions**

While we have shown that use of an inhibitor of the Wnt can rescue Akita<sup>+/-</sup> mice from *C. rodentium*-induced mortality, we have not yet been able to define the mechanism linking inhibition of porcupine/Wnt and survival from enteric infection during hyperglycemia. We have not identified the cell type responsible or a measurable link between Wnt and cells responsible for fluid balance. It is possible that Notch signalling links Wnt signalling and hyperglycemia. A study by Cheng et al. found that hyperglycemia inhibited Notch signalling, resulting in the skewed differentiation of intestinal cells towards a

secretory lineage<sup>148</sup>. Using a ketogenic (low carbohydrate) diet, these authors were able to restore intestinal cells differentiation toward normal characteristics. Future studies will need to assess Notch signalling by quantifying downstream differentiation markers such as Hes1 and Math1 in the colonic epithelium or the expression of ion or fluid transporters (i.e. aquaporins, slc26a3). It is also unknown whether intestinal (i.e. luminal) glucose concentrations play a role in dictating outcomes such as mortality during *C. rodentium* infection in our mouse models. We can assess this by using a ketogenic diet to see if a reduction in luminal glucose can impact Wnt or Notch signalling in the intestinal tract and rescue Akita<sup>+/-</sup> mice from *C. rodentium*-induced mortality.

Further studies should be also performed on AIEC infections in Akita<sup>+/-</sup> mice to evaluate the impact that hyperglycemia may play in the course of infection. Our current findings show that hyperglycemia promotes the overgrowth and tissue colonization of AIEC, but we did not assess any inflammatory markers or intestinal pathology. It is important to expand the scope of this research to other models of infection, as they will provide more insight into the molecular mechanisms that underly diabetes. It is also important to understand the relevance of our mouse models to enteric infections in humans. We have started this work and a recent re-analysis of the 2007 Walkerton *E. coli* outbreak identified hyperglycemia as an independent predictor

of worsened infection outcomes (**Fig. 36**). As millions of people currently live with diabetes and that number is expected to continually rise, this research can help to develop new therapeutics for this comorbidity of the disease and improve patient quality of life.

In diet-induced obese mice, we showed that both long- and short-term feeding of a high fat, high sucrose and low fibre diet were able to promote AIEC colonization and expansion. Long-term HFD also worsened pathology compared to chow-fed controls, however, it is currently unclear if short-term HFD feeding alters intestinal pathology during AIEC infection. We also determined that it was the low fibre content of the HFD that was sufficient to promote AIEC expansion, but the effects of long and short term feeding of diets lower in fibre on intestinal pathology still needs to be assessed. Our initial experiments with cellulose supplementation of the HFD showed no impact on the progression of infection, but future studies should look at the impact of the type of fibre (soluble vs. insoluble) and the type/amount of fibre combinations in the diet on AIEC infection outcomes. Our results show that the long-term HFD study had a much more profound effect on AIEC pathogen burden compared to short-term changes in diet. We do not yet understand the mechanisms underpinning this response. Our results imply that obesity has a small role on AIEC burden compared to diet, but it is possible that obesity and diet interact to regulate pathogen burden. To further study the impact of obesity independent of diet, a

genetically induced model of obesity, such as the MCR4<sup>-/-</sup> mouse, should be used.

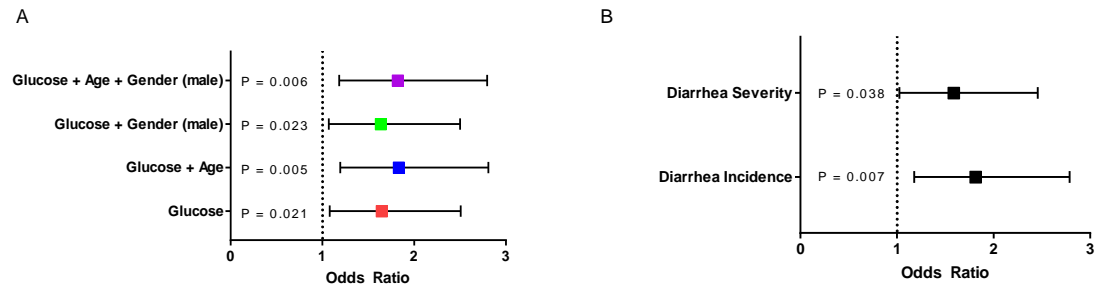


**Figure 36: Blood glucose indicative of type 2 diabetes is an independent risk factor predicting diarrhea during an *Escherichia coli* outbreak.** A logistic regression was performed to ascertain the effects of impaired fasting glucose, age, number of days fasting blood glucose was taken before the outbreak and gender on the likelihood that residents had diarrhea. Forest plot of the odds ratio for: A, Diarrhea incidence and B, severity in Walkerton residents (adjusted for age, # days post fasting blood glucose measured and gender; normal/intermediate fasting glucose vs. blood glucose indicative of type 2 diabetes). Statistical analysis conducted by Elizabeth Gunn at McMaster University.

## **Chapter 5 – References**

1. World Health Organization. Global report on obesity and overweight. (2018).
2. Lyznicki, J. M., Young, D. C., Riggs, J. A., Davis, R. M. & Dickinson, B. D. Obesity: Assessment and management in primary care. *Am. Fam. Physician* **63**, 2185–2196 (2001).
3. Noël, P. H. & Pugh, J. A. Management of overweight and obese adults. *Br. Med. J.* **325**, 757–761 (2002).
4. Birmingham, C. L., Muller, J. L., Palepu, A., Spinelli, J. J. & Anis, A. H. The cost of obesity in Canada. *Cmaj* **160**, 483–488 (1999).
5. Withrow, D. & Alter, D. A. The economic burden of obesity worldwide: A systematic review of the direct costs of obesity. *Obes. Rev.* **12**, 131–141 (2011).
6. Janssen, I. The Public Health Burden of Obesity in Canada. *Can. J. Diabetes* **37**, 90–96 (2013).
7. Kitahara, C. M. *et al.* Association between Class III Obesity (BMI of 40-59 kg/m<sup>2</sup>) and Mortality: A Pooled Analysis of 20 Prospective Studies. *PLoS Med.* **11**, 1–14 (2014).
8. Qasim, A. *et al.* On the origin of obesity: identifying the biological, environmental and cultural drivers of genetic risk among human populations. *Obes. Rev.* **19**, 121–149 (2018).
9. Ng, S. W. & Popkin, B. M. Time use and physical activity: A shift away from

- movement across the globe. *Obes. Rev.* **13**, 659–680 (2012).
10. Shields, M. & Tremblay, M. S. Sedentary behaviour and obesity. *Health Rep.* **19**, 19–30 (2008).
  11. Kenney, E. L. & Gortmaker, S. L. United States Adolescents' Television, Computer, Videogame, Smartphone, and Tablet Use: Associations with Sugary Drinks, Sleep, Physical Activity, and Obesity. *J. Pediatr.* **182**, 144–149 (2017).
  12. Kim, S. E., Kim, J. W. & Jee, Y. S. Relationship between smartphone addiction and physical activity in Chinese international students in Korea. *J. Behav. Addict.* **4**, 200–205 (2015).
  13. Ahmed, H. O. *et al.* The life styles causing overweight or obesity: Based on 5 years of experience in two centers in Sulaimani Governorate, Kurdistan Region/Iraq. *Int. J. Surg. Open* **11**, 22–29 (2018).
  14. Biddle, S. J. H. *et al.* Screen Time, Other Sedentary Behaviours, and Obesity Risk in Adults: A Review of Reviews. *Curr. Obes. Rep.* **6**, 134–147 (2017).
  15. Cordain, L. *et al.* Origins and evolution of the Western diet: health implications for the 21st century. *Am. J. Clin. Nutr.* **81**, 341–354 (2005).
  16. Moubarac, J. C. *et al.* Consumption of ultra-processed foods and likely impact on human health. Evidence from Canada. *Public Health Nutr.* **16**, 2240–2248 (2013).

17. Rolls, B. J. The Supersizing of America. *Nutr. Today* **38**, 42–53 (2003).
18. Bouchard, C. *et al.* The Response to Long-Term Overfeeding in Identical Twins. *N. Engl. J. Med.* **322**, 1477–1482 (1990).
19. Bouchard, C. Gene – Environment Interactions in the Etiology of Obesity : Defining the Fundamentals.
20. Sutton, G. M. *et al.* Diet-genotype interactions in the development of the obese, insulin-resistant phenotype of C57BL/6J mice lacking melanocortin-3 or -4 receptors. *Endocrinology* **147**, 2183–2196 (2006).
21. Cordain, L. *et al.* Plant-animal subsistence ratios and macronutrient energy estimations in worldwide hunter-gatherer diets. *Am. J. Clin. Nutr.* **71**, 682–692 (2000).
22. Kopp, W. How Western Diet And Lifestyle Drive The Pandemic Of Obesity And Civilization Diseases. *Diabetes, Metab. Syndr. Obes. Targets Ther.* **12**, 2221–2236 (2019).
23. Sampey, B. P. *et al.* Cafeteria diet is a robust model of human metabolic syndrome with liver and adipose inflammation: Comparison to high-fat diet. *Obesity* **19**, 1109–1117 (2011).
24. Martinez, K. B., Leone, V. & Chang, E. B. Western diets, gut dysbiosis, and metabolic diseases: Are they linked? *Gut Microbes* **8**, 130–142 (2017).
25. Leibel, R. L., Chung, W. K. & Chua, S. C. The molecular genetics of rodent single gene obesities. *J. Biol. Chem.* **272**, 31937–31940 (1997).

26. Augustine, K. A. & Rossi, R. M. Rodent mutant models of obesity and their correlations to human obesity. *Anat. Rec.* **257**, 64–72 (1999).
27. Ridaura, V. K. *et al.* Gut microbiota from twins discordant for obesity modulate metabolism in mice. *Science (80-. ).* **341**, (2013).
28. Bäckhed, F., Manchester, J. K., Semenkovich, C. F. & Gordon, J. I. Mechanisms underlying the resistance to diet-induced obesity in germ-free mice. *Proc. Natl. Acad. Sci. U. S. A.* **104**, 979–984 (2007).
29. Bäckhed, F. *et al.* The gut microbiota as an environmental factor that regulates fat storage. *Proc. Natl. Acad. Sci. U. S. A.* **101**, 15718–15723 (2004).
30. Turnbaugh, P. J., Bäckhed, F., Fulton, L. & Gordon, J. I. Diet-Induced Obesity Is Linked to Marked but Reversible Alterations in the Mouse Distal Gut Microbiome. *Cell Host Microbe* **3**, 213–223 (2008).
31. Kong, C., Gao, R., Yan, X., Huang, L. & Qin, H. *Probiotics improve gut microbiota dysbiosis in obese mice fed a high-fat or high-sucrose diet.* *Nutrition* (Elsevier Inc., 2018). doi:10.1016/j.nut.2018.10.002
32. Hamilton, M. K., Boudry, G., Lemay, D. G. & Raybould, H. E. Changes in intestinal barrier function and gut microbiota in high-fat diet-fed rats are dynamic and region dependent. *Am. J. Physiol. - Gastrointest. Liver Physiol.* **308**, G840–G851 (2015).
33. Foley, K. P. *et al.* Long term but not short term exposure to obesity related

- microbiota promotes host insulin resistance. *Nat. Commun.* **9**, 1–15 (2018).
34. Ghazarian, M., Luck, H., Revelo, X. S., Winer, S. & Winer, D. A. Immunopathology of adipose tissue during metabolic syndrome. *Turk Patoloji Derg.* **31**, 172–180 (2015).
35. Weisberg, S. P. *et al.* Obesity is associated with macrophage accumulation in adipose tissue Find the latest version : Obesity is associated with. *J Clin Invest.* **112**, 1796–1808 (2003).
36. Nguyen, M. T. A. *et al.* A subpopulation of macrophages infiltrates hypertrophic adipose tissue and is activated by free fatty acids via toll-like receptors 2 and 4 and JNK-dependent pathways. *J. Biol. Chem.* **282**, 35279–35292 (2007).
37. Lumeng, C. N. *et al.* Obesity induces a phenotypic switch in adipose tissue macrophage polarization Find the latest version : Obesity induces a phenotypic switch in adipose tissue macrophage polarization. *J Clin Invest* **117**, 175–184 (2007).
38. Zick, Y. Ser/Thr phosphorylation of IRS proteins: a molecular basis for insulin resistance. *Sci. STKE* **2005**, 1–3 (2005).
39. Biddinger, S. B. & Kahn, C. R. FROM MICE TO MEN: Insights into the Insulin Resistance Syndromes. *Annu. Rev. Physiol.* **68**, 123–158 (2006).
40. Winer, D. A., Winer, S., Chng, M. H. Y., Shen, L. & Engleman, E. G. B

- Lymphocytes in obesity-related adipose tissue inflammation and insulin resistance. *Cell. Mol. Life Sci.* **71**, 1033–1043 (2014).
41. Winer, D. A. *et al.* B Lymphocytes Promote Insulin Resistance through Modulation of T Lymphocytes and Production of Pathogenic IgG Antibody. *Nat Med* **17**, 610–617 (2011).
  42. McLaughlin, T. *et al.* T-Cell Profile in Adipose Tissue Is Associated With Insulin Resistance and Systemic Inflammation in Humans. *Arterioscler. Thromb. Vasc. Biol.* **34**, 2637–2643 (2014).
  43. Nishimura, S. *et al.* CD8<sup>+</sup> effector T cells contribute to macrophage recruitment and adipose tissue inflammation in obesity. *Nat. Med.* **15**, 914–920 (2009).
  44. Winer, S. *et al.* Normalization of obesity-associated insulin resistance through immunotherapy. *Nat. Med.* **15**, 921–929 (2009).
  45. Duffaut, C., Galitzky, J., Lafontan, M. & Bouloumié, A. Unexpected trafficking of immune cells within the adipose tissue during the onset of obesity. *Biochem. Biophys. Res. Commun.* **384**, 482–485 (2009).
  46. Jagannathan, M. *et al.* Toll-like receptors regulate B cell cytokine production in patients with diabetes. *Diabetologia* **53**, 1461–1471 (2010).
  47. DeFuria, J. *et al.* B cells promote inflammation in obesity and type 2 diabetes through regulation of T-cell function and an inflammatory cytokine profile. *Proc. Natl. Acad. Sci. U. S. A.* **110**, 5133–5138 (2013).

48. Vijay-Kumar, M. *et al.* Metabolic Syndrome and Altered Gut Microbiota in Mice Lacking Toll-Like Receptor 5. *Science* (80-. ). **328**, 228–231 (2010).
49. Koh, A., De Vadder, F., Kovatcheva-Datchary, P. & Bäckhed, F. From dietary fiber to host physiology: Short-chain fatty acids as key bacterial metabolites. *Cell* **165**, 1332–1345 (2016).
50. Schroeder, B. O. *et al.* Bifidobacteria or Fiber Protects against Diet-Induced Microbiota-Mediated Colonic Mucus Deterioration. *Cell Host Microbe* **23**, 27-40.e7 (2018).
51. Murphy, E. F. *et al.* Composition and energy harvesting capacity of the gut microbiota: Relationship to diet, obesity and time in mouse models. *Gut* **59**, 1635–1642 (2010).
52. Cândido, F. G. *et al.* Impact of dietary fat on gut microbiota and low-grade systemic inflammation: mechanisms and clinical implications on obesity. *Int. J. Food Sci. Nutr.* **0**, 1–19 (2017).
53. Cani, P. D., Bibiloni, R., Knauf, C., Neyrinck, A. M. & Delzenne, N. M. Changes in gut microbiota control metabolic diet-induced obesity and diabetes in mice. *Diabetes* **57**, 1470–81 (2008).
54. Guerville, M. *et al.* Western-diet consumption induces alteration of barrier function mechanisms in the ileum that correlates with metabolic endotoxemia in rats. *Am. J. Physiol. - Endocrinol. Metab.* **33**, ajpgendo.00372.2016 (2017).

55. Yajima, S. *et al.* Tumor necrosis factor-alpha mediates hyperglycemia-augmented gut barrier dysfunction in endotoxemia. *Crit. Care Med.* **37**, 1024–30 (2009).
56. Rodrigues, D. M., Sousa, A. J., Johnson-Henry, K. C., Sherman, P. M. & Gareau, M. G. Probiotics are effective for the prevention and treatment of *Citrobacter rodentium*-induced colitis in mice. *J. Infect. Dis.* **206**, 99–109 (2012).
57. Eder, K., Baffy, N., Falus, A. & Fulop, A. K. The major inflammatory mediator interleukin-6 and obesity. *Inflamm. Res.* **58**, 727–736 (2009).
58. Korbel, L. & Spencer, J. D. Diabetes mellitus and infection: An evaluation of hospital utilization and management costs in the United States. *J. Diabetes Complications* **29**, 192–195 (2015).
59. Shaw, J. E., Sicree, R. A. & Zimmet, P. Z. Global estimates of the prevalence of diabetes for 2010 and 2030. *Diabetes Res. Clin. Pract.* **87**, 4–14 (2010).
60. Calvet, H. M. & Yoshikawa, T. T. Infections in diabetes. *Infect. Dis. Clin. North Am.* **15**, 407–21, viii (2001).
61. Casqueiro, J., Casqueiro, J. & Alves, C. Infections in patients with diabetes mellitus: A review of pathogenesis. *Indian J. Endocrinol. Metab.* **16 Suppl 1**, S27-36 (2012).
62. Gupta, S., Koirala, J., Khardori, R. & Khardori, N. Infections in Diabetes Mellitus and Hyperglycemia. *Infect. Dis. Clin. North Am.* **21**, 617–638

(2007).

63. Shilling, A. M. & Raphael, J. Diabetes, Hyperglycemia, and Infections. *Best Pract. Res. Clin. Anaesthesiol.* **22**, 519–535 (2008).
64. Shah, B. R. & Hux, J. E. Quantifying the Risk of Infectious Diseases for People With Diabetes. *Diabetes Care* **26**, 510–513 (2003).
65. Peleg, A. Y., Weerathna, T., McCarthy, J. S. & Davis, T. M. E. Common infections in diabetes: pathogenesis, management and relationship to glycaemic control. *Diabetes. Metab. Res. Rev.* **23**, 3–13 (2007).
66. Benfield, T., Jensen, J. S. & Nordestgaard, B. G. Influence of diabetes and hyperglycaemia on infectious disease hospitalisation and outcome. *Diabetologia* **50**, 549–554 (2007).
67. Davis, T. M. E., Weerathne, T., Foong, Y., Mason, C. & Davis, W. A. Community-acquired infections in type 2 diabetic patients and their nondiabetic partners: The Fremantle Diabetes Study. *J. Diabetes Complications* **19**, 259–263 (2005).
68. Dewilde, S., Harris, T., Hosking, F. J. & Cook, D. G. Risk of Infection in Type 1 and Type 2 Diabetes Compared With the General Population: A Matched Cohort Study. *Diabetes Care* **2015**, 1–9 (2018).
69. Boyko EJ. Infection and Diabetes Mellitus. *Diabetes Am. 2nd Ed.* 485–496 (1995).
70. Baker, S. T. *et al.* Outcomes for general medical inpatients with diabetes

- mellitus and new hyperglycaemia. *Med. J. Aust.* **188**, 340–343 (2008).
71. Telzak, E. E., Greenberg, M. S. Z., Budnick, L. D., Blum, S. & Singh, T. Diabetes Mellitus ? A Newly Described Risk Factor for Infection from *Salmonella enteritidis*. **164**, 538–541 (1991).
72. Krausova, M. & Korinek, V. Wnt signaling in adult intestinal stem cells and cancer. *Cell. Signal.* **26**, 570–579 (2014).
73. Pinto, D. & Clevers, H. Wnt control of stem cells and differentiation in the intestinal epithelium. *Exp. Cell Res.* **306**, 357–363 (2005).
74. Pinto, D., Gregorieff, A., Begthel, H. & Clevers, H. Canonical Wnt signals are essential for homeostasis of the intestinal epithelium. *Genes Dev.* **17**, 1709–1713 (2003).
75. Nguyen, T. L. A., Vieira-Silva, S., Liston, A. & Raes, J. How informative is the mouse for human gut microbiota research? *DMM Dis. Model. Mech.* **8**, 1–16 (2015).
76. Treuting, P. M., Arends, M. J. & Dintzis, S. M. Lower Gastrointestinal Tract. in *Comparative Anatomy and Histology* 213–228 (Elsevier, 2018).  
doi:10.1016/B978-0-12-802900-8.00012-9
77. Sancho, E., Batlle, E. & Clevers, H. Live and let die in the intestinal epithelium. *Curr. Opin. Cell Biol.* **15**, 763–770 (2003).
78. Radtke, F. & Clevers, H. Self-renewal and cancer of the gut: two sides of a coin. *Science* **307**, 1904–1909 (2005).

79. Bevins, C. L. & Salzman, N. H. Paneth cells, antimicrobial peptides and maintenance of intestinal homeostasis. *Nat. Rev. Microbiol.* **9**, 356–368 (2011).
80. Cobo, E. R., Kisson-Singh, V., Moreau, F. & Chadee, K. Colonic MUC2 mucin regulates the expression and antimicrobial activity of  $\beta$ -defensin 2. *Mucosal Immunol.* 1–13 (2015). doi:10.1038/mi.2015.27
81. Hansson, G. C. Role of mucus layers in gut infection and inflammation. *Curr. Opin. Microbiol.* **15**, 57–62 (2012).
82. Marshman, E., Booth, C. & Potten, C. S. The intestinal epithelial stem cell. *BioEssays* **24**, 91–98 (2002).
83. Ireland, H., Houghton, C., Howard, L. & Winton, D. J. Cellular inheritance of a Cre-activated reporter gene to determine Paneth cell longevity in the murine small intestine. *Dev. Dyn.* **233**, 1332–1336 (2005).
84. Clevers, H. & Nusse, R. Wnt/ $\beta$ -catenin signaling and disease. *Cell* **149**, 1192–1205 (2012).
85. Fevr, T., Robine, S., Louvard, D. & Huelsken, J. Wnt /  $\beta$ -Catenin Is Essential for Intestinal Homeostasis and Maintenance of Intestinal Stem Cells. *Mol Cell Biol* **27**, 7551–7559 (2007).
86. Krausova, M. & Korinek, V. Wnt signaling in adult intestinal stem cells and cancer. *Cell. Signal.* **26**, 570–579 (2014).
87. Nusse, R. & Clevers, H. Wnt/ $\beta$ -Catenin Signaling, Disease, and Emerging

- Therapeutic Modalities. *Cell* **169**, 985–999 (2017).
88. Logan, C. Y. & Nusse, R. THE WNT SIGNALING PATHWAY IN DEVELOPMENT AND DISEASE. *Annu. Rev. Cell Dev. Biol.* **20**, 781–810 (2004).
89. Glinka, A. *et al.* LGR4 and LGR5 are R-spondin receptors mediating Wnt/ $\beta$ -catenin and Wnt/PCP signalling. *EMBO Rep.* **12**, 1055–1061 (2011).
90. Lau, W. De, Peng, W. C., Gros, P. & Clevers, H. The R-spondin / Lgr5 / Rnf43 module : regulator of Wnt signal strength The R-spondin / Lgr5 / Rnf43 module : regulator of Wnt signal strength. *Genes Dev.* **28**, 305–316 (2014).
91. Ruffner, H. *et al.* R-spondin potentiates Wnt/ $\beta$ -Catenin signaling through orphan receptors LGR4 and LGR5. *PLoS One* **7**, (2012).
92. Carmon, K. S., Lin, Q., Gong, X., Thomas, A. & Liu, Q. LGR5 interacts and cointernalizes with Wnt receptors to modulate Wnt/ $\beta$ -catenin signaling. *Mol. Cell. Biol.* **32**, 2054–2064 (2012).
93. Stanger, B. Z., Datar, R., Murtaugh, L. C. & Melton, D. A. Direct regulation of intestinal fate by Notch. **102**, 12443–12448 (2005).
94. Jensen, J. *et al.* Control of endodermal endocrine development by Hes-1[nature genetics 2000].pdf. **24**, (2000).
95. Tian, H. *et al.* Opposing activities of notch and wnt signaling regulate intestinal stem cells and gut homeostasis. *Cell Rep.* **11**, 33–42 (2015).
96. Vandussen, K. L. *et al.* Notch signaling modulates proliferation and

- differentiation of intestinal crypt base columnar stem cells. **497**, 488–497 (2012).
97. Liu, J. *et al.* Targeting Wnt-driven cancer through the inhibition of Porcupine by LGK974. *Proc. Natl. Acad. Sci.* **110**, 20224–20229 (2013).
98. Haegebarth, A. & Clevers, H. Wnt signaling, Lgr5, and stem cells in the intestine and skin. *Am. J. Pathol.* **174**, 715–721 (2009).
99. Liu, J. *et al.* Targeting Wnt-driven cancer through the inhibition of Porcupine by LGK974. *Proc. Natl. Acad. Sci.* **110**, 20224–20229 (2013).
100. Troll, J. V. *et al.* Microbiota promote secretory cell determination in the intestinal epithelium by modulating host Notch signaling. *Development* **145**, 1–7 (2018).
101. Bhinder, G. *et al.* Intestinal epithelium-specific MyD88 signaling impacts host susceptibility to infectious colitis by promoting protective goblet cell and antimicrobial responses. *Infect. Immun.* **82**, 3753–3763 (2014).
102. Sender, R., Fuchs, S. & Milo, R. Revised Estimates for the Number of Human and Bacteria Cells in the Body. *PLOS Biol.* **14**, e1002533 (2016).
103. Hung, T. Van & Suzuki, T. Dietary Fermentable Fiber Reduces Intestinal Barrier Defects and Inflammation in. (2018).  
doi:10.3945/jn.116.232538.Downloaded
104. Schley, P. D. & Field C.J.\*. The immune-enhancing effects of dietary fibres and prebiotics. *Br. J. Nutr.* **87**, 221–230 (2002).

105. Sun, Y. & O’Riordan, M. X. D. Regulation of Bacterial Pathogenesis by Intestinal Short-Chain Fatty Acids. in 93–118 (2013). doi:10.1016/B978-0-12-407672-3.00003-4
106. Turnbaugh, P. J. *et al.* An obesity-associated gut microbiome with increased capacity for energy harvest. *Nature* **444**, 1027–1031 (2006).
107. Kamada, N. *et al.* Regulated virulence controls the ability of a pathogen to compete with the gut microbiota. *Science (80-. )*. **336**, 1325–1329 (2012).
108. Schell, M. A. *et al.* The genome sequence of *Bifidobacterium longum* reflects its adaptation to the human gastrointestinal tract. *Proc. Natl. Acad. Sci. U. S. A.* **99**, 14422–14427 (2002).
109. Trejo, F. M., Minnaard, J., Perez, P. F. & De Antoni, G. L. Inhibition of *Clostridium difficile* growth and adhesion to enterocytes by *Bifidobacterium* supernatants. *Anaerobe* **12**, 186–193 (2006).
110. Rea, M. C. *et al.* Thuricin CD, a posttranslationally modified bacteriocin with a narrow spectrum of activity against *Clostridium difficile*. *Proc. Natl. Acad. Sci. U. S. A.* **107**, 9352–9357 (2010).
111. Mukherjee, S. & Hooper, L. V. Antimicrobial Defense of the Intestine. *Immunity* **42**, 28–39 (2015).
112. Brogden, K. A. Antimicrobial peptides: Pore formers or metabolic inhibitors in bacteria? *Nat. Rev. Microbiol.* **3**, 238–250 (2005).
113. Shi, N., Li, N., Duan, X. & Niu, H. Interaction between the gut microbiome

- and mucosal immune system. *Mil. Med. Res.* **4**, 1–7 (2017).
114. Macpherson, A. J. & Harris, N. L. Interactions between commensal bacteria and the chicken immune system. *Nat. Rev. Immunol.* **4**, 478–85 (2004).
115. I., I. *et al.* Specific microbiota direct the differentiation of Th17 cells in the mucosa of the small intestine. *Cell Host Microbe* **4**, 337–349 (2008).
116. Cavallari, J. F., Denou, E., Foley, K. P., Khan, W. I. & Schertzer, J. D. Different Th17 immunity in gut, liver, and adipose tissues during obesity: the role of diet, genetics, and microbes. *Gut Microbes* **7**, 82–89 (2016).
117. Garidou, L. *et al.* The Gut Microbiota Regulates Intestinal CD4 T Cells Expressing ROR $\gamma$ t and Controls Metabolic Disease. *Cell Metab.* **22**, 100–112 (2015).
118. Takahashi, S. *et al.* Follicular dendritic cell-secreted protein is decreased in experimental periodontitis concurrently with the increase of interleukin-17 expression and the Rankl/Opg mRNA ratio. *J. Periodontal Res.* **49**, 390–397 (2014).
119. Wang, X. *et al.* Interleukin-22 alleviates metabolic disorders and restores mucosal immunity in diabetes. *Nature* (2014). doi:10.1038/nature13564
120. Luck, H. *et al.* Regulation of obesity-related insulin resistance with gut anti-inflammatory agents. *Cell Metab.* **21**, 527–542 (2015).
121. McPhee, J. B. & Schertzer, J. D. Immunometabolism of obesity and

- diabetes: Microbiota link compartmentalized immunity in the gut to metabolic tissue inflammation. *Clin. Sci.* **129**, 1083–1096 (2015).
122. Wolk, K. *et al.* IL-22 increases the innate immunity of tissues. *Immunity* **21**, 241–254 (2004).
123. Muñoz, M. *et al.* Interleukin-22 Induces Interleukin-18 Expression from Epithelial Cells during Intestinal Infection. *Immunity* **42**, 321–331 (2015).
124. Blaschitz, C. & Raffatellu, M. Th17 Cytokines and the Gut Mucosal Barrier. 196–203 (2010). doi:10.1007/s10875-010-9368-7
125. Hasnain, S. Z. *et al.* Glycemic control in diabetes is restored by therapeutic manipulation of cytokines that regulate beta cell stress. *Nat Med* **20**, 1417–1426 (2014).
126. Zhao, R. *et al.* Elevated peripheral frequencies of th22 cells: A novel potent participant in obesity and type 2 diabetes. *PLoS One* **9**, (2014).
127. Dalmás, E. & Donath, M. Y. A role for interleukin-22 in the alleviation of metabolic syndrome. *Nat Med* **20**, 1379–1381 (2014).
128. Yang, L. *et al.* Amelioration of high fat diet induced liver lipogenesis and hepatic steatosis by interleukin-22. *J. Hepatol.* **53**, 339–347 (2010).
129. Gulhane, M. *et al.* High Fat Diets Induce Colonic Epithelial Cell Stress and Inflammation that is Reversed by IL-22. *Sci. Rep.* **6**, 28990 (2016).
130. Verdam, F. J. *et al.* Small intestinal alterations in severely obese hyperglycemic subjects. *J. Clin. Endocrinol. Metab.* **96**, 379–383 (2011).

131. Altmann, G. G. & Leblond, C. P. Factors influencing villus size in the small intestine of adult rats as revealed by transposition of intestinal segments. *Am. J. Anat.* **127**, 15–36 (1970).
132. Mayer, J. & Yannoni, C. Z. Increased Intestinal Absorption of Glucose in Three Forms of Obesity in the Mouse. *Am. J. Physiol. Content* **185**, 49–53 (1956).
133. Steinbach, G., Heymsfield, S., Olansen, N. E., Tighe, A. & Holt, P. R. Effect of Caloric Restriction on Colonic Proliferation in Obese Persons: Implications for Colon Cancer Prevention. *Cancer Res.* **54**, 1194–1197 (1994).
134. Padidar, S. *et al.* High-fat diet alters gene expression in the liver and colon: Links to increased development of aberrant crypt foci. *Dig. Dis. Sci.* **57**, 1866–1874 (2012).
135. Yang, W. C., Bancroft, L., Nicholas, C., Lozonchi, I. & Augenlicht, L. H. Targeted inactivation of p27kip1 is sufficient for large and small intestinal tumorigenesis in the mouse, which can be augmented by a Western-style high-risk diet. *Cancer Res.* **63**, 4990–4996 (2003).
136. Garci, J. M. A new link between diabetes and cancer : enhanced WNT / b - catenin signaling by high glucose. (2014). doi:10.1530/JME-13-0152
137. Wence-chavez, L. I. *et al.* Gene expression profiling demonstrates WNT /  $\beta$ -catenin pathway genes alteration in Mexican patients with colorec- tal

- cancer and diabetes mellitus. **22**, 1107–1114 (2017).
138. Magliano, D. J., Davis, W. A., Shaw, J. E., Bruce, D. G. & Davis, T. M. E. Incidence and predictors of all-cause and site-specific cancer in type 2 diabetes: The Fremantle Diabetes Study. *Eur. J. Endocrinol.* **167**, 589–599 (2012).
139. Smith, U. TCF7L2 and type 2 diabetes - We WNT to know. *Diabetologia* **50**, 5–7 (2007).
140. Sano, T., Ozaki, K., Kodama, Y., Matsuura, T. & Narama, I. Prevention of proliferative changes of forestomach mucosa by blood glucose control with insulin in alloxan-induced diabetic rats. *Cancer Sci.* **100**, 595–600 (2009).
141. Adachi, T. *et al.* Morphological changes and increased sucrase and isomaltase activity in small intestines of insulin-deficient and type 2 diabetic rats. *Endocrine Journal* **50**, 271–279 (2003).
142. Dorfman, T. *et al.* Enhanced intestinal epithelial cell proliferation in diabetic rats correlates with  $\beta$ -catenin accumulation. *J. Endocrinol.* **226**, 135–143 (2015).
143. Zhong, X. Y. *et al.* Lgr5 positive stem cells sorted from small intestines of diabetic mice differentiate into higher proportion of absorptive cells and Paneth cells in vitro. *Dev. Growth Differ.* **57**, 453–465 (2015).
144. Chocarro-Calvo, A., García-Martínez, J. M., Ardila-González, S., De la Vieja,

- A. & García-Jiménez, C. Glucose-Induced  $\beta$ -Catenin Acetylation Enhances Wnt Signaling in Cancer. *Mol. Cell* **49**, 474–486 (2013).
145. Cognard, E., Dargaville, C. G., Hay, D. L. & Shepherd, P. R. Identification of a pathway by which glucose regulates  $\beta$ -catenin signalling via the cAMP/protein kinase A pathway in  $\beta$ -cell models. *Biochem. J.* **449**, 803–811 (2013).
146. Chouhan, S., Singh, S., Athavale, D., Ramteke, P. & Pandey, V. Glucose induced activation of canonical Wnt signaling pathway in hepatocellular carcinoma is regulated by DKK4. *Nat. Publ. Gr.* 1–15 (2016).  
doi:10.1038/srep27558
147. Min, X. H. *et al.* Abnormal differentiation of intestinal epithelium and intestinal barrier dysfunction in diabetic mice associated with depressed Notch/NICD transduction in Notch/Hes1 signal pathway. *Cell Biol. Int.* **38**, 1194–1204 (2014).
148. Cheng, C.-W. *et al.* Ketone Body Signaling Mediates Intestinal Stem Cell Homeostasis and Adaptation to Diet. *Cell* **178**, 1115-1131.e15 (2019).
149. Mundy, R., MacDonald, T. T., Dougan, G., Frankel, G. & Wiles, S. *Citrobacter rodentium* of mice and man. *Cell. Microbiol.* **7**, 1697–1706 (2005).
150. Wiles, S. *et al.* Organ specificity, colonization and clearance dynamics in vivo following oral challenges with the murine pathogen *Citrobacter*

- rodentium. *Cell. Microbiol.* **6**, 963–972 (2004).
151. Deng, W., Vallance, B. A., Li, Y., Puente, J. L. & Finlay, B. B. *Citrobacter rodentium* translocated intimin receptor (Tir) is an essential virulence factor needed for actin condensation, intestinal colonization and colonic hyperplasia in mice. *Mol. Microbiol.* **48**, 95–115 (2003).
152. Levine, M. M. *Escherichia coli* that cause diarrhea: enterotoxigenic, enteropathogenic, enteroinvasive, enterohemorrhagic, and enteroadherent. *J. Infect. Dis.* **155**, 377–89 (1987).
153. Nataro, J. P., Kaper, J. B. Diarrheagenic *Escherichia coli*. *Clin. Microbiol. Rev.* **11**, 142–201 (1998).
154. Borenshtein, D., Nambiar, P. R., Groff, E. B., Fox, J. G. & Schauer, D. B. Development of fatal colitis in FVB Mice infected with *Citrobacter rodentium*. *Infect. Immun.* **75**, 3271–3281 (2007).
155. Borenshtein, D. *et al.* Diarrhea as a cause of mortality in a mouse model of infectious colitis. *Genome Biol.* **9**, R122 (2008).
156. Papapietro, O. *et al.* R-spondin 2 signalling mediates susceptibility to fatal infectious diarrhoea. *Nat. Commun.* **4**, 1898 (2013).
157. Wang, X. *et al.* Interleukin-22 alleviates metabolic disorders and restores mucosal immunity in diabetes. *Nature* **514**, 237–241 (2014).
158. Mattioli, B., Straface, E., Quaranta, M. G., Giordani, L. & Viora, M. Leptin promotes differentiation and survival of human dendritic cells and licenses

- them for Th1 priming. *J. Immunol.* **174**, 6820–6828 (2005).
159. Batra, A. *et al.* Leptin: A critical regulator of CD4+ T-cell polarization in vitro and in vivo. *Endocrinology* **151**, 56–62 (2010).
160. Lord, G. M. *et al.* Leptin modulates the T-cell immune response and reverses starvation-induced immunosuppression. *Nature* **394**, 897–901 (1998).
161. Aychek, T. *et al.* IL-23-mediated mononuclear phagocyte crosstalk protects mice from *Citrobacter rodentium*-induced colon immunopathology. *Nat Commun* **6**, 6525 (2015).
162. Martinez-Medina, M. *et al.* Molecular diversity of *Escherichia coli* in the human gut: New ecological evidence supporting the role of adherent-invasive *E. coli* (AIEC) in Crohn's disease. *Inflamm. Bowel Dis.* **15**, 872–882 (2009).
163. Glasser, A. *et al.* Adherent Invasive *Escherichia coli* Strains from Patients with Crohn's Disease Survive and Replicate within Macrophages without Inducing Host Cell Death Adherent Invasive *Escherichia coli* Strains from Patients with Crohn's Disease Survive and Replicate. *Infect. Immun. Immun* **69**, 5529–37 (2001).
164. Darfeuille-Michaud, A. *et al.* High prevalence of adherent-invasive *Escherichia coli* associated with ileal mucosa in Crohn's disease. *Gastroenterology* **127**, 412–421 (2004).

165. Baumgart, M. *et al.* Culture independent analysis of ileal mucosa reveals a selective increase in invasive *Escherichia coli* of novel phylogeny relative to depletion of Clostridiales in Crohn's disease involving the ileum. *ISME J.* **1**, 403–418 (2007).
166. Vejborg, R. M., Hancock, V., Petersen, A. M., Krogfelt, K. A. & Klemm, P. Comparative genomics of *Escherichia coli* isolated from patients with inflammatory bowel disease. *BMC Genomics* **12**, 316 (2011).
167. Calbo, E. & Garau, J. Of mice and men: innate immunity in pneumococcal pneumonia. *Int. J. Antimicrob. Agents* **35**, 107–113 (2010).
168. Eaves-Pyles, T. *et al.* *Escherichia coli* isolated from a Crohn's disease patient adheres, invades, and induces inflammatory responses in polarized intestinal epithelial cells. *Int. J. Med. Microbiol.* **298**, 397–409 (2008).
169. Spees, A. M., Wangdi, T. & Lopez, C. A. Streptomycin-Induced Inflammation Enhances *Escherichia coli* Gut. **4**, 1–10 (2013).
170. Oberc, A. M., Fiebig-Comyn, A. A., Tsai, C. N., Elhenawy, W. & Coombes, B. K. Antibiotics potentiate adherent-invasive *E. coli* infection and expansion. *Inflamm. Bowel Dis.* **25**, 711–721 (2019).
171. Elhenawy, W., Tsai, C. N. & Coombes, B. K. Host-Specific Adaptive Diversification of Crohn's Disease-Associated Adherent-Invasive *Escherichia coli*. *Cell Host Microbe* **25**, 301-312.e5 (2019).

172. McPhee, J. B. *et al.* Host defense peptide resistance contributes to colonization and maximal intestinal pathology by Crohn's disease-associated adherent-invasive *Escherichia coli*. *Infect. Immun.* **82**, 3383–3393 (2014).
173. Ding, S. *et al.* High-fat diet: Bacteria interactions promote intestinal inflammation which precedes and correlates with obesity and insulin resistance in mouse. *PLoS One* **5**, (2010).
174. Agus, A. *et al.* Western diet induces a shift in microbiota composition enhancing susceptibility to Adherent-Invasive *E. coli* infection and intestinal inflammation. *Sci. Rep.* **6**, 19032 (2016).
175. Schertzer, J. D., Green, H. J., Fowles, J. R., Duhamel, T. A. & Tupling, A. R. Effects of prolonged exercise and recovery on sarcoplasmic reticulum Ca<sup>2+</sup> cycling properties in rat muscle homogenates. *Acta Physiol. Scand.* **180**, 195–208 (2004).
176. Small, C. L. N., Reid-Yu, S. A., McPhee, J. B. & Coombes, B. K. Persistent infection with Crohn's disease-associated adherent-invasive *Escherichia coli* leads to chronic inflammation and intestinal fibrosis. *Nat. Commun.* **4**, 1–12 (2013).
177. Muller, L. M. a J. *et al.* Increased risk of common infections in patients with type 1 and type 2 diabetes mellitus. *Clin. Infect. Dis.* **41**, 281–288 (2005).

178. Diabetes and the Risk of Infection-. *Diabetes Care* (2001).
179. Lindström, P. The Physiology of Obese-Hyperglycemic Mice [ *ob/ob* Mice]. *Sci. World J.* **7**, 666–685 (2007).
180. Westman, S. Development of the obese-hyperglycaemic syndrome in mice. *Diabetologia* **4**, 141–149 (1968).
181. Edvell, A. & Lindström, P. Development of insulin secretory function in young obese hyperglycemic mice (Umeå ). *Metabolism* **44**, 906–913 (1995).
182. Edvell, A. Initiation of Increased Pancreatic Islet Growth in Young Normoglycemic Mice ( Umeå %./? )\*. **140**, 778–783 (1999).
183. Siegmund, B., Lehr, H. A. & Fantuzzi, G. Leptin: a pivotal mediator of intestinal inflammation in mice. *Gastroenterology* **122**, 2011–25 (2002).
184. Arnalich, F. *et al.* Relationship of Plasma Leptin to Plasma Cytokines and Human Survival in Sepsis and Septic Shock. *J. Infect. Dis.* **180**, 908–911 (1999).
185. Cani, P. D. *et al.* Metabolic Endotoxemia Initiates Obesity and Insulin Resistance. *Diabetes* **56**, 1761–1772 (2007).
186. Roberts, H. C., Hardie, L. J., Chappell, L. H. & Mercer, J. G. Parasite-induced anorexia: Leptin, insulin and corticosterone responses to infection with the nematode, *Nippostrongylus brasiliensis*. *Parasitology* **118**, 117–123 (1999).

187. Mancuso, P. *et al.* Leptin-Deficient Mice Exhibit Impaired Host Defense in Gram-Negative Pneumonia. *J. Immunol.* **168**, 4018–4024 (2002).
188. Hong, E.-G. *et al.* Nonobese, insulin-deficient Ins2Akita mice develop type 2 diabetes phenotypes including insulin resistance and cardiac remodeling. *Am. J. Physiol. Endocrinol. Metab.* **293**, E1687–E1696 (2007).
189. Naito, M. *et al.* Therapeutic impact of leptin on diabetes, diabetic complications, and longevity in insulin-deficient diabetic mice. *Diabetes* **60**, 2265–2273 (2011).
190. Berger, C. N. *et al.* Citrobacter rodentium Subverts ATP Flux and Cholesterol Homeostasis in Intestinal Epithelial Cells In Vivo. *Cell Metab.* **26**, 738-752.e6 (2017).
191. Radics, J., Königsmaier, L. & Marlovits, T. C. Structure of a pathogenic type 3 secretion system in action. *Nat. Struct. Mol. Biol.* **21**, 82–87 (2014).
192. Deng, W. *et al.* Regulation of type III secretion hierarchy of translocators and effectors in attaching and effacing bacterial pathogens. *Infect. Immun.* **73**, 2135–2146 (2005).
193. Frazier, T. H., Dibaise, J. K. & McClain, C. J. Gut microbiota, intestinal permeability, obesity-induced inflammation, and liver injury. *JPEN. J. Parenter. Enteral Nutr.* **35**, 14S-20S (2011).
194. Bekkevold, C. M., Robertson, K. L., Reinhard, M. K., Battles, A. H. & Rowland, N. E. Dehydration parameters and standards for laboratory

- mice. *J. Am. Assoc. Lab. Anim. Sci.* **52**, 233–239 (2013).
195. Tucci, V., Hardy, A. & Nolan, P. M. A comparison of physiological and behavioural parameters in C57BL/6J mice undergoing food or water restriction regimes. *Behav. Brain Res.* **173**, 22–29 (2006).
196. Silverstein, E. Urine specific gravity and osmolality in inbred strains of mice. *J. Appl. Physiol.* **16**, 194–196 (1961).
197. Grempler, R. *et al.* Empagliflozin, a novel selective sodium glucose cotransporter-2 (SGLT-2) inhibitor: Characterisation and comparison with other SGLT-2 inhibitors. *Diabetes, Obes. Metab.* **14**, 83–90 (2012).
198. Lioudaki, E., Whyte, M., Androulakis, E. S. & Konstantinos, G. The renal effects of SGLT-2 inhibitors and other anti-diabetic drugs : Clinical relevance and potential risks.
199. Vallianou, N. G., Geladari, E. & Kazazis, C. E. SGLT-2 inhibitors: Their pleiotropic properties. *Diabetes Metab. Syndr. Clin. Res. Rev.* 8–12 (2016). doi:10.1016/j.dsx.2016.12.003
200. Takebe, N. *et al.* Targeting Notch, Hedgehog, and Wnt Pathways in cancer stem cells: clinical update. *Nat Rev Clin Oncol* **12**, 445–464 (2015).
201. Papapietro, O. *et al.* R-Spondin 2 signalling mediates susceptibility to fatal infectious diarrhoea. *Nat. Commun.* (2013). doi:10.1038/ncomms2816
202. Kang, E., Yousefi, M. & Gruenheid, S. R-spondins are expressed by the intestinal stroma and are differentially regulated during *Citrobacter*

- rodentium- and dss-induced colitis in mice. *PLoS One* **11**, 1–13 (2016).
203. Small, C. L., Xing, L., McPhee, J. B., Law, H. T. & Coombes, B. K. Acute Infectious Gastroenteritis Potentiates a Crohn's Disease Pathobiont to Fuel Ongoing Inflammation in the Post-Infectious Period. *PLoS Pathog.* **12**, 1–20 (2016).
204. Shaler, C. R., Elhenawy, W. & Coombes, B. K. The Unique Lifestyle of Crohn's Disease-Associated Adherent-Invasive Escherichia coli. *J. Mol. Biol.* **431**, 2970–2981 (2019).
205. Nickerson, K. P. & McDonald, C. Crohn's Disease-Associated Adherent-Invasive Escherichia coli Adhesion Is Enhanced by Exposure to the Ubiquitous Dietary Polysaccharide Maltodextrin. *PLoS One* **7**, 1–13 (2012).
206. Karlsson, E. a & Beck, M. a. The burden of obesity on infectious disease. *Exp. Biol. Med. (Maywood)*. **235**, 1412–24 (2010).
207. Sen, T. *et al.* Diet-driven microbiota dysbiosis is associated with vagal remodeling and obesity. *Physiol. Behav.* **173**, 305–317 (2017).
208. Araújo, J. R., Tomas, J., Brenner, C. & Sansonetti, P. J. Impact of high-fat diet on the intestinal microbiota and small intestinal physiology before and after the onset of obesity. *Biochimie* **141**, 97–106 (2017).
209. Kless, C. *et al.* Diet-induced obesity causes metabolic impairment independent of alterations in gut barrier integrity. *Mol. Nutr. Food Res.* **59**, 968–978 (2015).

210. Winer, D. A., Luck, H., Tsai, S. & Winer, S. The Intestinal Immune System in Obesity and Insulin Resistance. *Cell Metab.* **23**, 413–426 (2016).
211. Teixeira, T. F. S., Collado, M. C., Ferreira, C. L. L. F., Bressan, J. & Peluzio, M. do C. G. Potential mechanisms for the emerging link between obesity and increased intestinal permeability. *Nutr. Res.* **32**, 637–647 (2012).
212. Cavallari, J. F. *et al.* Different Th17 immunity in gut , liver , and adipose tissues during obesity : the role of diet , genetics , and microbes. *Gut Microbes* **7**, 82–89 (2016).
213. Zou, J. *et al.* Fiber-Mediated Nourishment of Gut Microbiota Protects against Diet-Induced Obesity by Restoring IL-22-Mediated Colonic Health. *Cell Host Microbe* **23**, 41-53.e4 (2018).
214. Rubino, S. J., Geddes, K. & Girardin, S. E. Innate IL-17 and IL-22 responses to enteric bacterial pathogens. *Trends Immunol.* **33**, 112–118 (2012).
215. Schreiber, F., Arasteh, J. M. & Lawley, T. D. Pathogen Resistance Mediated by IL-22 Signaling at the Epithelial – Microbiota Interface. *J. Mol. Biol.* **427**, 3676–3682 (2015).
216. Valeri, M. & Raffatellu, M. Cytokines IL-17 and IL-22 in the host response to infection. *Pathog. Dis.* **74**, 1–15 (2016).
217. Zhang, H. jia *et al.* IL-17 is a protection effector against the adherent-invasive Escherichia coli in murine colitis. *Mol. Immunol.* **93**, 166–172 (2018).

218. McPhee, J. B. *et al.* Host defense peptide resistance contributes to colonization and maximal intestinal pathology by Crohn's disease-associated adherent-invasive Escherichia coli. *Infect. Immun.* **82**, 3383–3393 (2014).
219. Franceschi, C. *et al.* Inflammaging and anti-inflammaging: A systemic perspective on aging and longevity emerged from studies in humans. *Mech. Ageing Dev.* **128**, 92–105 (2007).
220. Bana, B. & Cabreiro, F. The Microbiome and Aging. *Annu. Rev. Genet.* **53**, annurev-genet-112618-043650 (2019).
221. Man, A. L., Gicheva, N. & Nicoletti, C. The impact of ageing on the intestinal epithelial barrier and immune system. *Cell. Immunol.* **289**, 112–118 (2014).
222. Olivieri, F. *et al.* Toll like receptor signaling in “ inflammaging ” : microRNA as new players. *Immun. Ageing* **10**, 1 (2013).
223. Thevaranjan, N. *et al.* Age-Associated Microbial Dysbiosis Promotes Intestinal Permeability, Systemic Inflammation, and Macrophage Dysfunction. *Cell Host Microbe* **21**, 455-466.e4 (2017).
224. Ma, X., Torbenson, M., Hamad, A. R. A., Soloski, M. J. & Li, Z. High-fat diet modulates non-CD1d-restricted natural killer T cells and regulatory T cells in mouse colon and exacerbates experimental colitis. *Clin. Exp. Immunol.* **151**, 130–138 (2008).

225. Laffin, M. *et al.* A high-sugar diet rapidly enhances susceptibility to colitis via depletion of luminal short-chain fatty acids in mice. *Sci. Rep.* **9**, 12294 (2019).
226. Wang, H. *et al.* Dietary non-digestible polysaccharides ameliorate intestinal epithelial barrier dysfunction in IL-10 knockout mice. *J. Crohn's Colitis* **10**, 1076–1086 (2016).
227. Desai, M. S. *et al.* A Dietary Fiber-Deprived Gut Microbiota Degrades the Colonic Mucus Barrier and Enhances Pathogen Susceptibility. *Cell* **167**, 1339-1353.e21 (2016).
228. Ogata, M., Ogita, T., Tari, H., Arakawa, T. & Suzuki, T. Supplemental psyllium fibre regulates the intestinal barrier and inflammation in normal and colitic mice. 661–672 (2017).  
doi:10.1017/S0007114517002586
229. Llewellyn, S. R. *et al.* Interactions Between Diet and the Intestinal Microbiota Alter Intestinal Permeability and Colitis Severity in Mice. *Gastroenterology* **154**, 1037-1046.e2 (2018).
230. Jangra, S., Raja, S. K., Sharma, R. K., Pothuraju, R. & Mohanty, A. K. Ameliorative effect of fermentable fibres on adiposity and insulin resistance in C57BL/6 mice fed a high-fat and sucrose diet. *Food Funct.* **10**, 3696–3705 (2019).
231. Thaiss, C. A. *et al.* Hyperglycemia drives intestinal barrier dysfunction and

- risk for enteric infection. *Science (80-. )*. **359**, 1376–1383 (2018).
232. Allen, T. J., Cooper, M. E. & Lan, H. Y. Use of genetic mouse models in the study of diabetic nephropathy. *Curr. Diab. Rep.* **4**, 435–440 (2004).
233. Thaiss, C. A. *et al.* Hyperglycemia drives intestinal barrier dysfunction and risk for enteric infection. **1383**, 1376–1383 (2018).
234. Furman, B. L. Streptozotocin-Induced Diabetic Models in Mice and Rats. *Curr. Protoc. Pharmacol.* **70**, 5.47.1-5.47.20 (2015).
235. Goyal, S. N. *et al.* Challenges and issues with streptozotocin-induced diabetes - A clinically relevant animal model to understand the diabetes pathogenesis and evaluate therapeutics. *Chem. Biol. Interact.* **244**, 49–63 (2016).
236. Koley, H. *et al.* Mice with Streptozotocin-Induced Hyperglycemia are Susceptible to Invasive Enteric Bacterial Infection. *Jpn. J. Infect. Dis.* **70**, 111–114 (2017).
237. Radenković, M., Stojanović, M. & Prostran, M. Experimental diabetes induced by alloxan and streptozotocin: The current state of the art. *J. Pharmacol. Toxicol. Methods* **78**, 13–31 (2016).
238. Srinivasan, K. & Ramarao, P. Animal models in type 2 diabetes research: An overview K. *Indian J. Med. Res.* **136**, 451–472 (2012).
239. Deeds, M. C. *et al.* Single dose streptozotocin-induced diabetes: Considerations for study design in islet transplantation models. *Lab. Anim.*

- 45**, 131–140 (2011).
240. Lenzen, S. The mechanisms of alloxan- and streptozotocin-induced diabetes. *Diabetologia* **51**, 216–226 (2008).
241. Eleazu, C. O., Eleazu, K. C., Chukwuma, S. & Essien, U. N. Review of the mechanism of cell death resulting from streptozotocin challenge in experimental animals, its practical use and potential risk to humans. *J. Diabetes Metab. Disord.* **12**, 1–7 (2013).
242. Nørgaard, S. A. *et al.* Optimising streptozotocin dosing to minimise renal toxicity and impairment of stomach emptying in male 129/Sv mice. *Lab. Anim.* **0**, 1–12 (2019).
243. Kellett, G. L., Brot-Laroche, E., Mace, O. J. & Leturque, A. Sugar Absorption in the Intestine: The Role of GLUT2. *Annu. Rev. Nutr.* **28**, 35–54 (2008).
244. Kwon, O. *et al.* Inhibition of the intestinal glucose transporter GLUT2 by flavonoids. *FASEB J.* **21**, 366–377 (2007).
245. Imaeda, A., Kaneko, T., Aoki, T., Kondo, Y. & Nagase, H. DNA damage and the effect of antioxidants in streptozotocin-treated mice. *Food Chem. Toxicol.* **40**, 979–987 (2002).
246. Rerup, C. C. Drugs producing diabetes through damage of the insulin secreting cells. *Pharmacol. Rev.* **22**, 485–518 (1970).
247. Rossini, A. A., Williams, R. M., Appel, M. C. & Like, A. A. Sex differences in the multiple-dose streptozotocin model of diabetes. *Endocrinology* **103**,

1518–1520 (1978).

248. Wang, X. *et al.* Interleukin-22 alleviates metabolic disorders and restores mucosal immunity in diabetes. *Nature* **514**, 237–241 (2014).
249. Borenshtein, D. *et al.* Decreased expression of colonic Slc26a3 and carbonic anhydrase IV as a cause of fatal infectious diarrhea in mice. *Infect. Immun.* **77**, 3639–3650 (2009).
250. Fre, S. *et al.* Notch Lineages and Activity in Intestinal Stem Cells Determined by a New Set of Knock-In Mice. **6**, (2011).
251. Fre, S., Huyghe, M., Mourikis, P., Robine, S. & Louvard, D. Notch signals control the fate of immature progenitor cells in the intestine. **435**, (2005).
252. Zhen, Q. I. & Ye-guang, C. Regulation of intestinal stem cell fate specification. **58**, 570–578 (2015).
253. Sukhotnik, I. *et al.* Activated Notch signaling cascade is correlated with stem cell differentiation toward absorptive progenitors after massive small bowel resection in a rat. 247–255 (2018).  
doi:10.1152/ajpgi.00139.2017
254. Lee, Y. S. *et al.* Inflammation is necessary for long-term but not short-term high-fat diet-induced insulin resistance. *Diabetes* **60**, 2474–2483 (2011).
255. Cousin, B. *et al.* Immuno-metabolism and adipose tissue: The key role of hematopoietic stem cells. *Biochimie* (2015).  
doi:10.1016/j.biochi.2015.06.012

256. Simpson, H. L. & Campbell, B. J. Review article: dietary fibre-microbiota interactions. *Aliment. Pharmacol. Ther.* **42**, 158–179 (2015).
257. Shang, Y. *et al.* Short Term High Fat Diet Induces Obesity-Enhancing Changes in Mouse Gut Microbiota That are Partially Reversed by Cessation of the High Fat Diet. *Lipids* **52**, 1–13 (2017).
258. Vieira, E. L. M. *et al.* Oral administration of sodium butyrate attenuates inflammation and mucosal lesion in experimental acute ulcerative colitis. *J. Nutr. Biochem.* **23**, 430–436 (2012).
259. Li, Z. *et al.* Butyrate reduces appetite and activates brown adipose tissue via the gut-brain neural circuit. *Gut* **67**, 1269–1279 (2018).
260. Leonel, A. J. & Alvarez-Leite, J. I. Butyrate: Implications for intestinal function. *Curr. Opin. Clin. Nutr. Metab. Care* **15**, 474–479 (2012).
261. Perry, R. J. *et al.* Acetate mediates a microbiome-brain-B cell axis promoting metabolic Syndrome. *Nature* **534**, 213–217 (2016).
262. Pellizzon, M. A. & Ricci, M. R. The common use of improper control diets in diet-induced metabolic disease research confounds data interpretation: The fiber factor. *Nutr. Metab.* **15**, 1–6 (2018).
263. Saucillo, D. C., Gerriets, V. A., Sheng, J., Rathmell, J. C. & Maciver, N. J. Leptin metabolically licenses T cells for activation to link nutrition and immunity. *J. Immunol.* **192**, 136–44 (2014).
264. Howard, J. K. *et al.* Leptin protects mice from starvation-induced lymphoid

- atrophy and increases thymic cellularity in ob/ob mice. *J. Clin. Invest.* **104**, 1051–1059 (1999).
265. Kühnen, P., Krude, H. & Biebermann, H. Melanocortin-4 Receptor Signalling: Importance for Weight Regulation and Obesity Treatment. *Trends Mol. Med.* **25**, 136–148 (2019).
266. Balthasar, N. *et al.* Divergence of melanocortin pathways in the control of food intake and energy expenditure. *Cell* **123**, 493–505 (2005).
267. Kumar, K. G. *et al.* Analysis of the therapeutic functions of novel melanocortin receptor agonists in MC3R- and MC4R-deficient C57BL/6J mice. *Peptides* **30**, 1892–1900 (2009).
268. Baldini, G. & Phelan, K. D. The melanocortin pathway and control of appetite-progress and therapeutic implications. *J. Endocrinol.* **241**, R1–R33 (2019).
269. Warden, C. H. & Fisler, J. S. Comparisons of Diets Used in Animal Models of High-Fat Feeding. *Cell Metab.* **7**, 277 (2008).
270. Wise, A. & Gilbert, D. J. The variability of dietary fibre in laboratory animal diets and its relevance to the control of experimental conditions. *Food Cosmet. Toxicol.* **18**, 643–648 (1980).
271. Marques, F. Z. *et al.* High-fiber diet and acetate supplementation change the gut microbiota and prevent the development of hypertension and heart failure in hypertensive mice. *Circulation* **135**, 964–977 (2017).

272. Sasaki, D. *et al.* Low amounts of dietary fibre increase in vitro production of short-chain fatty acids without changing human colonic microbiota structure. *Sci. Rep.* **8**, 1–7 (2018).
273. Ivarsson, E. Dietary Fibre and Gut Microbiota. 201–211 (2008).
274. Dalby, M. J., Ross, A. W., Walker, A. W. & Morgan, P. J. Dietary Uncoupling of Gut Microbiota and Energy Harvesting from Obesity and Glucose Tolerance in Mice. *Cell Rep.* **21**, 1521–1533 (2017).
275. Fuentes-Zaragoza, E., Riquelme-Navarrete, M. J., Sánchez-Zapata, E. & Pérez-Álvarez, J. A. Resistant starch as functional ingredient: A review. *Food Res. Int.* **43**, 931–942 (2010).
276. Sajilata, M. G., Singhal, R. S. & Kulkarni, P. R. Resistant starch - A review. *Compr. Rev. Food Sci. Food Saf.* **5**, 1–17 (2006).
277. Zou, J. *et al.* Fiber-Mediated Nourishment of Gut Microbiota Protects against Diet-Induced Obesity by Restoring IL-22-Mediated Colonic Health. *Cell Host Microbe* **23**, 41-53.e4 (2018).
278. Buddington, K. K., Donahoo, J. B. & Buddington, R. Dietary oligofructose and inulin protect mice from enteric and systemic pathogens and tumor inducers. *J. Nutr.* **132**, 472–477 (2002).
279. Cheng, L. *et al.* High fat diet exacerbates dextran sulfate sodium induced colitis through disturbing mucosal dendritic cell homeostasis. *Int. Immunopharmacol.* **40**, 1–10 (2016).

280. Wirtz, S., Neufert, C., Weigmann, B. & Neurath, M. F. Chemically induced mouse models of intestinal inflammation. *Nat. Protoc.* **2**, 541–546 (2007).
281. Silveira, A. L. M. *et al.* Preventive rather than therapeutic treatment with high fiber diet attenuates clinical and inflammatory markers of acute and chronic DSS-induced colitis in mice. *Eur. J. Nutr.* **56**, 179–191 (2017).
282. Eichele, D. D. & Kharbanda, K. K. Dextran sodium sulfate colitis murine model: An indispensable tool for advancing our understanding of inflammatory bowel diseases pathogenesis. *World J. Gastroenterol.* **23**, 6016–6029 (2017).